IN VITRO EVALUATION OF COMB-TYPE POLY(ETHYLENE GLYCOL)-CELL INTERACTIONS AND COMPARISON WITH LINEAR POLY(ETHYLENE GLYCOL)

A Thesis Submitted to
the Graduate School of Engineering and Sciences of
İzmir Institute of Technology
in Partial Fulfillment of the Requirements for the Degree of

MASTER OF SCIENCE

in Biotechnology

by
Tuğba TOKER

December 2012
İZMİR

We approve the thesis of **Tuğba TOKER**

Examining Committee Members:

_____

Assoc. Prof. Dr. Volga BULMUŞ
Department of Chemical Engineering
İzmir Institute of Technology

_____

Prof. Dr. Serdar ÖZÇELİK
Department of Chemistry
İzmir Institute of Technology

_____

Assist. Prof. Dr. Devrim PESEN OKVUR
Department of Molecular Biology and Genetics
İzmir Institute of Technology

10 December 2012

_____

Assoc. Prof. Dr. Volga BULMUŞ
Supervisor, Department of Chemical Engineering
İzmir Institute of Technology

_____

Assoc. Prof. Dr. Yusuf BARAN
Co-Supervisor, Department of Molecular Biology and Genetics
İzmir Institute of Technology

_____

Assoc. Prof. Dr. Volga BULMUŞ
Head of the Department of Biotechnology and Bioengineering

_____

Prof. Dr. R. Tuğrul SENGER
Dean of the Graduate School of Engineering and Sciences

ACKNOWLEDGMENTS

Firstly, I would like to express my sincere gratitude to my thesis supervisor Assoc. Prof. Dr. Volga BULMUŞ for giving me the chance to work on this study. She gave me guidance, encouragement, support and patient throughout my thesis and my life. Although she always says ‘‘You live your afraids, mustn’t worry, you can defeat them’’, I know that she encouraged me to me and my life.

I also want to thank my co-supervisor Assoc. Prof. Dr Yusuf BARAN and Assist. Prof. Dr. Hadi M. ZAREİE for his academic support and comments.

I am thankful to Ekrem ÖZER for his help and guidance for solving my research problems. Fortunately he is our labmate because of his energy, hopeful and high sound. I would like to thank my colleagues, Işıl KURTULUŞ, Esra AYDINLIOĞLU and Damla TAYKOZ for their help and support throughout the study. I also thank Melis KARTAL for sparing her time for me in Cancer Genetic Laboratory.

I am also grateful to specialist Işın ÖZÇELİK and Salih GÜNNAZ for their help and support throughout the NMR experiments.

I would also like to thank staff of Biotechnology and Bioengineering Research and Application Center; Özgür YILMAZER who trained me for cell culture studies in a patient manner and Dane RUSÇUKLU. They are worthy for me.

Grateful thanks go to Hande ORŞAHİN, who became a real friend, sister and homemate since 2003. I would like to thank my other sisters Gözde ÖZYILDIRIM, Şeyda ŞENİŞLER and my new homemate Ceren SÜNGÜÇ also Ezgi BARAN and E.Aysu SAĞDIÇ for their endless friendship and emotional support. I appreciate you; Abdurrahman DEMİR for being such a great partner, your endless care and logical approaches were the best motivation for me.

Lastly and most importantly, I would like to express special thanks to my mother Reyhan, my sister Funda and my father M. Uğur TOKER to whom I dedicate this thesis for their never ending love, support and encouragements during my thesis and my life. Finally, my little niece Elif ÇELİKOĞLU, welcome to my world.

ABSTRACT

IN VITRO EVALUATION OF COMB-TYPE POLY(ETHYLENE GLYCOL)-CELL INTERACTIONS AND COMPARISON WITH LINEAR POLY(ETHYLENE GLYCOL)

The aim of this study is to investigate physicochemical characteristics and *in vitro* cell interactions of comb-type poly(ethylene glycol) (M_n= 10 700 and M_n= 20 200 g/mol, p(PEG-A) 10K and p(PEG-A) 20K, respectively) in comparison with linear poly(ethylene glycol) (M_n= 10 000 and M_n= 20 000 g/mol, PEG 10K and PEG 20K, respectively) of equivalent molecular weight. *In vitro* cytotoxicity, cell uptake and intracellular distribution profile of comb-type and linear polymers were investigated using human lung adenocarcinoma epithelial cells (A549).

The dynamic light scattering (DLS) analysis showed that the comb-type polymers had smaller hydrodynamic diameters (D_h) (4.5±0.3 nm - 5.9±0.3 nm) than linear PEGs (5.6±0.5 nm - 7.8 ±0.2 nm) in water and phosphate buffer solution at pH 7.4. While the D_h of p(PEG-A) 10K and 20K in RPMI 1640 and RPMI 1640 containing 10% FBS ranged between 44.4±1.8 nm and 58±5.3 nm, the D_h of PEG 10K and 20K in the same media were between 54.5±4.7 nm and 63.5±2 nm. According to the AFM analysis, PEG 10K forms supramolecular linear structures whereas p(PEG-A) 10K forms spherical structures.

None of the polymers caused significant cytotoxic effect on A549 cells under the conditions tested via a cell viability assay. Cell uptake studies via flow cytometry showed that the uptake of p(PEG-A) 10K by A549 cells was significantly higher than the other polymers tested. All polymers were internalized by A549 cells via an active transport mechanism. The uptake increased with increasing polymer concentrations. None of the polymers affected the cell cycle of A549 cells under the conditions tested. Both the comb-type and linear PEGs were found to localize in the lysosomes of A549 cells.

ÖZET

TARAK TİPİ POLİ(ETİLEN GLİKOL)-HÜCRE ETKİLEŞİMLERİNİN *İN VİTRO* DEĞERLENDİRİLMESİ VE LİNEER POLİ(ETİLEN GLİKOL) İLE KARŞILAŞTIRILMASI

Bu çalışmanın amacı, eşdeğer moleküler ağırlığa sahip tarak-tipi PEG (MA= 10 700 ve MA=20 200 g/mol, p(PEG-A) 10K ve p(PEG-A) 20K, sırasıyla) ve lineer PEG'in (MA= 10 000 ve MA=20 000 g/mol, PEG 10K ve PEG 20K, sırasıyla) fizikokimyasal karakteristliklerinin ve *in vitro* hücre etkileşimlerinin karşılaştırmalı olarak incelenmesidir. Dört farklı polimerin, *in vitro* sitotoksisite, hücre alımı, hücre-içi dağılım profilleri ve hücre döngüsüne etkileri insan akciğer adenokarsinom epitel hücrelerinde (A549) incelendi.

Dinamik ışık saçılımı (DLS) analizleri, tarak-tipi polimerin hidrodinamik çaplarının (4.5±0.3 nm - 5.9±0.3 nm) lineer PEG'e göre (5.6±0.5 nm - 7.8 ±0.2 nm) suda ve fosfat tampon çözeltisinde daha küçük olduğunu gösterdi. Hücre kültür ortamında, RPMI 1640 ve 10% FBS içeren RPMI 1640, p(PEG-A) 10K and 20K'nın hidrodinamik çapları 44.4±1.8 nm ve 58±5.3 nm iken, PEG 10K and 20K'nın 54.5±4.7 nm ve 63.5±2 nm'dir. AFM analizleri, PEG 10K supramoleküler lineer form yapısındayken, p(PEG-A) 10K'nın küresel yapıda olduğunu göstermiştir.

Polimerler, A549 hücrelerinde önemli derecede sitotoksik etki göstermemiştir. Hücre alımı çalışmaları, A549 hücrelerine p(PEG-A) 10K'nın diğer polimerlere göre önemli derecede fazla alındığını göstermiştir. Tüm polimerler A549 hücreleri tarafından aktif taşıma ile alınmıştır. Hücre alımı, artan polimer konsantrasyonuyla artmıştır. A549 hücrelerinin hücre döngüsüne, polimerlerin etkisi gözlenmemiştir. Polimerler, A549 hücrelerinin lizozomlarında lokalize olmuştur.

TABLE OF CONTENTS

LIST OF FIGURES

Figure **Page**

LIST OF TABLES

Table **Page**

CHAPTER 1

INTRODUCTION

Poly(ethylene glycol) (PEG) is a non-toxic, non-immunogenic and uncharged polymer that consists of repeating ethylene oxide units along a linear polymer backbone (Figure 1.1). PEG has been widely used in pharmaceutical applications due to its low toxicity, low protein adsorption property and non-immunogenicity. Biomolecular therapeutics display better in vivo properties and performance when covalently conjugated with PEG chains (Zalipsky 1995). PEG having varying molecular weights and narrow polydispersity* is commercially available and has been widely used for preperation of protein conjugates, PEG-liposomes and micelles and PEG-drug conjugates for pharmaceutical applications (Zalipsky and Milton Harris 1997).

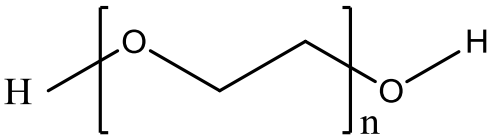

Figure 1.1. The chemical structure of linear PEG

Conjugating biomolecules with PEG, a strategy termed PEGylation, is now an important method not only for therapy, but also diagnosis and organic biocatalysis (Veronese and Pasut 2005).

*Polydispersity index (PDI) is a measure of molecular weight distribution of polymers. The PDI has a value equal to or greater than 1.If the polymer chains are uniform in chain length, the PDI is equal to 1 (Rogošić, Mencer, and Gomzi 1996).

PEGylation of therapeutics has several advantages: PEG reduces immunogenicity of the therapeutics molecules. The hydrodynamic volume of the therapeutic molecules increases after PEGylation, which results in increased *in vivo* circulation half-lifes of therapeutics by reducing renal clearance and restricting body distribution. PEGylation also increases stability and solubility of biomolecules and protects biomolecules againts degradation by enzymes (Zalipsky and Milton Harris 1997).

Despite these favorable properties of PEGylation, there are several disadvantages of PEGylation technology:

1. PEG is a non-degradable polymer. Below 20 kDa molecular weight, it is excreted from the body via kidneys. However above 50 kDa molecular weight, it is eliminated more slowly and it accumulates at liver that leads to macromolecular syndrome (Bouladjine et al. 2009, Veronese and Pasut 2005).

2. While the higher molecular weight PEG can protect therapeutics better, the nondegradable structure of PEG, which leads to accumulation at liver, limits the use of high molecular weight polymers in therapeutic applications.

3. PEG has poor cell uptake because of hydrophilic nature and large hydrodynamic volume (Caliceti and Veronese 2003). This is especially important for formulations or therapeutics that need to reach intracellular targets, such as anticancer drug carrying nanoparticles and DNA/RNA based therapeutics. It has been reported that PEGylated conjugates showed little uptake due to the shielding effect of PEG inhibiting electrostatic interactions with anionic cell surfaces (Kunath et al. 2003).

4. Also PEGylation may decrease pharmacological activity of biotherapeutics. Interferon-alpha-2a modified with 40 kDa PEG retains only 7% of the initial therapeutic activity of the protein (Bailon et al. 2001).

In recent years new PEG architectures have been developed to improve the applications of PEGylation technology. These include branched PEGs such as 3-armed, 4-armed, star and comb-type PEGs.

Comb-type PEG polymers that are formed by grafting multiple linear PEG oligomers to methacrylate or acrylate polymer backbones, have attracted attention as superior alternatives to linear and multi-armed PEGs (Figure 1.2) (Ryan et al. 2009, Sayers et al. 2009). Due to their umbrella-like shape, comb-type PEGs can be more efficient in enhancing the circulation half-life of biomolecules in body by increasing resistance to degradative enzymes. The most important advantage of comb-type PEG

over linear and multi-armed PEGs is that it contains short PEG side chains attached to the backbone via the degradable ester bonds. Upon degradation of ester bonds, short PEG chains and also the remaining backbone are released. These short segments are in the bio-eliminable molecular weight range (Magnusson et al. 2010). Due to enzyme degradable and hydrolyzable ester linker, comb-type PEG may overcome the limitations of linear PEG, linked to its nondegradable structure such as liver accumulation problem. Another important feature of comb-type PEG is that it can be synthesized with controlled molecular weight, narrow molecular weight distribution and defined-end group at mild laboratory conditions via controlled/living radical polymerization techniques such as reversible addition fragmentation chain transfer (RAFT) polymerization and atom transfer radical polymerization (ATRP) techniques (Ryan et al. 2009, Moad, Rizzardo, and Thang 2009, Lowe, Hoyle, and Bowman 2010). In recent publications, comb-type PEG has shown to improve *in vivo* half-life of proteins and stability of nucleic acids against nucleases (Gunasekaran et al. 2011).

The aim of this thesis is to investigate interactions of comb-type PEG, poly(polyethylene glycol) methyl ether acrylate (PEG-A) with *in vitro* cultured cells in comparison with linear PEG. To do this, comb-type PEGs having two different molecular weights were first synthesized via RAFT polymerization and physicochemically characterized using Nuclear Magnetic Resonance (NMR), Gel Permeation Chromatography (GPC), Dynamic Light Scattering (DLS) and Atomic Force Microscopy (AFM). Commercially available linear PEGs of equivalent molecular weigths were also analyzed using the same techniques. Comb-type and linear PEGs were then tested in *in vitro* cytotoxicity, cell uptake, cell cycle and intracellular distribution experiments using a human lung adenocarcinoma epithelial cell line (A549). The methods and results are presented in Chapters 3 and 4, respectively.

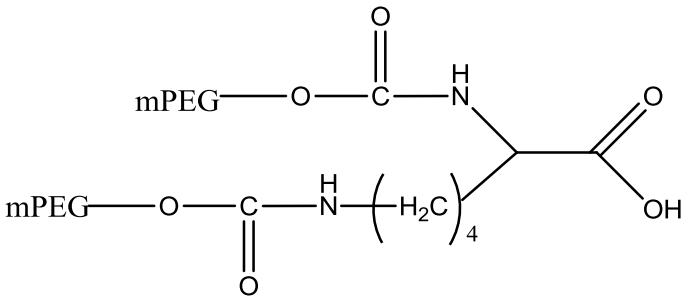

Branched-PEG2

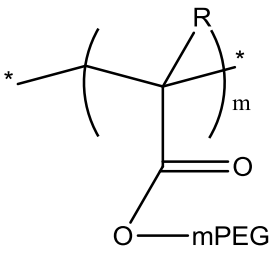

R=H or R=CH_3

Comb-type PEG

Figure 1.2. The chemical structure of branched and comb-type PEG

CHAPTER 2

LITERATURE REVIEW

2.1. PEGylation Technology

Advances in molecular biology and biotechnology have led to proteins, peptides, RNA and DNA-based biomacromolecular therapeutics that can be used for treatment of various diseases. For treatment of today, a large number of biopharmaceuticals are commercially available for human use. Despite their enormous potential, biopharmaceuticals have some important limitations *in vivo* such as immunogenicity, low solubility and nonspecific biodistribution (Veronese and Pasut 2005). In addition, biopharmaceuticals are prone to degradation by enzymes and rapidly excreted from the body in minutes (Jevševar, Kunstelj, and Porekar 2010).

PEGylation which is the covalent attachment of poly(ethylene glycol) (PEG) chains to bioactive substances has been used to overcome these limitations. PEGylation was first proposed by *Davis et al.* in 1970 to improve pharmacokinetic properties of proteins (Harris, Martin, and Modi 2001, Matsushima et al. 2001).

The PEGylation Technology has been widely used in pharmaceutical applications to improve properties of proteins, enzymes and anticancer drugs. It has also been used to prepare, stealth micelles and liposomes as efficient drug delivery vehicles. In addition, PEG hydrogels have been used for wound covering and cell encapsulation (Zalipsky and Milton Harris 1997).

PEGylation improves pharmacokinetic properties of biotherapeutics and drug delivery systems via various ways: PEG increases hydrodynamic volume of biomolecules/systems it is attached to (Figure 2.1) (Veronese and Pasut 2005, Harris, Martin, and Modi 2001). This reduces the rapid clearance by kidneys. PEGylation enhances the biological half-life of biomolecules/drug delivery systems by providing enhanced resistance against enzymes, reduced immunogenecity and recognition by reticuloendothelial system by shielding their surfaces (Gunasekaran et al. 2011). Acording to Figure 2.1 PEG shields the protein surface from degrading enzymes and

antibodies by steric hindrance. Moreover, the size of the conjugate increases so that the kidney clearance of the PEGylated protein decreases (Veronese and Pasut 2005).

PEGylation may also alter the biodistribution of biomolecules/drug delivery systems. Briefly, it increases the overall yield of the therapy.

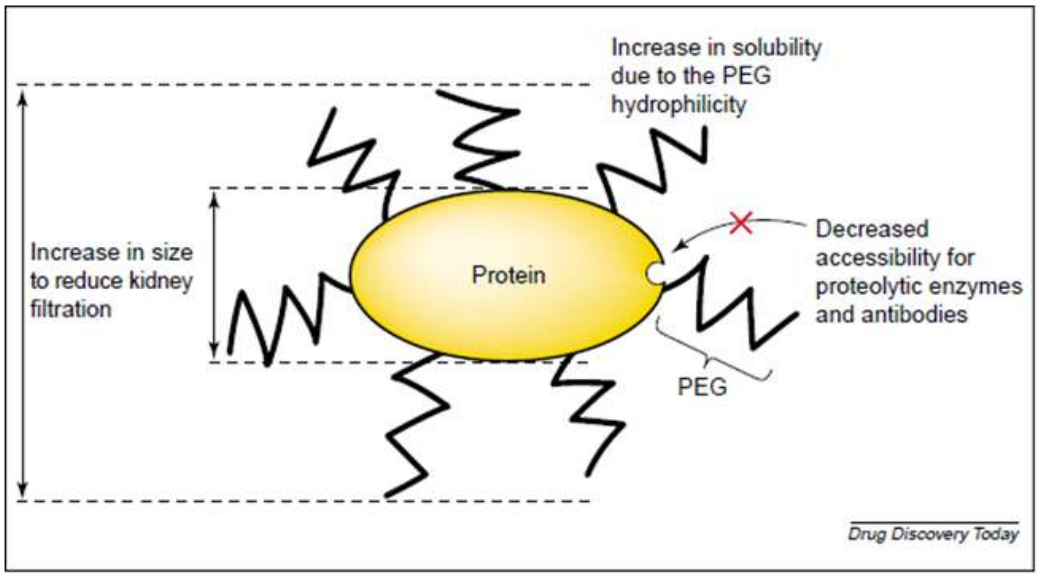

Figure 2.1. A protein-PEG conjugate

Along with these important advantages, PEGylation has several limitations: Biotherapeutics' pharmacological activity often decreases after PEGylation. Even though decreasing the pharmacological activity of biotherapeutics, PEGylation is the preferable method to increase the blood circulation half-life of biotherapeutics. Several protein therapeutics are taken up in the liver. By masking both recognition sites and charges, PEGylation reduces the protein uptake by liver cells (Kompella and Lee 2001). The liver clearance of PEG is size-dependent indicating a minimum around a molecular weight of 50 kDa. The higher-molecular-weight PEGs accumulate in the Kupffer cells of liver tissue (Caliceti and Veronese 2003, YAMAOKA, TABATA, and IKADA 1995, 1994). It is not easy to estimate the kidney excretion limit of PEG by looking only at the kidney clearance threshold of proteins (~60 kDa, albumin). Because, the high water affinity of PEG increases the polymer's hydrodynamic volume up to 3–5 times that of a globular protein with an equivalent molecular weight. Therefore, kidney clearance threshold for PEG is 3-5 times smaller when compared with globular proteins. The linear and flexible nature of the chains help PEG to cross the glomerular membranes by

a ‘snake-like’ movements (Veronese and Pasut 2005, Jevševar, Kunstelj, and Porekar 2010).

Another important limitation of PEGylation has been reported to be the poor cellular uptake of linear PEG. *Kunath et al*. prepeared RGD peptide-polyethylenimine (PEI)- PEG copolymers and reported that PEG can reduce the positive charge of PEI and also the cellular uptake of the copolymer. The poor uptake was attributed to the shielding effect of PEG inhibiting electrostatic interactions with anionic cell surface preventing nonspecific uptake. It is also possible that PEG blocks statistically exist as a cloud conformation due to the high flexibility of PEG chains. This conformation may prevent interactions between targeting RGD residues of the copolymers and integrin receptors on the cell surface. Therefore RGD peptide with PEG spacer did not lead to an effective targeting (Kunath et al. 2003, Torchilin et al. 1994). In gene therapy, PEGylation of adenovirus vectors (Ads) is an efficient strategy. Although high transduction efficiency, which is characteristic property of Ads, decreased owing to the steric hindrance of CAR by PEG chains. While PEG-Ads decreased gene expression in CAR-positive cells, RGD-PEG-Ad enhanced gene expression about 200-fold higher than PEG-Ads (Eto et al. 2005).

During PEG conjugation, the biological activity loss of therapeutics have been prevented by exploiting a different architecture of linear PEG used for modification. It was indicated that the activity loss of enzymes (such as asparaginase or uricase) was greatly circumvented by using branched PEG instead of linear PEG due to the hindrance by the bulky structure of the polymer approaching to the active site cleft (Figure 2.2). The high steric hindrance of branched PEG may be advocated to explain the lower inactivation of enzymes as compared to linear PEG of the same size (Veronese 2001).

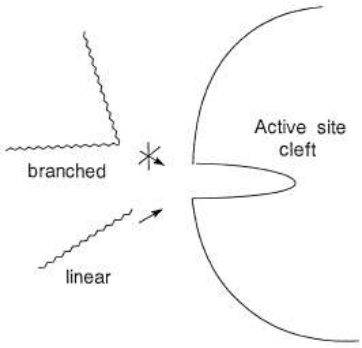

Figure 2.2. Branched PEG has the advantage of a lower inactivation of the enzymes during conjugation

2.2. Types of PEG Conjugates

To date, a number of PEGylated proteins have been approved for human use. Examples of the approved PEGylated protein therapeutics are listed in Table 2.1. Both linear and branched PEG architectures have been used to prepare these commercially available PEGylated therapeutics.

Table 2.1. Examples of FDA-approved PEGylated drugs in the market

Conjugate/Company	Type of PEGylation	Disease /Treatment	Year of Approval	Ref.
PEG-adenosine Deaminase (Adagen®)	Linear PEG	Severe combined immunodeficiency disease (SCID)	1990	(Graham 2003)
PEG-asparaginase (Oncaspar®)	Linear PEG	Leukemia	1994	(Levy et al. 1988)
PEG-interferon-α2b (PegIntron®)	Branched PEG 12kDa	Hepatitis C	2000	(Grace et al. 2001)
PEG-interferon-α2a (Pegasys®)	Branched PEG 40kDa	Hepatitis C	2002	(Bailon et al. 2001)
PEG-human growth hormone mutein antagonist (Somavert®)	Linear PEG 5kDa	Acromegaly	2002	(Trainer et al. 2000)
PEG-anti-VEGF aptamer (Pegaptanib, Macugen™)	Branched PEG 40kDa	Wet age associated macular degeneration	2004	(Ng et al. 2006)

Different PEG architectures that have been reported in the literature to date is shown by Figure 2.3. Among these architectures, linear PEG derivatives having molecular weights between 5kDa and 20 kDa have been often used as PEGylation reagents (Veronese 2001). For example, *Gilbert and Park-Cho* (Gilbert and Park-Cho

2000) used linear monomethoxyPEG (12 kDa) to develop PEG-interferon a-2b (IFN-a-2b). These conjugates improved pharmacokinetic properties of IFN-a-2b in both humans and animals. The second type of PEG architectures that has been widely used in PEGylation is the multi-arm PEGs. Two or more linear PEG chains are covalently linked through a core to prepare multi-arm PEGs. Among multi-arm PEGs, two-arm PEGs have been used in clinically approved PEGylated protein therapeutics. *Bailon et al.* (Bailon et al. 2001) conjugated IFN-a-2a with an N-hydroxysuccinimide (NHS) ester derivative of two-arm PEG (total molecular weigth 40 kDa, each linear PEG chain 20 kDa). These conjugates also showed improved pharmacokinetic properties in animals and healthy humans.

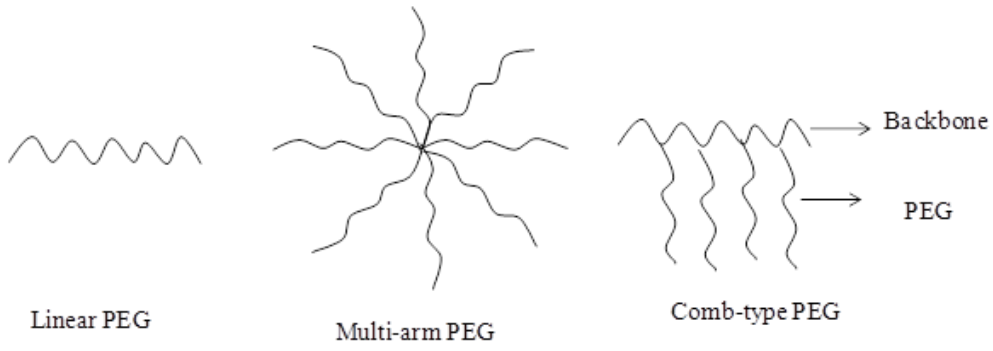

Figure 2.3. Types of PEGs backbones and architectures

Conjugation of multi-arm PEGs to proteins increases pH and thermal stability of proteins and provides greater stability toward proteolytic digestion. When compared to linear PEG, multi-arm PEGs with single reactive functional group have been proven more useful in polypeptide and protein. Lysine is the amino acid spacer between two PEG molecules in two-arm PEG that offers the advantages of higher protection of protein surface as compared to the linear form. Generally, it provides lower immunogenicity, higher retention in blood and decreased enzyme inactivation during the conjugation (Caliceti, Schiavon, and Veronese 1999). It is indicated that PEG and PEG2 (two-arm) derivatives show very different accumulation profiles in the examined organs. According to the literature data, the linear PEG derivative does not show specific localization in peripheral districts also low amounts of linear PEG' conjugates are found in all the tissues. On the other hand, the PEG2 adduct accumulates at significant extent in liver and spleen that rich of reticulo-endothelial cells. Therefore, branched shape of this polymer can affect the cell/ conjugate interaction process and the

higher accumulation of the PEG2 derivative can more efficiently stimulate the cell phagocytic process with respect to the linear one (Bailon et al. 2001, Caliceti, Schiavon, and Veronese 1999, Bendele et al. 1998).

Multi-arm PEGs have been more efficient in improving the biological half-life of protein therapeutics by providing higher steric hindrance effect because of its umbrella-like shape, thus leading to more efficiently reduction in immunogenicity and better resistance against proteolysis (Ryan et al. 2008, Roberts, Bentley, and Harris 2012, Ryan et al. 2009). Figure 2.4 shows the difference in the steric hindrance effect of linear and two-arm PEGs. The umbrella-like structure of branched PEG defines the higher capacity in rejecting approaching cells or molecules as compared to linear PEG of the same size (Veronese 2001).

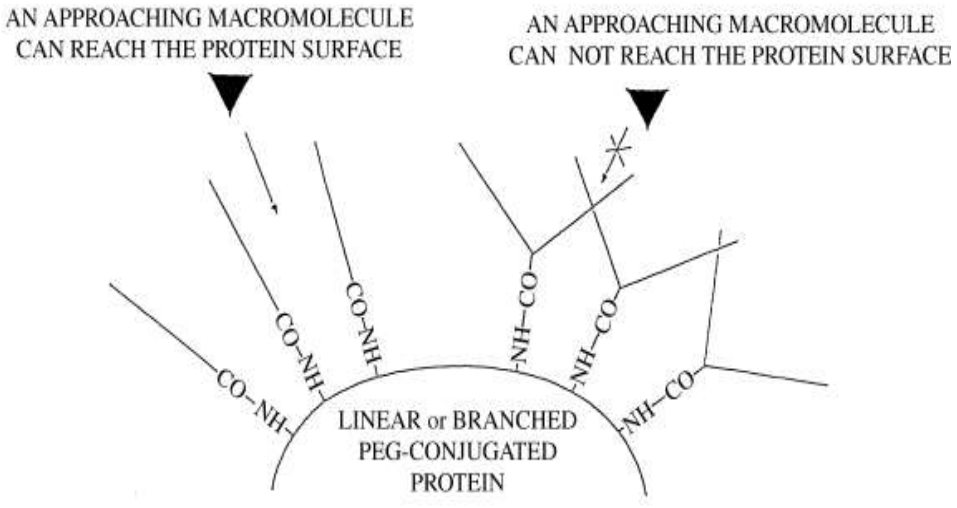

Figure 2.4. Linear and Branched PEG-conjugated protein

Comb-type PEG is a new entry to PEG architecture inventory. Comb-type PEGs that are composed of multiple PEG chains grafted to methacrylate or acrylate polymer backbone have demonstrated to be potent alternatives to linear and multi-arm PEGs for enhancing the pharmacokinetics of protein drugs (Sayers et al. 2009). These promising PEG architectures have recently been used in conjugation with biomolecules reported only by a few publications. The comb-type structure provides an umbrella-shaped conjugate and this architecture can increase resistance to proteolytic and nuclease attacks and reduce immunogenicity because of enhanced steric effect. It has been shown that comb-type PEG, when compared with linear PEG of equivalent molecular weight, exhibits greater steric hindrance, hence enhances biostability and lowers clearance rates

of the conjugated biotherapeutics (Gunasekaran et al. 2011, Ryan et al. 2009, Ryan et al. 2011). Figure 2.5 and Figure 2.6 shows linear PEG and comb-type PEG protein conjugates. Moreover, comb-type PEG polymers can be easily synthesized by reversible addition fragmentation chain transfer (RAFT) polymerization (Moad, Rizzardo, and Thang 2009) and atom transfer radical polymerization (ATRP) techniques (De et al. 2008) that are relatively new techniques enabling synthesis of polymers with varying architectures, such as block and star copolymers, controlled molecular weights and narrow polydispersities, and also defined end-group functionalities. End-group functionality of polymers allow to crucial synthetic strategies to be applied for site-specific PEGylation (Gunasekaran et al. 2011). Because of these properties, PEGylation using comb-type polymers may play an important role in enhancing the potential of both gene and protein therapeutics (Asayama et al. 1998, Srividhya et al. 2006).

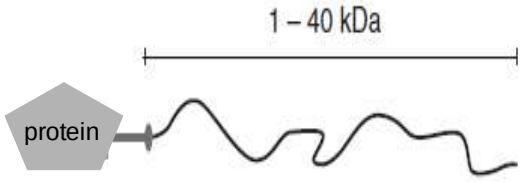

Figure 2.5. Linear-PEG conjugated protein

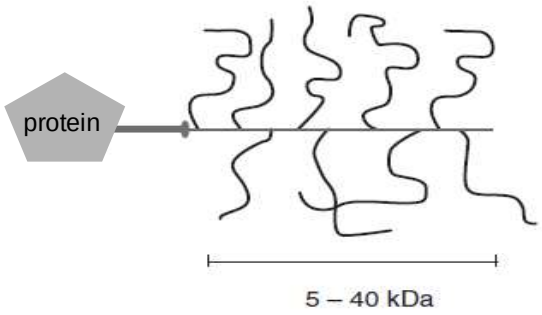

Figure 2.6. The comb-type PEG conjugated protein

2.2.1. Comb-type PEGylated Biomolecules as Potential Therapeutics

Heredia et al. (Heredia et al. 2008) synthesized a poly(polyethylene glycol methyl ether acrylate) p(PEG-A) (comb-type PEG-A) with a pyridyl disulfide end functionality via reversible addition fragmentation chain-transfer (RAFT) polymerization, to conjugate with a-thiol-modified of siRNA. The authors showed a 88% conjugation yield. Following the same conjugation method (Figure 2.7) *Gunasekaran et al.* (Gunasekaran et al. 2011) prepared siRNA comb-type PEG-A conjugates using pyridyl disulfide-functional poly(polyethylene glycol methyl ether acrylate) p(PEGA)s with two different molecular weights (low molecular weight (LMWC) and high molecular weight (HMWC)). The conjugates were shown to be cleavable as they contained reversible disulphide linkages. Moreover, when compared to thiol-modified and unmodified siRNA, siRNA-p(PEG-A) conjugates sharply increased nuclease resistance and serum stability. The unmodified siRNA and thiol-modified siRNA were completely degraded within 10 and 48 h in 80% active fetal bovine serum (FBS), respectively. However, LMWC and HMWC degraded much slower; the HMWC degradation was only 16% at 72 h. A previous study (Kim et al. 2006) indicated that in 50% fetal bovine serum, the siRNA-linear PEG (M_n= 5 000) conjugates had higher stability than non-modified siRNA. The unmodified siRNA showed almost complete degradation after 8 h incubation in the serum-containing medium. In contrast, the siRNA–PEG conjugate could last up to 16 h without a significant loss of integrity in the same condition. PEG-based polymers with high stable siRNA conjugates can be contributed to the steric hindrance effect of the polymer by preventing the interactions between the nucleases and siRNA. Even though not directly comparable, umbrella-like shape of p(PEGA) attribute to provide greater protection of siRNA. The higher serum stability of siRNA-p(PEG-A) conjugates relative to siRNA-linear PEG conjugates can be attributed to the umbrella-like shape of p(PEG-A), potentially providing greater protection to siRNA.

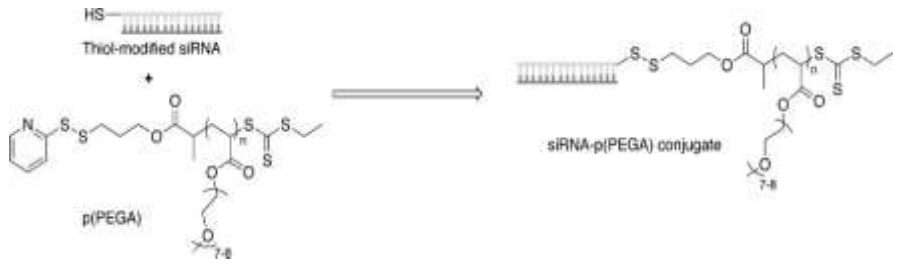

Figure 2.7. Conjugation of thiol-modified siRNA with RAFT-synthesized pyridyldisulfide functionalized p(PEGA) (Gunasekaran et al. 2011)

Gao et al. (Gao et al. 2009) reported comb-type poly(oligo(ethylene glycol) methyl ether methacrylate) [p(OEGMA)] (Number average moleculer weight: 120 kDA, PDI: 1.4) conjugate with myoglobin protein. After administration of these conjugates to mice, distribution phase of the myoglobin-p(OEGMA) conjugate [hydrodynamic radius (Rh): 13 nm] showed a 41-fold increase in blood exposure, also final elimination phase was prolonged until 18 hours compared to unmodified myoglobin (Rh:1.7 nm). This exciting results indicated that comb-type PEG stably and dramatically prolongs the half-life of a protein after intravenous administration *in vivo*.

Similarly, *Gao et al.* (Gao et al. 2010) reported the conjugates of poly(oligoethylene glycol) methyl ether methacrylate p(OEGMA) with Green Fluorescent Protein (GFP). The authors showed that the blood exposure of the conjugate (hydrodynamic radius (Rh): 21 nm) was increased 15-fold when compared to unmodified protein (Rh: 3.0 nm) after intravenous administration to mice. Besides, compared to the unmodified protein, the conjugate showed a 50-fold increase in tumor accumulation, 24 h after intravenous administration to tumor-bearing mice. These results showed that comb-type PEG conjugation improves significantly *in vivo* pharmacological profile of a protein.

Ryan et al. (Ryan et al. 2009) conjugated Salmon calcitonin (sCT) via its N-terminal cysteine to a comb-typePEG, sCT-Poly$PEG_{6,5K}$ (Number average molecular weight: 6.5 kDA) and linear PEG, sCT-PolyPEG_{5K} (Number average molecular weight: 5 kDa) to investigate benefits of site-specific attachment to a comb-shaped polymer. Intracellular cyclic adenosine monophosphate (cAMP) was used for measuring the bioactivity of conjugates in human breast cancer (T47D) cells *in vitro*. Both analysis by RP-HPLC and cAMP activities showed that after 30 min of incubation in rat liver homogenate, sCT was totally degraded and sCT-PEG_{5K} retains only 7% of its

bioactivity after 30 min. In comparison, sCT-PolyPEG®$_{6.5K}$ showed a much slower rate of liver metabolism and more resistance to liver enzymes. According to biological activities of sCT-PolyPEG®$_{6.5K}$ and sCT-PEG$_{5K}$ conjugates *in vitro,* compared with non-modified sCT, sCT-PolyPEG$_{6,5K}$ and sCT-PolyPEG$_{5K}$ maintained 85% and 92% of the bioactivity. Using lactate dehydrogenase (LDH) assay, cytotoxicity of conjugates was assessed and this assay indicated that both polymers were non-toxic. While both sCT-PolyPEG®$_{6.5K}$ and sCT-PEG$_{5K}$ were resistant to metabolism by serine proteases, homogenates and serum, PolyPEG®$_{6.5K}$ showed higher resistance than other. Besides, non-modified form of the protein was degraded and sCT-PEG$_{5K}$ showed far less bioactivity when compared to PolyPEG®$_{6.5K}$. While both conjugates reduced serum calcium levels, PolyPEG®$_{6.5K}$ increased the $T_{1/2}$ and AUC of serum sCT with respect to sCT-PEG$_{5K}$ and sCT. In order to assess concentration and hypocalcaemic response of sCT in the blood plasma following i.v. administration to rats, pharmacokinetics and *in vivo* biological efficacy of sCT-PEG$_{5K}$ and sCT-PolyPEG®$_{6.5K}$ were evaulated. Both types of conjugates and sCT had similar hypocalcaemic effects and they reached a maximum at 240 min, but sCT-PolyPEG®$_{6.5K}$ reached a maximum at 120 min compared sCT and sCT-PEG$_{5K}$. Therefore, PolyPEG® improved pharmacokinetic profiles of sCT.

CHAPTER 3

MATERIALS AND METHODS

3.1. Materials

Poly(ethylene glycol) methyl ether acrylate (PEG-A) (number-average molecular weight M_n = 480 g/mol) was purchased from Aldrich. Poly(polyethylene glycol) methyl ether acrylate p(PEG-A) (M_n= 10 700 g/mol, *PDI*= 1,21 p(PEG-A) 10K and M_n= 20 200g/mol, *PDI*=1,26 p(PEG-A) 20K) was synthesized according to the procedure reported elsewehere (Heredia et al. 2008). A brief description of the polymer synthesis is given in the section below. Thiol PEG, mPEG-SH (M_n= 10 000 g/mol, *PDI*=<1.08 PEG 10K) was purchased from Nanocs. O-[2-(3-Mercaptopropionylamino)ethyl]-O′-methylpolyethylene glycol 20′000 (M_n= 20 000 g/mol, *PDI*=<1.08 PEG 20K) was bought from Fluka. 3-(Benzylsulfanylthiocarbonylsulfanyl)-propionic acid (BSPA) that was synthesized by Assoc. Prof. Dr. V. Bulmuş at University of New South Wales, Sydney according to a procedure reported elsewhere (Boyer, Bulmus, and Davis 2009) was used as received. The initiator, 2,2′- Azoisobutyronitrile (AIBN) was crystallized twice from methanol prior to use.

All other chemicals were used as received. Diethyl ether, acetonitrile, N,N-dimethylformamide, triethylamine (TEA), hexylamine (HEA), tris(2-carboxyethyl)phosphine hydrochloride (TCEP), deuterated water (D2O), deuterated chloroform (CDCl3), N'N-dimethylacetamide (DMAc, HPCL grade ≥ %99.9) were purchased from Sigma. Oregon Green® 488 Maleimide and Propidium Iodide were bought from Invitrogen. Dialysis membrane (MWCO= 3 500) was purchased from Spectrum® Laboratories.

RPMI-1640 (Roswell Park Memorial Institute 1640 Medium) medium (L-Glutamine, HEPES 25mM) and FBS (Foetal Bovine Serum) were obtained from Gibco. PBS (phosphate buffer saline solution, pH 7.1, 0.1 mM) was prepared using relevant mono and dibasic salts and NaCl. Thiazolyl Blue Tetrazolium Blue (MTT) reagent was

bought from Sigma- Aldrich. LysoTracker® Red DND-99 and DAPI dilactate (organel dyes) were purchased from Invitrogen.

Human lung adenocarcinoma epithelial (A549) cells were kindly donated by Assoc. Prof. Dr. Y. Baran and Biotechnology and Bioengineering Research and Application Center, İzmir Institute of Technology, İzmir, Turkey.

3.2. Methods

3.2.1. Synthesis of Poly(ethylene glycol) Methyl Ether Acrylate p(PEG-A)

Poly(polyethylene glycol methyl ether acrylate) p(PEG-A) was synthesized according to the literature (Heredia et al. 2008). The polymerization reaction is shown in Figure 3.1. Briefly, BSPA, PEG-A and AIBN were dissolved in acetonitrile. The solution was purged with nitrogen for 15 min at 0°C and then immersed in an oil-bath at 65°C. At the end of polymerization time, the solution was partially evaporated under vacuum. The polymer was then precipitated in cold diethyl ether to remove any traces of monomers and unreacted RAFT agent. The precipitation process was then repeated ten times. The precipitated polymer was collected and dried under vacuum.

For the synthesis of p(PEG-A) having M_n and *PDI* of 10 700 g/mol and 1.21, respectively, BSPA (6 mg, 0.0261 mmol), PEG-A (0.72 g, 0.0015 mol) and AIBN (0.75 mg, 0.0051 mmol) were mixed in 1.5 ml of acetonitrile to yield a mole ratio of $[BSPA]_0/[PEG\text{-}A]_0/[AIBN]_0$= 1/30/0.2. The polymerization time was 4 h. For the synthesis of p(PEG-A) having M_n and *PDI* of 20 200g/mol and 1.26, respectively, BSPA (6 mg, 0.0261 mmol), PEG-A (0.72 g, 0.0015 mol) and AIBN (0.75 mg, 0.0051 mmol) were mixed in 1.5 ml acetonitrile to yield a mol ratio of $[BSPA]_0/[PEG\text{-}A]_0/[AIBN]_0$ = 1/60/0.2. The polymerization time was 6 h.

The polymers were characterized by gel permeation chromatography (GPC) using DMAc as mobile phase and ^{1}H-NMR spectroscopy using D_2O as a solvent. Monomer conversions were determined by ^{1}H-NMR spectroscopy of the polymerization mixture (before purification of the polymer) by comparing the area of the vinylic protons ($\delta \sim 5.4\text{-}6.3$ ppm, (3H)) to the area of the PEG characteristic protons ($\delta \sim 4{,}3$ ppm, (2H)).

The number average molecular weight (M_n) was estimated by ^{1}H-NMR of the purified polymer using 3.1:

M_n= [(I^{CH} at 4.0 ppm / (I^{phenyl})/5) × MW_{PEG-A}] + MW_{RAFT}, with I^{CH} at 4.0 ppm, I^{phenyl}, MW_{PEG-A} and MW_{RAFT} (3.1) correspond to the intensity of signal at 4.0 ppm and intensity of signal at 7.2-7.4 ppm, molecular weight of PEG-A monomer and molecular weight of RAFT agent, respectively.

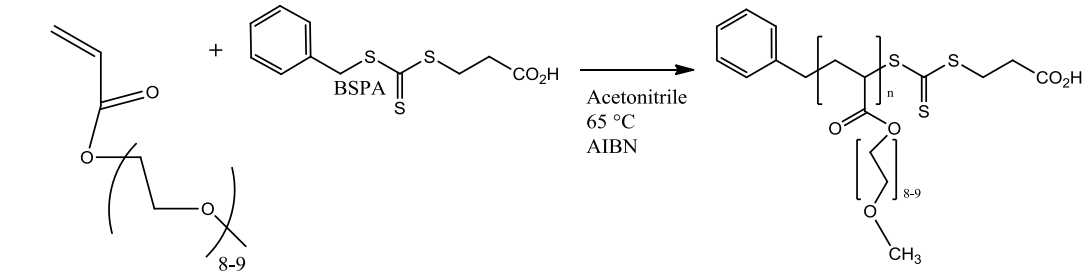

Poly(ethylene glycol) methyl ether acrylate (PEG-A)

Poly(polyethylene glycol) methyl ether acrylate p(PEG-A)

Figure 3.1. Synthesis of polyethylene glycol ethyl methyl ether acrylate p(PEG-A) (M_n=10 700 and 20 200g/mol)

3.2.2. End-group Modification of p(PEG-A) via Aminolysis

The RAFT end-group of the polymers was aminolyzed to yield thiol-ended polymers as shown in Figure 3.2. Briefly, for each polymer, p(PEG-A) (0,006 M), HEA (0,06 M) and TEA (0,06 M) were dissolved in acetonitrile. The solutions were purged for 15 min with nitrogen to remove oxygen and then left to be shaken at room temperature for 24 h. After reaction time, acetonitrile was removed by vacuum evaporation. The polymers were then precipitated in cold diethyl ether (10 times) and dried under vacuum. The product was then characterized by ^{1}H-NMR spectroscopy using D_2O as a solvent. Also RAFT end-group modification conditions for PEG-A (M_n= 10 700 and 20 200g/mol) was as follows: $[PEG\text{-}A]_0/[HEA]_0/[TEA]_0$ = 1/10/10. The reaction conditions for both polymers (M_n= 10 700 and 20 200g/mol) are detailed in Table 3.1.

Table 3.1. The aminolysis conditions.

Polymers	Polymer (g) (mole)	HEA (g) (mole)	TEA (g) (mole)	Solvent Amount (ml)
p(PEG-A) M_n=10 700	0.15, 1.4×10^{-5}	0.14, 1.4×10^{-4}	0.14, 1.4×10^{-4}	2,1
p(PEG-A) M_n=20 200	0.15, $0{,}74\times 10^{-5}$	7,3, $0{,}74\times 10^{-4}$	7,3, $0{,}74\times 10^{-4}$	1,1

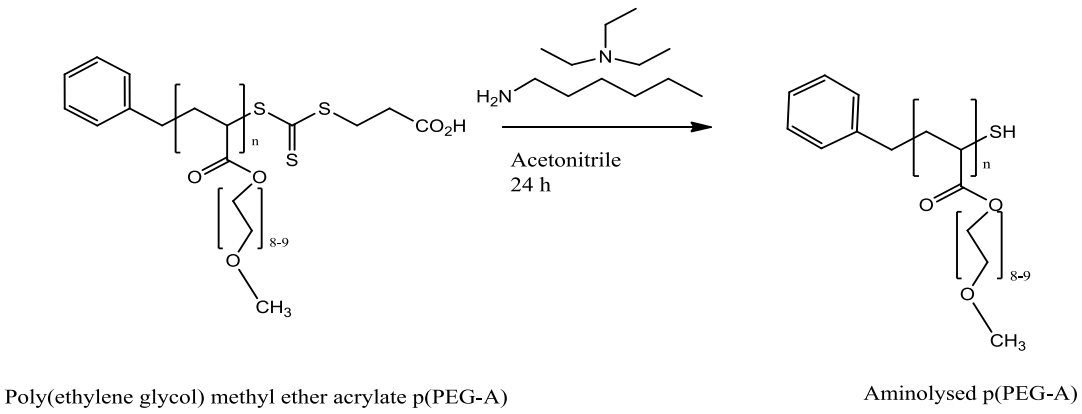

Poly(ethylene glycol) methyl ether acrylate p(PEG-A)

Aminolysed p(PEG-A)

Figure 3.2. Chemical modification of PEG-A (M_n= 10 700; 20 200g/mol) end-group by aminolysis

3.2.2.1. Preparation of Ethylene Glycol Ended-Polymers for Cytotoxicity Experiments

Since both the RAFT synthesized comb-type polymers and purchased linear polymers possessed a reactive thiol end-group, the monomeric unit (ethylene glycol) was used to cap the thiol-end groups before cytotoxicity experiments. The reaction is shown in Figure 3.3. The thiol-terminated polymers were reacted with poly(ethylene glycol) methly ether acrylate monomer (PEG-A) in the presence of tris(2-carboxyethyl)phosphine hydrochloride (TCEP). For each polymer (0.11 g, 0,01 M), TCEP (0,2 M) and monomer (0.2 M) were dissolved in phosphate buffer solution at pH

7.1. The solution was purged with nitrogen for 30 min and left to be stirred. After 20 h, fresh TCEP (0,2 M) was added to the reaction medium under nitrogen. After another 4 h, the polymer was purified by dialysis against water using a membrane with a MW cut off 3500 Da for 4 days and finally freeze-dried. The final product was characterized by ^{1}H NMR spectroscopy using D_2O as a solvent.

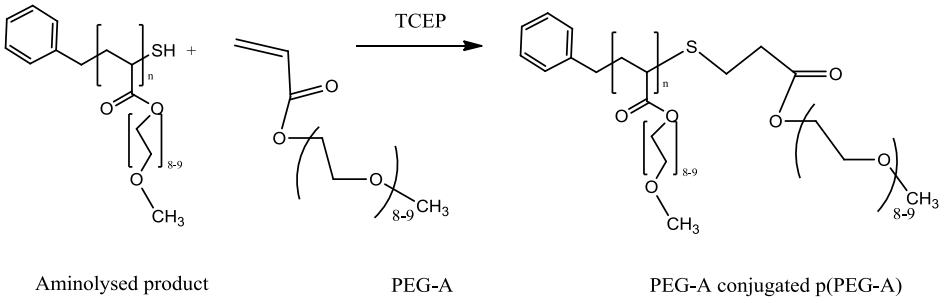

Figure 3.3. Preparation of ethylene glycol ended comb-type polymers

3.2.2.2. Preparation of Fluorescent Labelled Polymers for Cell Uptake and Intracellular Distribution Experiments

p(PEG-A)s and PEGs were labeled with Oregon Green maleimide 488. Firstly Oregon Green maleimide 488 (5 mg, 1.08×10^{-5} mol) was dissolved in 108 µl DMF to have a stock dye solution of 100 mM. The dye solution (24.5µl, 0,25 $\times10^{-5}$ mol) was added to polymer solution in phosphate buffer solution (0.1M, 500 µl, 0.05×10^{-5} mol). TCEP (0.02 M, 2.8 mg, 1 $\times10^{-5}$ mol) dissolved in phosphate buffer solution at pH 7.1 was also added to the reaction mixture. The reaction solution was purged with nitrogen for 10 min and gently shaken overnight at 37°C. The product was then dialyzed against water using a membrane with a MW cut off of 3500 Da for 4 days and finally freze-dried. The labelling of polymers was verified using fluorescence spectrometer (Varian Cary Eclipse Fluorescence Spectrometer) and the degree of labelling was determined via UV-vis spectroscopy (Perkin Elmer Lambda 25 UV/Vis Spectrometer).

3.2.3. Physicochemical Characterization of Polymers

3.2.3.1. NMR and GPC Analyses

^{1}H Nuclear Magnetic Resonance (NMR) spectroscopy was used to determine monomer conversions, molecular weigth of polymers and end-group modifications. All ^{1}H-NMR spectra were taken using Varian VNMRJ 400 spectrometer at Izmir Institute of Technology or Varian Mercury Plus 400 Actively Shielded NMR System at EBILTEM NMR Laboratory, Ege University, Izmir.

Gel permeation chromotography (GPC) was used to determine the molecular weight and molecular weight distribution of the polymers. N,N-Dimethylacetamide (DMAc) containing 0,05 % w/v LiBr was used as a mobile phase in GPC analyses. GPC analyses were performed using a Shimadzu modular system comprising an SIL-10AD auto injector, PSS Gram 30 A° and 100 A° (10 μM, 8x300 mm) guard column and an RID-10A refractive-index detector. Calibration was performed with poly(methyl methacrylate) standards with low polydispersity with molecular weight ranging from 410 to 67 000 g/mol.

3.2.3.2. DLS Analysis

Dynamic light scattering (DLS) was used to measure the hydrodynamic radius (Rh) of linear PEG and comb-type p(PEG-A) in 5 different media: water, phosphate buffer saline (PBS) at pH 7.4, PBS containing 10% fetal bovine serum (FBS), cell culture medium RPMI-1640, and RPMI-1640 containing 10% FBS. 0.05 mM polymer solutions were prepared in 5 different media and DLS analyses were performed for each polymer solution. For measurements, the polymer solutions, (40 μL) was taken into ZEN0040 Microcuvettes and placed into a Zetasizer Nano ZS (Malvern, UK) (measurement range 0.3nm – 10.0 microns; light source He-Ne laser 633nm Max 5mW; Power 100 VA). The measurements were repeated 9 times. Measurement duration was adjusted automatically. The refractive index of PEG and p(PEG-A) was 1.46 and 1.48, respectively. The properties of dispersant that were used for measurements are listed in Table 3.2.

Table 3.2. The properties of dispersants used for DLS measurements

	Water	PBS	PBS containing 10% fetal bovine serum (FBS),	RPMI-1640	RPMI-1640 containing 10% FBS
Refractive index	1.33 (Schiebener et al. 1990)	1.33	1.33	1.33 (Yunus and Rahman 1988)	1.33
Viscosity(Bihari et al. 2008)	0.88	0.88	0.88	0.1	0.1

3.2.3.3. AFM Analysis

Atomic Force Microscope (AFM) images of polymers were taken using an AFM (Solver Pro 7 from NT-MDT, NanoMagnetics Instruments, Ankara) in the tapping mode that gave topographical and phase contrast images. 0.05 mM polymer concentrations in distilled water was placed on silicon substrate, and the samples were dried under atmospheric conditions at room temperature.

3.2.4. Cell Culture Experiments

A549 cells (Human lung adenocarcinoma epithelial cell line) were grown in RPMI 1640 medium (RPMI) supplemented with 10% fetal bovine serum (FBS), 1% Penicillin–Streptomycin as antibiotic in flasks. The cells were maintained between 80-90% confluency in a dark cell incubator having 5% carbondioxide (CO_2) and 95% humidity at 37ºC (Masters 2000).

3.2.4.1. MTT Cell Viability Assay

The effect of linear PEG and comb-type p(PEG-A)s on the viability of cells was determined by a 3-(4,5-dimethylthiazol-2-yl)-2,5-diphenyl tetrazolium bromide (MTT) Cell Viability assay (Berg, Hansen, and Nielsen 2009). The assay measures the ability of living cells to reduce a tetrazolium dye, MTT, to its insoluble formazan giving a purple color.

Briefly, A549 cells were seeded a day prior to sample exposure at 5000 cells/well (96 well plate) in culture medium containing 10% FBS/RPMI. Polymer sample stocks were prepared in PBS solution, followed by dilution in culture medium. The final concentration of PBS exposed to the cells was no more than 0.5% (v/v) for the duration of the experiment. Varying concentrations (25, 50, 100 and 200 μM) of polymers were added to the cells (0.5–4.6 mg/ml) and then incubated at 37 °C/5% CO_2 for 24 and 72h. Following the 24 and 72 h incubation, the viability of the cell was determined by MTT Cell Viability assay. 3-(4,5-dimethylthiazol-2-yl)-2,5-diphenyl tetrazolium bromide (MTT) dye was added to wells according to manufacturer' protocol. The plates were incubated at 37 °C for 3-4 h and metabolic activity was detected by spectrophotometric analysis. The fluorescence was then recorded at 544Ex/590Em nm (Varioskan Flash, Thermo Electron Corparation, Finland). The cell viability (%) was calculated relative to the positive control (cells not treated with polymers) according to 3.2. The statistical significance of the results was detected using Analysis of variance (ANOVA) Minitab 15 (Minitab Inc., State College, PA, USA).

$$\text{Cell Viability}(\%) = \frac{V_{\text{sample}}}{V_{\text{positive}}} \times 100 \qquad (3.2)$$

Where,

V sample = viable cell absorbance value in the sample well

V positive = viable cell absorbance value in the positive control (non treated well)

3.2.4.2. Flow Cytometry Analyses

3.2.4.2.1. Cell Uptake

Uptake of linear PEG and comb-type p(PEG-A) by A549 cells was investigated using flow cytometry (BD FACSCanto™ A Flow Cytometer, BD Biosciences, San Jose, USA). Firstly, all Oregon Green labelled polymers (linear PEG and comb-type p(PEG-A)) were prepeared for stock solution in PBS (0,002M) including 50 μM polymer concentrations. A549 cells (1ml, $6x10^4$ per well) were seeded in 12 well plates and incubated in a humidified atmosphere (37ºC and 4 ºC, 5% CO2) for 24 hours. For 12,5 μM and 25 μM polymer concentrations, stock solution was diluted. After 24 hours; Oregon Green labelled polymers were added wells (20 μl) including 12,5 μM polymer concentration. Thus final concentration of wells were 0.04 mM. The cells and polymers were incubated for 1, 3, 6 h at either 4 or 37 °C. Each treatment was performed in triplicate. For 25 μM and 50 μM polymer concentrations, respective volumes (20 μl) from polymer stock solutions (0,002M) were added to the wells. The cells and polymers were incubated for 1 hour at either 37 °C. At the end of incubation, medium was collected and the wells were washed with cold PBS. The cells were harvested by trypsinization and after washing, collected cells were centrifuged for 5 minutes. Supernatant was removed and pellet was re-suspended with 200 μl cold PBS. Data from 10,000 events were collected per sample and analysed by using FacsDiva V.5.0.3 software. To detect Oregon green solid state 488 laser used for excitation and 530/30 filter configuration for Oregon green maleimide were used for detection.

3.2.4.2.2. Cell Cycle

The effect of linear PEG and comb-type p(PEG-A) on the cycle of A549 cells was also investigated using flow cytometry. Firstly, all polymers were prepeared for stock solution in PBS (1 mM). A549 cells (1ml, $5x10^5$ per well) were seeded in 6 well plates and incubated in a humidified atmosphere (37ºC, 5% CO2) for 24 and 72 hours. 200 μl of each polymer from stock solution was added to wells to yield a final well concentration were 0,16 mM. Each treatment was performed in triplicate. Cells without any treatment were considered as negative control. Cells and polymers were incubated

for 24 and 72 hours. In addition to this, A549 cells (1ml, $5x10^5$ per well) were seeded in 6 well plates and incubated in a humidified atmosphere (37ºC, 5% CO_2) and 4 ºC to detect of only cells cell cycle at this temperature. After the incubation time, medium was removed and the wells were washed with cold PBS twice. The cells were harvested by trypsinization and washing with cold PBS twice. Collected cells were centrifuged and supernatant was removed. The pellet was dissolved with PBS (5 ml) and centrifuged. The supernatant was removed and the cells were fixed in cold ethanol (4 ml) in order to fixation of cells. After fixation, cells were centrifuged at 4°C for 10 minutes at 1200 rpm. Supernatant was removed and pellet was dissolved in PBS (4 ml). The cells were centrifuged again at 4°C for 10 minutes at 1200 rpm and pellet was dissolved in 0.1 % Triton X-100 (1 ml) including PBS solution. The cells were then treated with RNase A (100 µl, 200 µg/ml) and incubated for 30 minutes at 37 ◦C. At the end of incubation, Diploid nuclei were then stained with Propidium iodide (100 µl, 1 mg/ml) and incubated for 15 minutes at room temperature. Analysis was then performed using a FACSCanto A (BD Biosciences, San Jose, USA). To detect Propidium iodide, green solid state 488 laser was used for excitation, 556/LP and 585/40 filter configurations for PI were used for detection. The data on cellular DNA content and cell cycle were analyzed by ModFit LT V.3.0 software (Yılmazel Çakmak 2011).

3.2.4.2.3. Intracellular Distribution

DAPI is a widely-used nuclear counterstain that stains nuclei specifically. For A549 cell lines, DAPI has been shown to stain efficiently the nuclei of A549 cells (Bhawe et al. 2004). Firstly, stock solutions of Oregon Green labelled polymers (linear PEG and comb-type p(PEG-A)) were prepeared in PBS (0,002 M). A549 cells (1ml, $5x10^5$ per well) were grown on coverslips inside 6 well plates with culture medium containing 10% FBS/RPMI and incubated in a humidified atmosphere (37ºC, 5% CO_2) for 24 hours. After incubation, Oregon Green labelled polymers were added to wells (20 µl). Thus final concentration of polymers in wells were 0.04 mM. The cells and polymers were incubated for 1 hour at 37 °C. After incubation period, the medium containing polymers was removed by washing with PBS three times. Subsequently, cells were fixed using fresh 2% paraformaldehyde for 20 minutes. After washing three times with PBS, cells were permeabilized with 0.1 % Triton X-100 (1 ml) including

PBS solution. Next, cells were blocked with 3% BSA in 0.1 % Triton X-100 (0,5 ml) inPBS solution for 30 minutes. Cells were then treated with 300 nM (300 µl) DAPI in PBS for 5 min at dark according to the manufacturer protocol. The wells were washed thoroughly with PBS two times for 10 minutes in dark. Excess buffer was drained from coverslip and mounted. The fluorescent images were visualized by fluorescence microscope (Olympus ix71, USA).

LysoTracker® Red DND-99 was used to stain lysosomes of A549 cells according to manufacturer protocol. Briefly, A549 cells (1ml, $5x10^5$ per well) were grown on coverslips inside 6 well plates with culture medium containing 10% FBS/RPMI and incubated in a humidified atmosphere (37ºC, 5% CO_2) for 24 hours. After incubation, Oregon Green labelled polymers (0,002 M) were added to wells (20 µl) and incubated for 1 hour at 37 °C. The medium containing polymers was removed by washing with PBS three times. Before imaging, cells were incubated with 100 nM LysoTracker Red DND-99 (Invitrogen) in culture medium containing 10% FBS/RPMI for 1 hour in a humidified atmosphere (37ºC, 5% CO_2). The wells were then washed three times with PBS and imaged using a fluorescence microscope. Excitation wavelengths were 358 nm, 496 nm, 577 nm and emission wavelengths were 461 nm, 524 nm, 590 nm for DAPI, Oregon green, and LysoTracker Red DND-99 respectively.

CHAPTER 4

RESULTS AND DISCUSSIONS

4.1. Physicochemical Characterization of Poly(ethylene glycol) Methyl Ether Acrylate p(PEG-A) and Linear PEG

4.1.1. Chemical Structure and Molecular Weight Characterization

Poly(polyethylene glycol) methyl ether acrylate p(PEG-A) with different molecular weights were synthesized by reversible addition fragmentation chain transfer (RAFT) polymerization according to the method reported in a previous publication (Heredia et al. 2008). The RAFT polymerization mechanism provides control over the molecular weight and molecular weight distribution (polydispersity index, *PDI*) of polymers (Rogošić, Mencer, and Gomzi 1996). The number average molecular weight (M_n) of the polymers synthesized by RAFT-controlled mechanism can theoretically be calculated according to 4.1. In this equation, the monomer conversion was determined by ^{1}H-NMR analyses of the polymerization mixtures as described in previous publications and given in Appendix A (A.1 and A.2) (Boyer et al. 2009, Boyer, Bulmus, and Davis 2009). The actual M_n of the synthesized polymers was determined by both ^{1}H-NMR and gel permeation chromatography (GPC) analyses of purified polymers Appendix A (A.3 and A.4). A measure of molecular weight distribution, polydispersity index (*PDI*), was also determined by GPC. The polymerization conditions and the properties of the resultant polymers are given in Table 4.1. The number-average molecular weight (M_n) was calculated from the ^{1}H-NMR spectra of the polymers by taking the integral ratio of the characteristic peaks of the RAFT agent end-group (7.4 and 7.2 ppm) to the characteristic peak of methylene of poly(PEG-A) (4.15 ppm) (Figure 4.1 and 4.2). These experimental M_n values obtained by NMR were in good agreement with the theoretical M_n values obtained from 4.1. Moreover, the *PDI* values that were determined by GPC showed narrow distribution of polymer chains. Thus, the low *PDI* values and the good agreement of the theoretical and experimental M_n values showed that the polymerization of PEG-A was controlled by the RAFT polymerization.

Theoretical molecular weight (M_n) = (conversion (%) × $[M]_0/[RAFT]_0$ × $MW_{(monomer)}$) + MW_{RAFT}. (4.1)

Where $[M]_0$ is the initial monomer concentration, $[RAFT]_0$ is the initial concentration of the RAFT agent, $MW_{(monomer)}$ is the molecular weight of the monomer, MW_{RAFT} is the molecular weight of the RAFT agent (Moad, Rizzardo, and Thang 2005, Lowe and McCormick 2007).

Table 4.1. RAFT polymerization conditions and the properties of p(PEG-A) 10 and 20K obtained from RAFT polymerizations

Polymer Code	$[BSPA]_0/[PEG\text{-}A]_0/[AIBN]_0$[a]	Time (hours)	Conversions[b] (mol %)	M_n[c] (g/mol)	M_n[d] (g/mol)	PDI[e]	$M_{n,\,theo}$[f] (g/mol)
p(PEG-A) 10K	1/30/0.2	4	60	10 700	9 314	1,21	8912
p(PEG-A) 20K	1/60/0.2	6	78	20 200	17 978	1,26	22 736

[a] The molar ratio of monomer, RAFT agent and initiator. [b] The monomer conversion and [c] the number average molecular weight determined by ^{1}H-NMR. [d] the number average molecular weight determined by GPC. [e] Polydispersity index determined by GPC. [f] The theoretical moleculer weight calculated by $M_{n,\,theo}$ = (conversion (%) × [M]/[RAFT] × $MW_{(monomer)}$) + MW_{RAFT}.

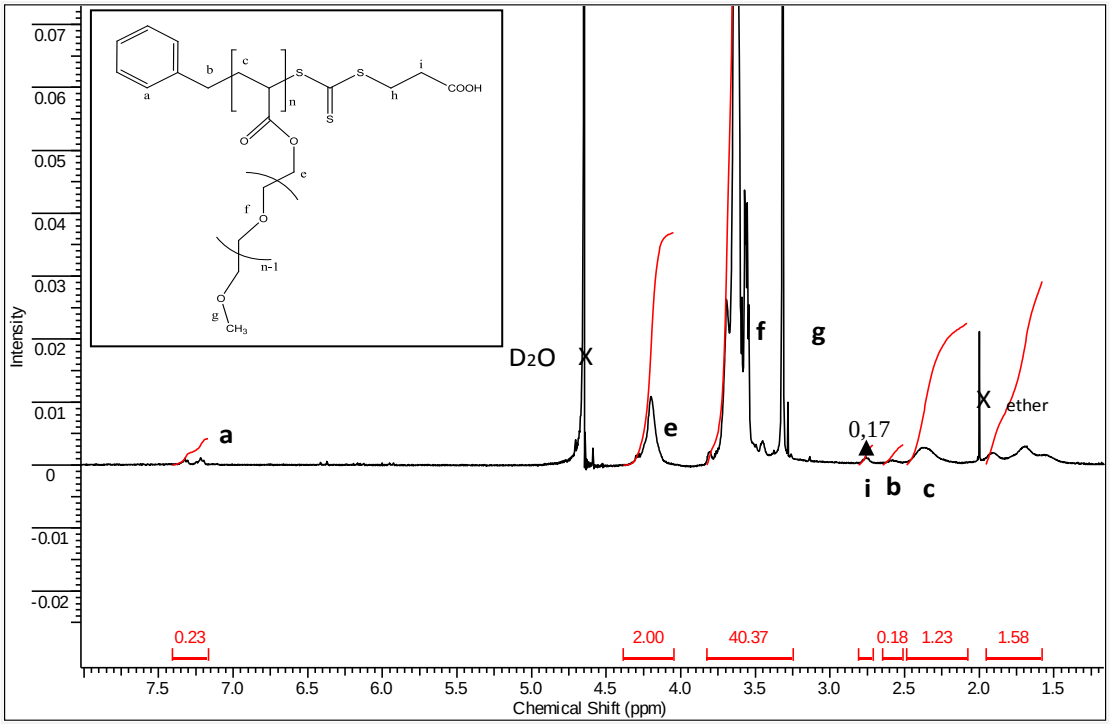

Figure 4.1. ^{1}H-NMR spectrum of purified p(PEG-A) 10K (M_n determined by ^{1}H-NMR = 10 700 g/mol, M_n determined by GPC = 9 314 g/mol and *PDI* = 1,21)

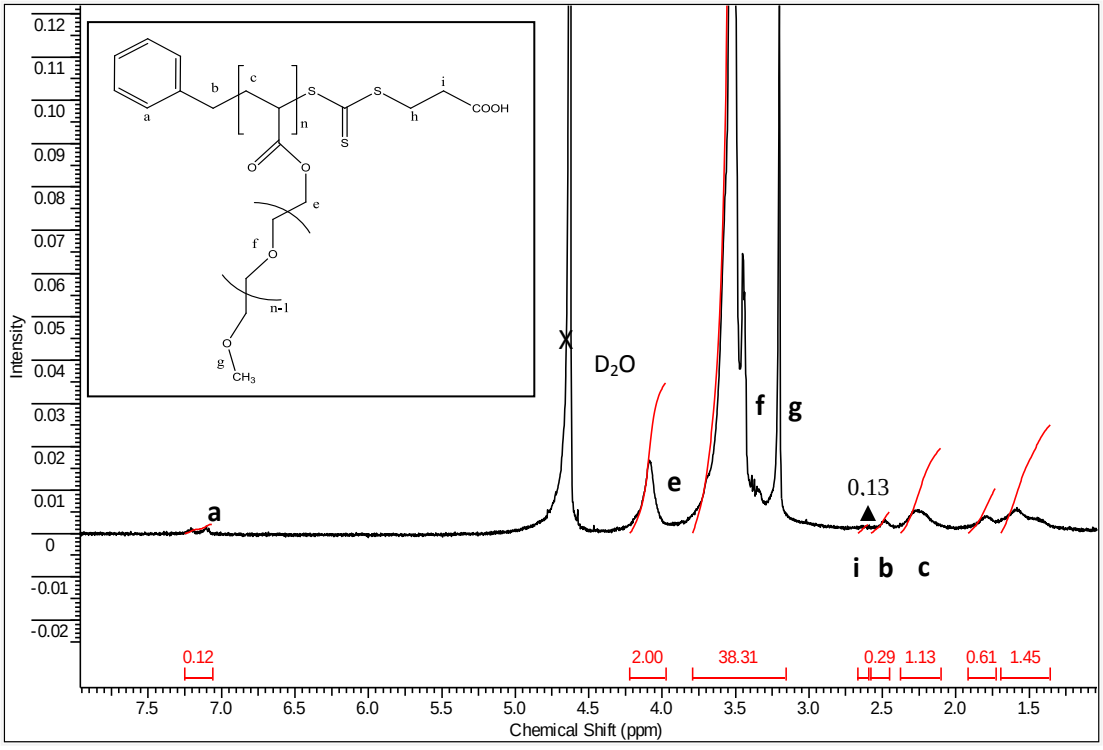

Figure 4.2. ^{1}H-NMR spectrum of purified p(PEG-A) 20K (M_n determined by ^{1}H-NMR = 20 200 g/mol, M_n determined by GPC = 17 978 g/mol and *PDI* = 1,26)

4.1.2. Dynamic Light Scattering Analysis

The molecular size is an important parameter affecting the interactions of polymers with cells (Bures et al. 2001). Hydrodynamic size measurements of comb-type (p(PEG-A) 10K and 20K) and linear (PEG 10K and 20K) PEGs were performed in five different media using dynamic light scattering (DLS). Representative DLS data and results determined from DLS data are given in Appendix A (Figure A.4) and Table 4.2, respectively.

Table 4.2. Average hydrodynamic diameters (D_h) of polymers in different media (nm) (Measurements are the average±standard error of 9 different measurements)

	H_2O	PBS	PBS (containing 10% FBS)	RPMI 1640	RPMI 1640 (containing 10% FBS)
PEG 10K	5.6±0.5	5.8±0.2	6.9±0.2	54.5±4.7	55.5±1
PEG 20K	7.8±0.3	7.8±0.2	6.9±0.3	55.9±5.8	63.5±2
p(PEG-A) 10K	4.5±0.3	5.6±1	6.4±0.4	44.4±1.8	51.5±4
p(PEG-A) 20K	5.9±0.3	5.5±0.2	6.3±0.8	58±5.3	57.5±1.6

The hydrodynamic diameter of comb-type PEG, p(PEG-A) polymers, was consistently found to be smaller than that of linear PEGs (except in RPMI 1640 medium only). This was attributted to the more compact architecture of the comb-type PEG with respect to linear PEG of the same molecular weight. The hydrophobic poly(acrylate) backbone and the hdyrophilic short PEG segments should take a more compact conformation in water when compared with the expanded, fully-solvated conformation of linear PEG backbone. In a previous study, hydrodynamic radius (R_h) of PEG 20K in water was measured as 3.45±2.5 (nm) which was quite close to the the size of linear PEG 20K obtained in this study (Linegar et al. 2010). The hydrodynamic diameters in water did not change significantly when PBS at pH 7.4 was used as a dispersant. Because of the non-charged structure of linear PEG and comb-type PEG, both polymers are not affected by the ions exist in PBS. In PBS containing 10% FBS, there was no significant change in hydrodynamic diameter of both types of PEG. PEG is known to

have non-fouling, protein-repelling character (Pacetti and Roorda 2010). Thus the presence of serum proteins is not expected to cause any change in the conformation of neither linear PEG chains nor comb-type PEG chains.

The hydrodynamic diameter (D_h) of linear PEG and comb-type PEG was also investigated in cell culture medium, RPMI 1640, or RPMI 1640 containing 10% FBS, which mimicks to some extent the physiological environment. The interactions of various components such as glucose, salts, amino acids present in RPMI 1640 or serum proteins present in RPMI 1640 containing serum with the polymers are important in mediating the uptake of macromolecules and particulates by cells (Wiogo et al. 2011). Such interactions are expected to cause conformation and hydrodynamic size changes in polymer chains, which should be detected easily via DLS measurements. Indeed, the D_h values of the polymers in RPMI 1640 containing 10% FBS and RPMI 1640 only sharply increased with respect to the D_h values in water and PBS (Table 4.2). There was no significant change in diameters obtained in RPMI 1640 containing 10% FBS and RPMI 1640 only, indicating that the increase in diameters was not caused by the interactions of serum proteins with the polymers. The components of RPMI 1640 solution, i.e. glucose, amino acids may interact with both linear and comb-type PEGs possibly through the formation of hydrogen bonds between these components and oxygen of PEG. Importantly, there was no significant difference between the D_h values of comb-type PEGs (p(PEG-A)) and those of linear PEGs in both media, suggesting that the presence of hydrophobic -C-C- backbone of comb-type PEG does not lead to hydrophobic interactions with serum proteins or other components of RPMI 1640.

4.1.3. AFM Analysis

The AFM images of linear PEG having 10 000 g/mol (PEG 10K) and comb-type PEG having 10 700 g/mol (p(PEG-A) 10K) are presented in Figure 4.3. Both samples were prepared at the same concentration (0.05 mM) and imaged using tapping mode. Interestingly, while PEG 10K sample appeared to have linear structures, p(PEG-A) 10K appeared to form spherical structures. The width of the linear structures observed with PEG 10K sample was about 37.5 nm. The diameter of spherical structures observed with p(PEG-A) 10K was about 125 nm. These results suggest that both types of polymers undergo supramolecular associations, and the interchain interactions of linear and comb-type PEG differ significantly during the drying of samples before AFM

measurements. These interchain associations may be due to hydrophobic interactions between comb-type PEG chains and H bonding between linear PEG chains. Further investigations on the AFM measurements of these samples would be required in future: The concentration of polymer samples may be further reduced or the samples can be analyzed directly in solution (eliminating drying process) to better understand the morphology differences between these polymers in aqueous solutions.

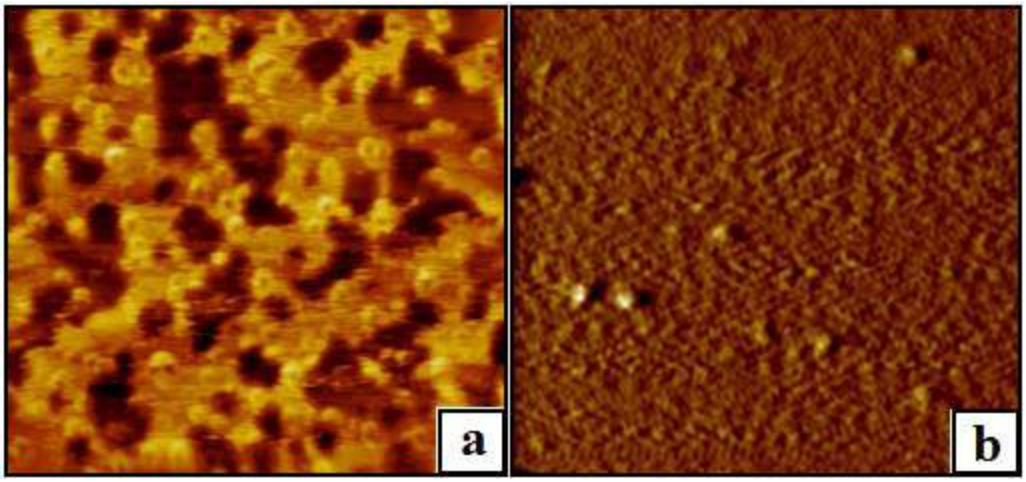

Figure 4.3. AFM images of (a) p(PEG-A) 10K (2 x 2 μm) (b) PEG10K (1 x 1 μm)

4.2. End-group Modifications of Comb-type and Linear PEG

End-group modification of polymers prepared by reversible addition–fragmentation chain transfer (RAFT) polymerization has been widely carried out in literature by conversion of thiocarbonylthio end-group of the polymers into thiol groups which are able to conjugate easily with biomolecules, fluorescent molecules or other bioactive compounds (Boyer, Bulmus, and Davis 2009). The removal of the RAFT end-group via such modifications is also useful to eliminate the possible toxicity of these groups (Pissuwan et al. 2010). A common synthetic route for the conversion of the RAFT end-group to thiol is the reduction or aminolysis of this group (Whittaker et al. 2006, Li et al. 2008, Thomas et al. 2004). In this study, aminolysis of the comb-type PEGs synthesized by RAFT polymerization was carried out to convert these groups to thiols and subsequently attach (1) an ethylene glycol group to prepare ethylene glycol capped p(PEG-A) for cytotoxicity experiments or (2) a fluorescent dye to prepare fluorescent-labelled p(PEG-A) for cell uptake and intracellular distribution experiments.

The linear PEGs that were supplied from a manufacturer have already possesed a thiol end-group. They therefore were subjected directly to conjugation with (1) ethylene glycol group to prepare ethylene glycol capped PEG for cytotoxicity and cell cycle experiments or (2) a fluorescent dye to prepare fluorescent-labelled PEG for cell uptake and intracellular distribution experiments.

4.2.1. Aminolysis of Comb-type PEG

In order to create thiol end-group on the RAFT synthesized comb-type polymers, p(PEG-A) 10K and p(PEG-A) 20K were first aminolyzed. In the relevant literature, it is well-known that the trithiocarbonate RAFT end group can be easily reduced to thiol via a primary or secondary amine (Li et al. 2008, Thomas et al. 2004). A thiol group contains a carbon-bonded sulfhydryl (–C–SH or R–SH) group which allows easy and selective conjugation of biorelated molecules or flourescence dyes having unsaturated double bonds such as acrylate or maleimide to the end-group thiol modified polymers (Li et al. 2008). The aminolysis of p(PEG-A) 10K and 20K were performed in the presence of triethylamine (TEA) and hexylamine (HEA) at a $[PEG\text{-}A]_0/[HEA]_0/[TEA]_0$ mol ratio of 1/10/10 for 24 hours. The aminolysis reaction was monitored by UV-vis spectrophotometry. The polymers after aminolysis and purification were further analyzed by ^{1}H-NMR spectroscopy to verify the removal of the RAFT end-group.

As determined from the UV-vis spectroscopy of p(PEG-A) 20K before aminolysis, the RAFT end-group of the polymer has a maximum UV absorption at ~305 nm (Figure 4.5). After aminolysis this group leaves the polymer (Figure 3.2) and thus changes its structure leading to the shift of the maximum absorption wavelenght from 305 nm to 280 nm (Boyer et al. 2009). Figure 4.5 shows representative Uv-vis spectra of p(PEG-A) 20K before and after aminolysis, clearly revealing the cleavage of the RAFT end-group from the polymer chains. The control spectrum of amines only (TEA and HEA) shows that the presence of amines in the reaction medium does not interfere with the measurement of the RAFT end-group. Similar successful aminolysis reactions were reported in the literature. For example *Boyer et al*. reported the aminolysis of poly(hydroxypropylacrylamide) (PHPMA) via a similar method. The

authors also showed the disappearance of RAFT group signal at ~305 nm after aminolysis (Boyer et al. 2009).

^{1}H-NMR spectrum of aminolyzed p(PEG-A) 10K after purification is shown in Figure 4.4. In this spectrum, one can see that there are not any characteristic signals of the RAFT end-group at 2,70-2,80 ppm. This result evidences directly the success of aminolysis reaction which results in the formation of thiol-ended p(PEG-A) ready for subsequent modifications.

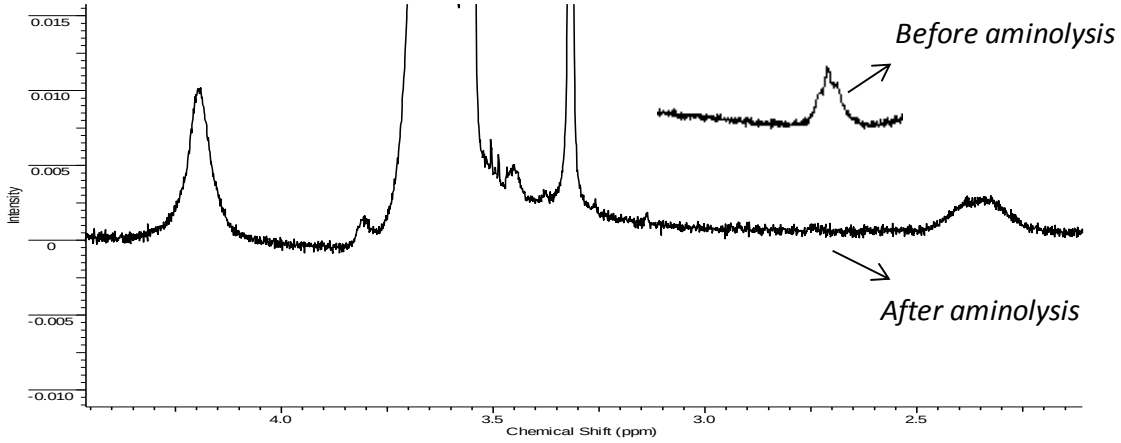

Figure 4.4 ^{1}H-NMR spectrum of aminolyzed p(PEG-A) 10K after purification

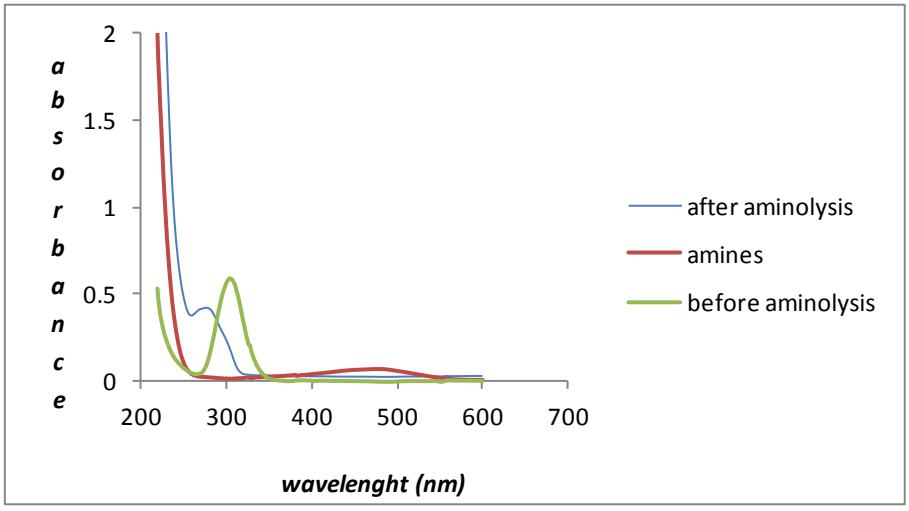

Figure 4.5. UV spectra of p(PEG-A) 20K in acetonitrile before and after aminolysis

4.2.2. Ethylene Glycol Ended-Polymers for Cytotoxicity Experiments

The thiol end-groups of both linear and comb-type PEGs used in this study are potentially toxic as they are highly reactive chemical groups. *Chang et al*. showed that the thiol chain end was a significant source of toxicity and suggested that the toxicity can be reduced dramatically by masking the free thiol (Chang et al. 2009). Thus with the help of postpolymerization treatments, toxicity can be eliminated (Pissuwan et al. 2010).

Considering this, the thiol end-groups of commercial PEGs and aminolyzed p(PEG-A)s were masked by reacting with poly(ethylene glycol) methyl ether acrylate (PEG-A) (the repeating unit of p(PEG-A)). The polymers were then purified by dialysis to remove the excess of monomer which is a highly toxic compound. ^{1}H-NMR spectroscopy of the purified polymers showed the absence of PEG-A monomer signals between 5,80 ppm and 6.4 ppm, thus indicating the complete removal of the excess monomer (Appendix B).

4.2.3. Fluorescent Dye Labelled Polymers for Cell Uptake Experiments

Fluorophores absorb light energy of a specific wavelength and re-emit light upon light excitation. This property can be used to stain biomolecules or polymers. A maleimide derivative of a fluorophore, Oregon Green® 488 Maleimide (OG) was used as an "ene" reagent that was conjugated to thiol-ended polymers through thiol-ene addition reaction. This created OG-labelled polymers with excitation/emission maxima of ~496/524 nm. Oregon Green® 488 maleimide has also been used by others as a thiol-reactive fluorophore to react with thiol groups on biomolecules to give fluorescent labelled biomolecules (Hermanson 1996).

To enable the study of cell uptake and intracellular distribution profiles of comb-type and linear PEGs, polymers were labelled with Oregon Green® 488 Maleimide. The fluorescence intensity of labelled polymers was analysed by fluorescence spectroscopy. The fluorophore number per polymer chain was also determined using Uv-vis spectroscopy at 491 nm (the extinction coefficient of OG at 491 nm = 81 000 M^{-1} cu^{-1}).

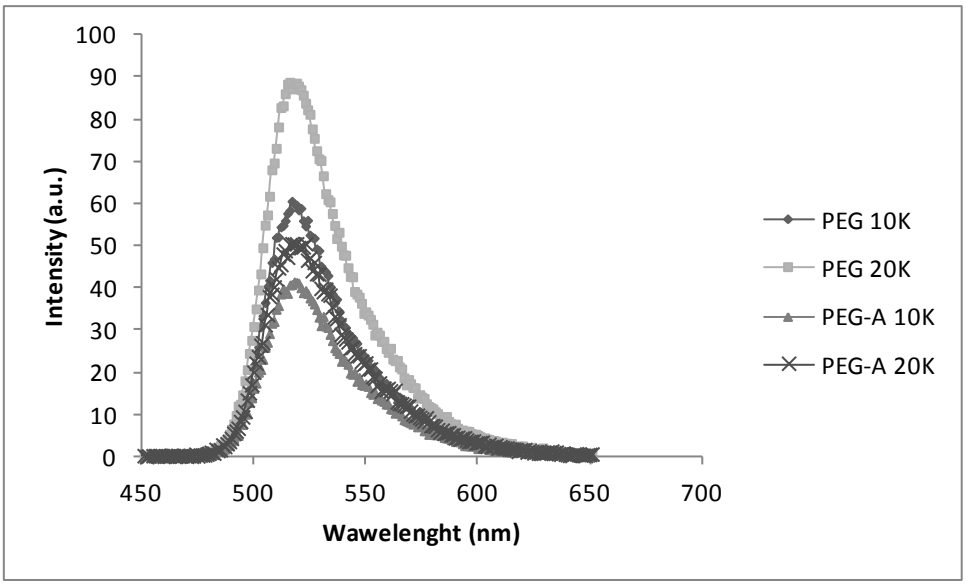

Figure 4.6. Fluorescence spectra of Oregon Green® 488 labelled polymers. The concentration of all polymers was 0,0002 M. The spectra were with polymer solutions in deonize water.

Fluorescence spectra of OG labelled polymers are shown in Figure 4.6. Considering that the equivalent concentrations for each polymer samples were used in the measurements, one can easily see that the fluorescence intensity of the linear polymers, PEG 10K and PEG 20K were higher than that of the comb-type PEGs, p(PEG-A) 10K and p(PEG-A) 20K. This might be attributed to the inefficient end-group modification of comb-type PEGs as these polymers might have less end-groups available for dye attachment compared to linear PEGs.

To quantify the labelling degree of the polymers (μg of OG/ mg of polymer), the comb-type and linear PEGs at the same molar concentrations were analysed by UV-vis Spectroscopy at 491 nm (Figure 4.7).

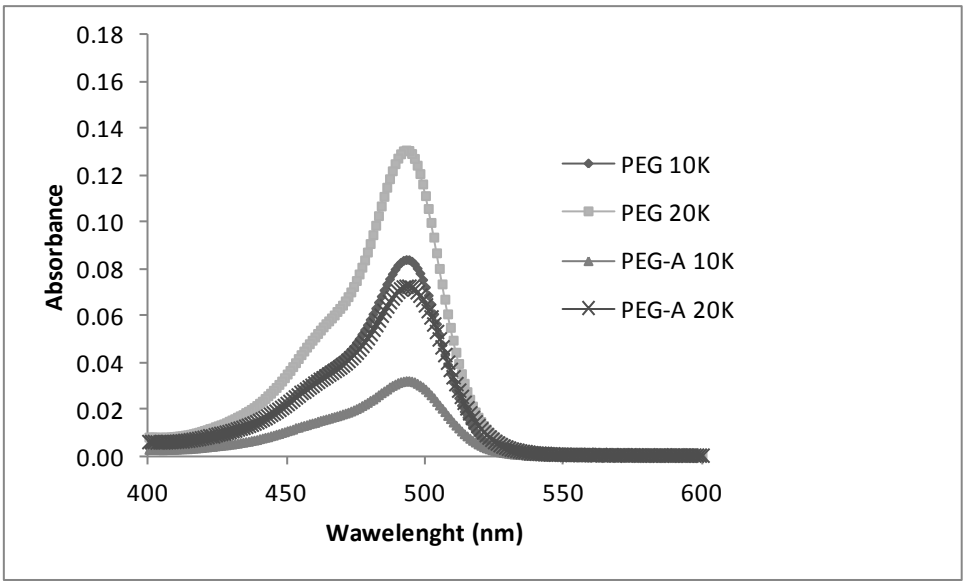

Figure 4.7. UV-vis spectra of Oregon Green® labelled polymers. The concentration of all polymers was 0,0002 M. The spectra were with polymer solutions in deonize water.

Supporting the flourescence spectroscopy results, linear PEG 20K had the highest absorbance compared to the other polymers when detected with UV-vis spectroscopy. Based on the absorbance values of polymer solutions at 491 nm and the extinction coefficient of the dye, the OG content of polymers (μg of OG/ mg of polymer) was calculated according to the 4.2 considering all the dilutions made during measurements:

$$\text{Abs}_{\text{labelled polymers}} = \varepsilon \times \text{concentration of dye x path lenght} \qquad (4.2)$$

Where Abs is the absorbance of the polymer solution at 491 nm, ε is the extinction coefficient of the dye at 491 nm (81 000 M^{-1} cu^{-1} according to the manufacturer). Using polymer molar concentrations used in the measurements, the degree of labeling (μg of OG/ mg of polymer) was calculated. The degree of labelling for each polymer is given in Table 4.3.

Table 4.3. The OG content of linear and comb-type PEGs as determined from Uv-vis spectroscopy measurements

	μg dye/ mg polymer
PEG 10K	3.04
PEG 20K	2.28
p(PEG-A) 10K	0.94
p(PEG-A) 20K	1.44

4.3. Cell Culture Results

A549 cells (a human lung adenocarcinoma epithelial cell line) was used as adherent model carcinoma cell line to investigate cytotoxicity, cell uptake, cell cycle and intracellular distribution profiles of linear and comb-type PEGs. A549 cell line was used as a model cancer cell line as the lung cancer is one of the most common cancer types worlwide. Importantly, it has been shown in the literature that the uptake of linear PEG by A549 cells is not favorable (Kunath et al. 2003).

4.3.1. MTT Cell Viability Assay

The effect of linear and comb-type PEG on the viability of *in vitro* cultured A549 cells were investigated using 3-(4,5-dimethylthiazol-2-yl)-2,5-diphenyl tetrazolium bromide (MTT) cell viability assay (Berg, Hansen, and Nielsen 2009). In this assay, the ability of living cells to reduce a redox dye (tetrazole) into fluorescent dye (purple formazan) was measured. Viable cells signal fluorescence because their metabolic activity reduces the dye whereas the non-viable cells do not signal. The absorbance was measured at 570 nm using a microplate reader and depicted as a percentage relative to the untreated control cells.

The comb-type PEG (p(PEG-A) 10K and p(PEG-A) 20K) and linear PEG (PEG 10K and PEG 20K) at varying polymer concentrations (25 μM, 50 μM, 100 μM and 200 μM) were incubated with A549 for 24 or 72 hours. The cytotoxcitiy experiments were

performed in five-replicate. The percent viability of the cells treated with polymers was calculated according to the control (cells with no treatment) using Equation 3-1 (in Materials and Methods Section). The viability of A549 cells after treatment with the polymers for 24 h and 72 his shown Figure 4.8 and 4.9, respectively. Tables 4.4 and 4.5 summarize the percentage cell viability together with statistical analysis results.

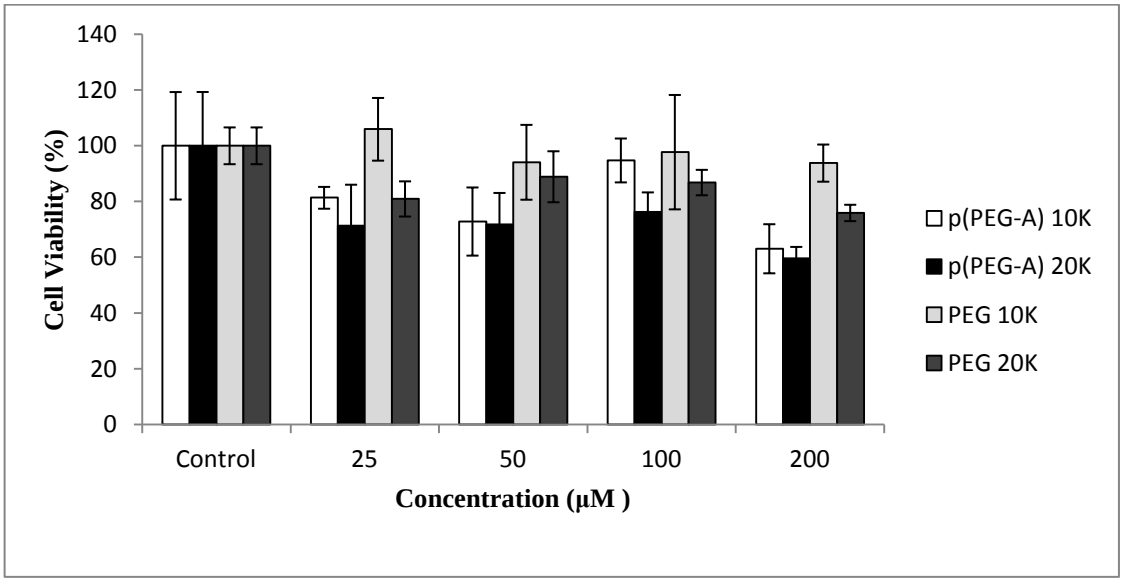

Figure 4.8. Viability of A549 cells after incubation with comb-type PEGs (p(PEG-A) 10K and p(PEG-A) 20K) and linear PEGs (PEG 10K and PEG 20K) for 24 h. Control is the cells with no treatment.

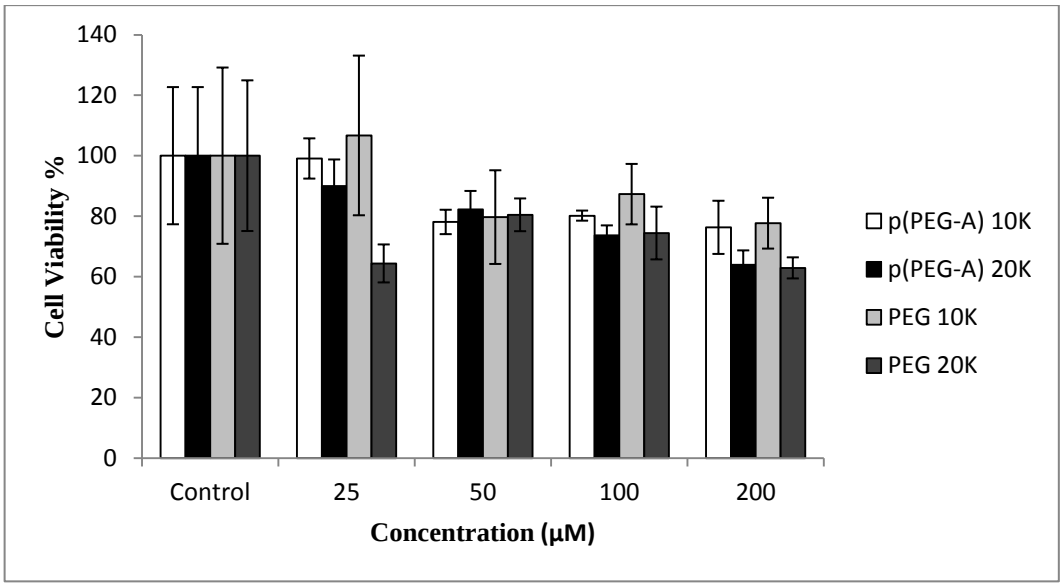

Figure 4.9. Viability of A549 cells after incubation with comb-type PEGs (p(PEG-A) 10K and p(PEG-A) 20K) and linear PEGs (PEG 10K and PEG 20K) for 72 h. Control is the cells with no treatment.

From Figure 4.8 PEG 10K caused no significant inhibition on A549 cell viability (93,79%) at the concentrations tested ($p>0.05$). PEG 20K caused the lowest cell viability (75,92%) only at 200 µM concentration. However, p(PEG-A) 10K and p(PEG-A) 20K caused statistically significant reduction on the cell viability ($p<0.05$). At 200 µM concentration, p(PEG-A) 10K (63,08%) and p(PEG-A) 20K (59,64%) showed maximum toxic effect ($p<0.05$). However, even these maximum values were above the 50% cell viability, showing that p(PEG-A) do not cause a major toxicity on A549 cells after 24 h incubation.

Table 4.4. Percent Viability of A549 cells after incubation with comb-type PEGs (p(PEG-A) 10K and p(PEG-A) 20K) and linear PEGs (PEG 10K and PEG 20K) for 24 h.

	Polymers			
Concentrations	p(PEG-A) 10K	p(PEG-A) 20K	PEG 10K	PEG 20K
Control	$100\pm19.27^{a,A}$	$100\pm19.3^{a,A}$	$100\pm6.60^{a,A}$	$100\pm6.60^{a,A}$
25 μM	$73.29\pm3.92^{bc,AB}$	$71.25\pm14.3^{b,AB}$	$105.92\pm11.24^{a,A}$	$80.94\pm6.31^{bc,B}$
50 μM	$72.83\pm12.22^{bc,A}$	$71.89\pm11.3^{b,A}$	$94.08\pm13.42^{a,A}$	$88.90\pm9.14^{ab,A}$
100 μM	$84.75\pm7.87^{ab,A}$	$76.29\pm7.0^{b,A}$	$97.72\pm20.51^{a,A}$	$86.82\pm4.56^{bc,A}$
200 μM	$63.08\pm8.80^{c,AB}$	$59.64\pm4.1^{b,A}$	$93.79\pm6.66^{a,B}$	$75.92\pm2.93^{c,A}$

[a-c] Values within each concentration followed by the same letter are not significantly different ($p > 0.05$).
[A-B] Values within each polymer followed by the same letter are not significantly different ($p > 0.05$).
Data are means values ± one standard deviation (n=5).

In literature, *Pissuwan et al*. (Pissuwan et al. 2010) investigated the effect of p(PEG-A) (M_n = 11 100 g/mol) on the viability of three different cell lines (CHO-K1, NIH3T3, and Raw264.7) for 24 h and 72 h upto 1 mM or ∼10 mg/mL polymer concentratios. After incubating the cells with the polymers the cell viability was evaulated by a CellTiter-Blue assay. p(PEG-A) did not cause any significant cytotoxic effect on any of the cell types over 24 h. Also it was noted that p(PEG-A) was nontoxic over 72 h to CHO-K1 and NIH3T3 cells while it showed dose-dependent toxicity on RAW264.7 cells. These results indicate that the effect of p(PEG-A) on the viability of cells depends on the cell type.

The viability of A549 cells after treatment with the polymers for 72 h is shown in Figure 4.9 and Table 4.5. From the figure Figure 4.10, PEG 10K and PEG 20K caused slight inhibition on the viability of A549 cells (77,9%) and (62,9%), respectively at 200 μM ($p<0.05$). Compared to 24 h results, PEG 10K and PEG 20K showed more cytotoxic effect on A549 cells in 72 h. However, the effect of p(PEG-A) 10K and p(PEG-A) 20K on the cell viability was less than the effect of the same polymers in 24 h. It is possible that the cell growth in 72 h minimizes the cytotoxic effect of p(PEG-A).

Table 4.5. Percent Viability of A549 cells after incubation with comb-type PEGs (p(PEG-A) 10K and p(PEG-A) 20K) and linear PEGs (PEG 10K and PEG 20K) for 72 h.

	Polymers			
Concentrations	p(PEG-A) 10K	p(PEG-A) 20K	PEG 10K	PEG 20K
Control	$100\pm22.69^{a,A}$	$100\pm22.69^{a,A}$	$100\pm29.2^{a,A}$	$100\pm29.2^{a,A}$
25 μM	$99{,}07\pm6.66^{ab,A}$	$89.95\pm8.8^{ab,A}$	$106.7\pm26.4^{a,A}$	$64.6\pm6.3^{b,B}$
50 μM	$78.08\pm4.03^{bc,A}$	$82.23\pm6.1^{abc,A}$	$79.7\pm15.5^{a,A}$	$80.4\pm5.4^{ab,A}$
100 μM	$80.17\pm1.67^{abc,A}$	$73.67\pm3.3^{bc,A}$	$87.3\pm10.0^{a,A}$	$74.4\pm8.7^{ab,A}$
200 μM	$76.29\pm8.79^{c,A}$	$63.86\pm4.8^{c,B}$	$77.7\pm8.4^{a,AB}$	$62.9\pm3.5^{b,B}$

$^{a-c}$ Values within each concentration followed by the same letter are not significantly different ($p > 0.05$).
$^{A-B}$ Values within each polymer followed by the same letter are not significantly different ($p > 0.05$).
Data are means values ± standard deviation (n=5).

4.3.2. Cell Uptake

Uptake of OG-labelled linear and comb-type PEGs by A549 cells was investigated using flow cytometry that enabled quantitative analysis of fluorescence–associated cells at an extremely rapid rate. Firstly, four different polymers at 12.5 μM concentration was incubated with cells at 37ºC for 1, 3 and 6 hours. The mean green fluorescence values (total fluorescence collected in the channel normalized accroding to the total cell count in the A549-cells region) were used to indicate the cell uptake of polymers. It should be noted that as the degree of labelling differed for each polymer type (Table 4.3), the mean green fluorescence values obtained with each type of polymer were normalized according to the labelling degree of p(PEG-A) 10K, the polymer with the lowest labelling degree. Additionally, the uptake of polymers with no label was also investigated by flow cytometry as a control experiment (Appendix C).

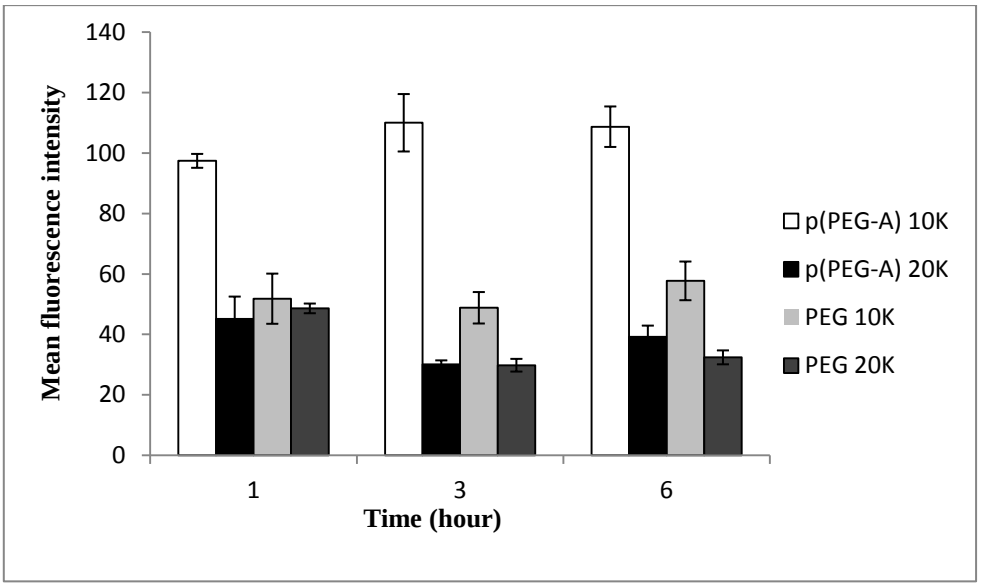

Figure 4.10. Uptake of comb-type PEGs (p(PEG-A) 10K and p(PEG-A) 20K) and linear PEGs (PEG 10K and PEG 20K) by A549 cells in 1, 3 and 6 hours at 37 °C. The polymer concentration was 12.5 μM. Experiments were performed in triplicate.

In addition, Figure 4.10 shows the mean fluorescence intensity (per cell) as a function of incubation time and polymer type. The maximum cell uptake was observed with p(PEG-A) 10K. The other polymers showed similar uptake profiles for 1 hour incubation. For 3 and 6 hours, the uptake of PEG 10K was slightly higher than p(PEG-A) 20K and PEG 20K, however it was still far less than p(PEG-A) 10K. p(PEG-A) 10K is has the smallest hydrodynamic volume (Table 4.2). It might be easier for cells to take up the most compact polymer structure. For all polymer samples, the mean cell uptake at 37 °C was not a function of time.

Table 4.6. Mean Fluorescence Intensity of comb-type PEGs (p(PEG-A) 10K and p(PEG-A) 20K) and linear PEGs (PEG 10K and PEG 20K) by A549 cells in 1, 3 and 6 hours at 37 °C. The polymer concentration was 12.5 μM.

	Polymers			
Mean Fluorescence Intensity(hour)	p(PEG-A) 10K	p(PEG-A) 20K	PEG 10K	PEG 20K
1.	$94.67\pm2.31^{a,A}$	$45.15\pm7.24^{a,B}$	$51.82\pm8.34^{a,B}$	$48.65\pm1.64^{a,B}$
3.	$110.00\pm9.54^{a,A}$	$30.14\pm1.36^{b,C}$	$48.77\pm5.24^{a,B}$	$29.82\pm2.09^{b,C}$
6.	$108.67\pm6.66^{a,A}$	$39.17\pm3.68^{ab,C}$	$56.99\pm6.43^{a,B}$	$32.43\pm2.28^{b,C}$

[a-b] Values within each mean fluorescence intensity followed by the same letter are not significantly different ($p > 0.05$).
[A-C] Values within each polymer followed by the same letter are not significantly different ($p > 0.05$).
Data are means values ± one standard deviation (n=3).

The time-dependent cell uptake of polymers was also analyzed at 4 °C by flow cytometry. As seen in Figure 4.11 when compared to the uptake at 37 °C, cell-associated mean fluorescence of all polymers significantly decreased at 4 °C. Endocytosis, phagocytosis and pinocytosis are known as general cell entry mechanisms for various extracellular materials. These mechanismsare energy-dependent, thus they are hindered at low temperatures (such as 4 °C) (Marsh and McMahon 1999, Silverstein, Steinman, and Cohn 1977).

Interestingly, the uptake of both p(PEG-A) and PEG having 20K molecular weight by A549 cells at 4 °C increased with time. This effect was more profound with linear PEG 20K. This observation suggests that the higher molecular weight polymers enter A549 cells via a passive mechanism. This mechanism needs to be investigated in future studies.

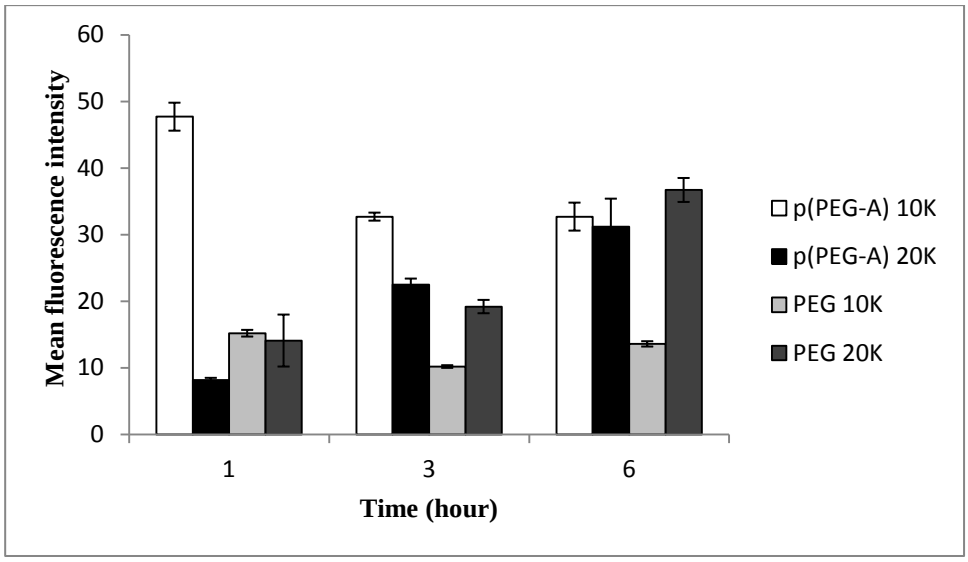

Figure 4.11. Uptake of comb-type PEGs (p(PEG-A) 10K and p(PEG-A) 20K) and linear PEGs (PEG 10K and PEG 20K) by A549 cells in 1, 3 and 6 hours at 4 °C. The polymer concentration was 12.5 μM. Experiments were performed in triplicate.

Table 4.7. Mean Fluorescence Intensity of comb-type PEGs (p(PEG-A) 10K and p(PEG-A) 20K) and linear PEGs (PEG 10K and PEG 20K) by A549 cells in 1, 3 and 6 hours at 4 °C. The polymer concentration was 12.5 μM.

	Polymers			
Mean Fluorescence Intensity(hour)	p(PEG-A) 10K	p(PEG-A) 20K	PEG 10K	PEG 20K
1.	$47.67\pm2.08^{a,A}$	$8.48\pm0,3^{a,C}$	$15.51\pm0.52^{a,B}$	$14.10\pm3.87^{a,BC}$
3.	$32.66\pm0.57^{c,A}$	$22.52\pm0.86^{b,B}$	$10.24\pm0.17^{c,D}$	$19.17\pm1.03^{a,C}$
6.	$40.30\pm2.08^{b,A}$	$37.97\pm4.24^{c,A}$	$13.58\pm6.35^{b,B}$	$36.6\pm1.76^{b,A}$

[a-c] Values within each mean fluorescence intensity followed by the same letter are not significantly different ($p > 0.05$).
[A-D] Values within each polymer followed by the same letter are not significantly different ($p > 0.05$).
Data are means values ± one standard deviation (n=3).

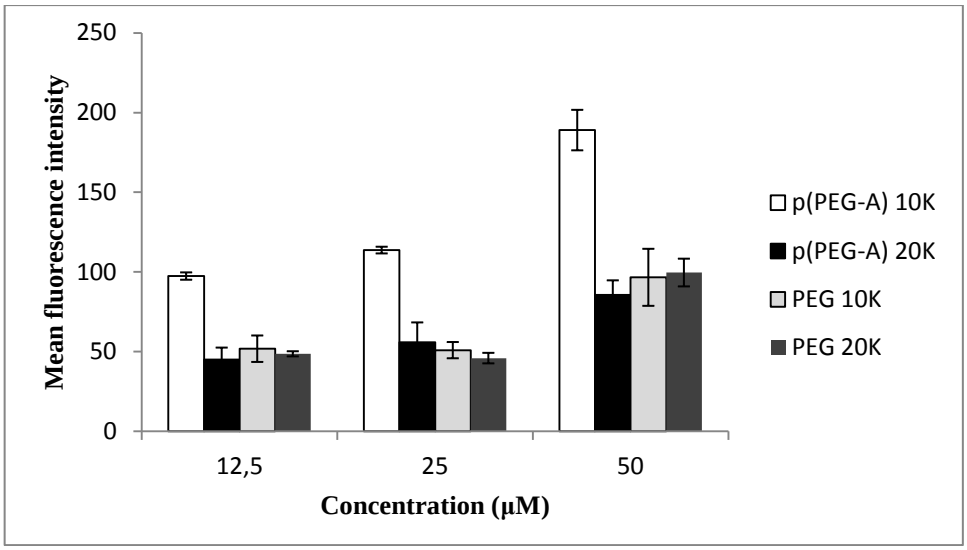

Figure 4.12. Uptake of comb-type PEGs (p(PEG-A) 10K and p(PEG-A) 20K) and linear PEGs (PEG 10K and PEG 20K) at varying concentrations (12,5, 25 and 50 µM) by A549 cells in 1 hours at 37 °C. Experiments were performed in triplicate.

To determine whether the active cell uptake is dependent on the dose of polymers, varying concentrations of polymers were incubated with A549 cells at 37 ºC for 1 hour (Figure 4.12). The data indicated that the uptake of all polymers by A549 cells increased with increasing polymer concentrations in the studied range. p(PEG-A) 10K appeared to have the highest uptake at all concentrations when compared to other polymers tested.

Table 4.8. Mean Fluorescence Intensity of comb-type PEGs (p(PEG-A) 10K and p(PEG-A) 20K) and linear PEGs (PEG 10K and PEG 20K) by A549 cells in 1 hour at 37 °C. The polymer concentration was 12.5 μM, 25 μM and 50 μM.

Mean Fluorescence Intensity (concentration)	Polymers			
	p(PEG-A) 10K	p(PEG-A) 20K	PEG 10K	PEG 20K
12.5 μM	$94.67\pm2.31^{a,A}$	$45.15\pm7.24^{a,B}$	$51.82\pm8.34^{a,B}$	$48.65\pm1.64^{a,B}$
25 μM	$113.67\pm2.08^{b,A}$	$55.95\pm12.40^{ab,B}$	$50.91\pm5.11^{a,B}$	$45.90\pm3.29^{a,B}$
50 μM	$189.0\pm12.73^{c,A}$	$85.51\pm9.23^{b,B}$	$96.59\pm17.86^{b,B}$	$99.57\pm8.75^{b,B}$

[a-c] Values within each mean fluorescence intensity followed by the same letter are not significantly different ($p > 0.05$).
[A-B] Values within each polymer followed by the same letter are not significantly different ($p > 0.05$).
Data are means values ± one standard deviation (n=3).

4.3.3. Cell Cycle

Since p(PEG-A) 10K and p(PEG-A) 20K at 200 μM concentration caused statistically significant reduction on the cell viability (63,08% and 59,64%, respectively) in 24 hours, whereas there was no significant cytotoxic effect of linear PEGs. Considering these results, the effect of both types of polymers on the cell cycle was investigated by incubating four different polymers at 200 μM concentration with A549 cells at 37 ºC for 24 hours.

Cell division is divided into two stages: mitosis (M) which is the process of nuclear division and interphase which is the interlude between two M phases. Interphase consists of G1, S and G2 phases. G1, S, G2 and M phases are the traditional subdivisions of the standard cell cycle. Replication of DNA occurs in S phase. S phase is preceded by G1 phase during which the cell is preparing for DNA synthesis and followed by G2 phase during which the cell prepares for mitosis (Vermeulen, Van Bockstaele, and Berneman 2003).

To investigate the effects of polymers on cell cycle, DNA-content was measured by flow cytometry after propidium iodine (PI) staining. Additionally, DNA distribution was analyzed by ModFit software. The flow cytometry data are given in Appendix D.

Figure 4.13 and Figure 4.14 show the DNA distribution of A549 cells determined from the flow cytometry data. The results indicated that none of the polymers caused an arrest on cell cycle over 24 or 72 hour compared to control experiment. At 72 hour, the result indicates that the rate of DNA synthesis was retarded and thus slowed the progress of cells through S phase. However, the percentage of G2/M cells did not alter when compared to control experiments. G1 and S phases did not display an arrest and were nearly close to G1 and S phases of untreated control A549 cells. Also, DNA distribution of A549 cells after 24 hour treatment at 4 and 37 °C was shown in Appendix D (Figure D.3). Cells at 4 °C do not lose their viability as indicated by cell cycle experiment results.

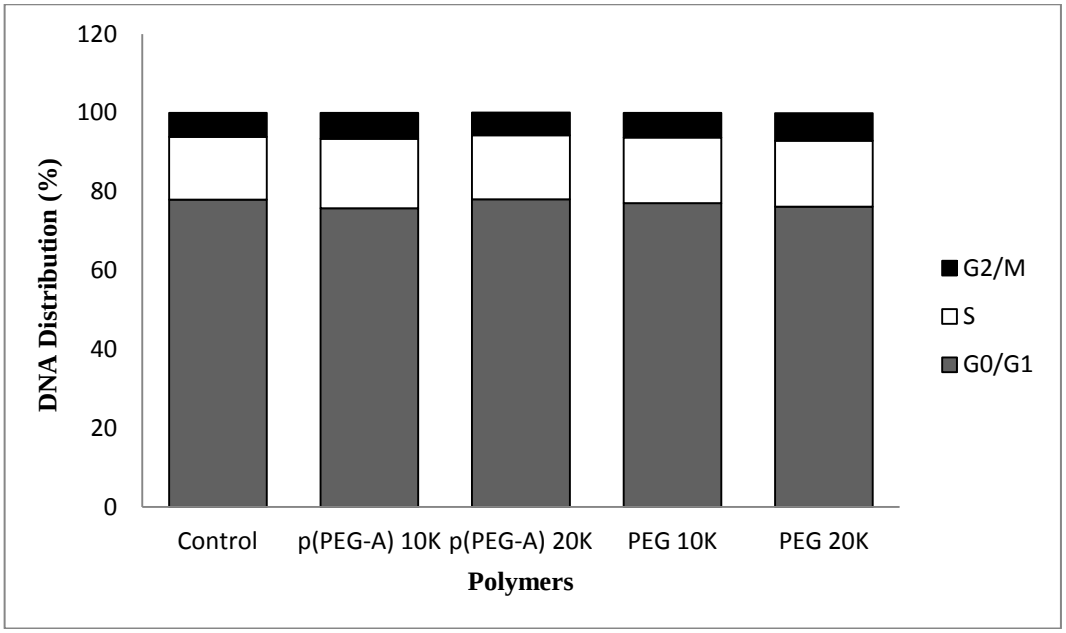

Figure 4.13. DNA distribution of A549 cells after 24 hour treatment with polymers at 200 μM. Experiments were performed in triplicate.

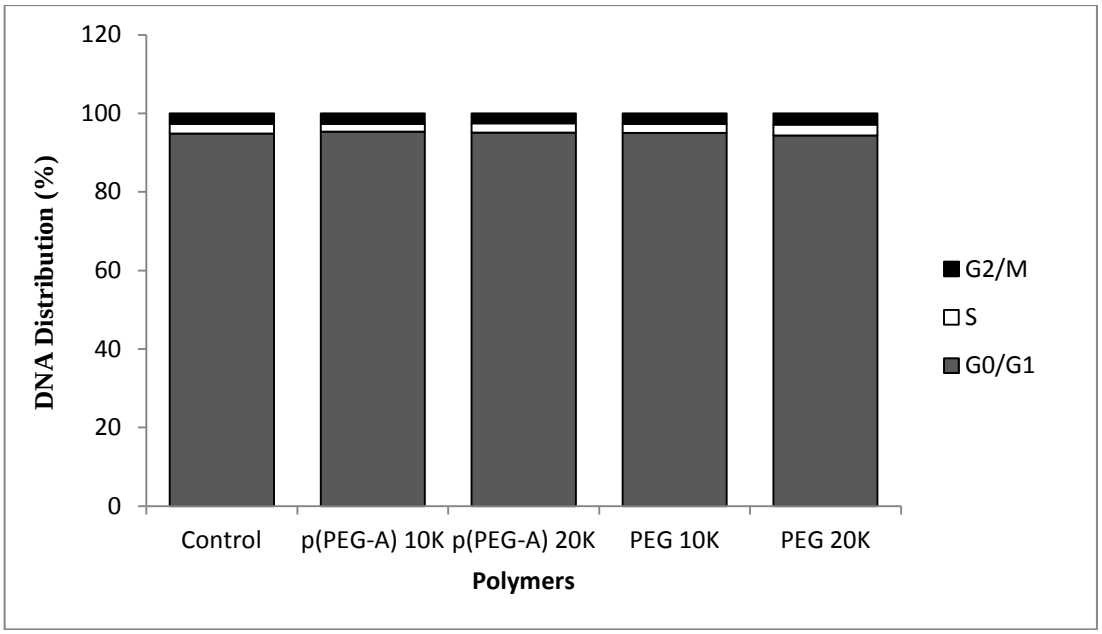

Figure 4.14. DNA distribution of A549 cells after 72 hour treatment with polymers at 200 μM. Experiments were performed in duplicate.

4.3.4. Intracellular Distribution

To investigate intracellular localization of polymers, green-fluorescent labelled polymers were incubated with cells followed by staining nucleus with blue fluorescent dye or lysosomes with red fluorescent dye, and then imaging by a fluorescence microscope. The fluorescence images are shown in Figures 4.15 – 4.22. In all cases, polymers were taken up by A549 cells, as green fluorescence was apparent inside the cells. None of the polymers entered the nucleus of cells, as expected. It was seen in emerged images that polymers localized mostly in lysosomes, and partially within cytoplasm. These results together with flow cytometry analyses suggest that both comb-type and linear PEGs are taken up by cells via energy-dependent active mechanism, such as endocytosis as a common mechanism for soluble macromolecules.

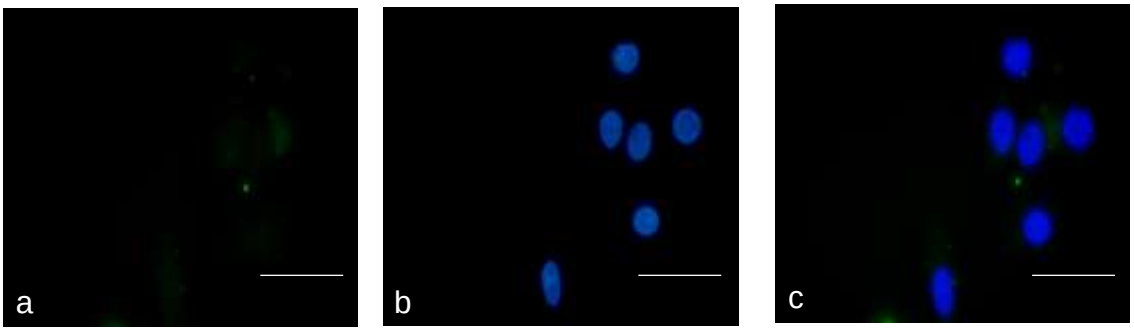

Figure 4.15. Fluorescence microscopic images of A549 cells after 1 hour incubation with (a) Oregon green labeled with p(PEG-A) 10K (green), (b) colabeled with DAPI (blue); (c) merged image of a and b: ×100 (scale bar: 30 μm)

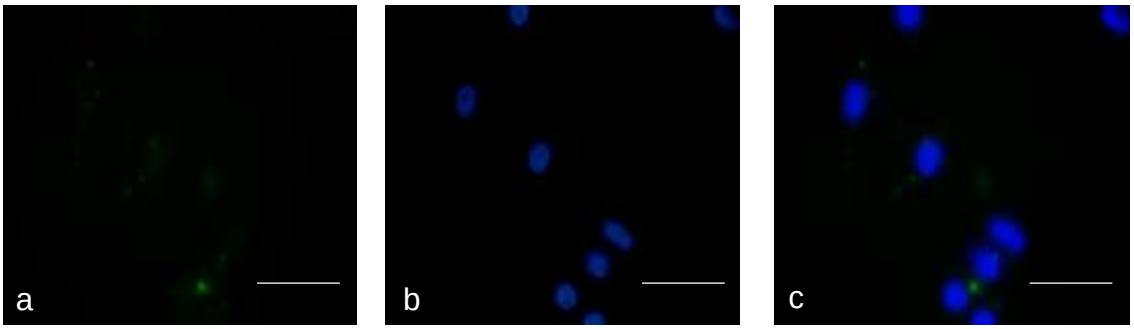

Figure 4.16. Fluorescence microscopic images of A549 cells after 1 hour incubation with (a) Oregon green labeled with PEG 10K (green), (b) colabeled with DAPI (blue); (c) merged image of a and b: ×100 (scale bar: 30 μm)

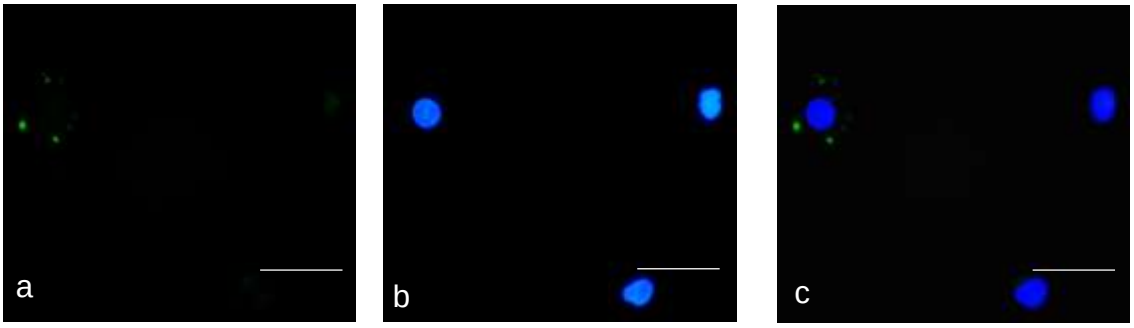

Figure 4.17. Fluorescence microscopic images of A549 cells after 1 hour incubation with (a) Oregon green labeled with p(PEG-A) 20K (green), (b) colabeled with DAPI (blue); (c) merged image of a and b: ×100 (scale bar: 30 μm)

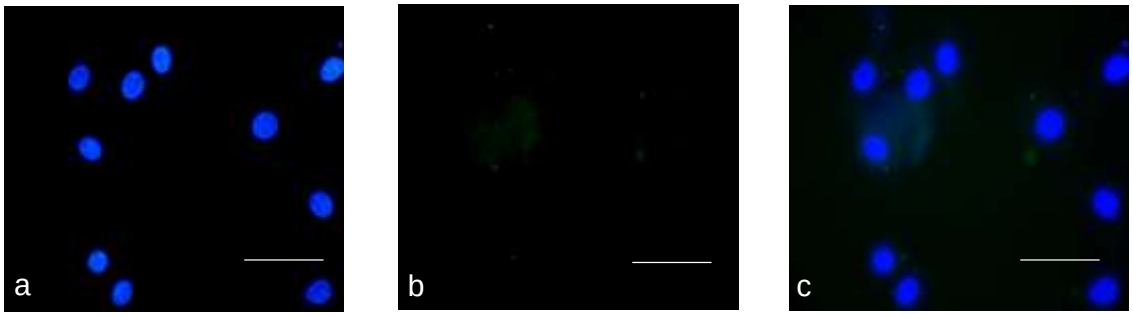

Figure 4.18. Fluorescence microscopic images of A549 cells after 1 hour incubation with (a) Oregon green labeled with PEG 20K (green), (b) colabeled with DAPI (blue); (c) merged image of a and b: ×100 (scale bar: 30 μm)

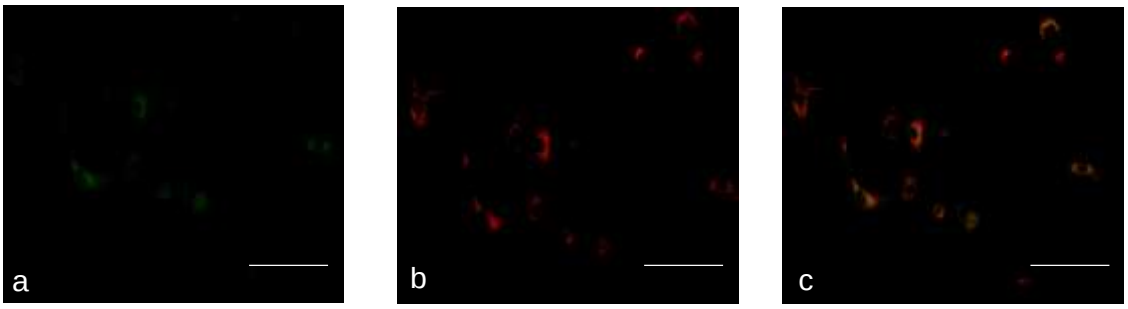

Figure 4.19. Fluorescence microscopic images of A549 cells after 1 hour incubation with (a) Oregon green labeled with p(PEG-A) 10K (green), (b) colabeled with LysoTracker® Red DND-99 (red); (c) merged image of a and b: ×40 (scale bar: 30 μm)

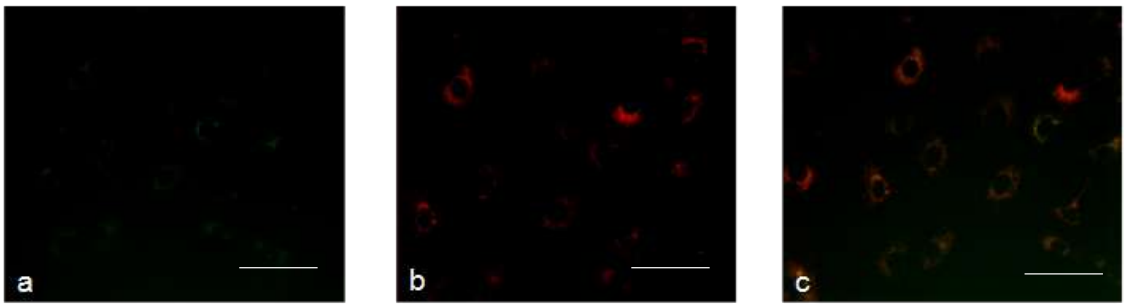

Figure 4.20. Fluorescence microscopic images of A549 cells after 1 hour incubation with (a) Oregon green labeled with PEG 10K (green), (b) colabeled LysoTracker® Red DND-99 (red); (c) merged image of a and b: ×40 (scale bar: 30 μm)

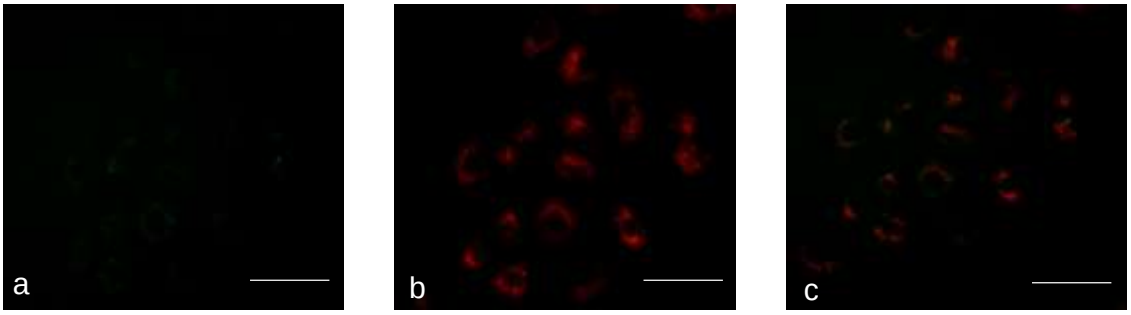

Figure 4.21. Fluorescence microscopic images of A549 cells after 1 hour incubation with (a) Oregon green labeled with p(PEG-A) 20K (green) , (b) colabelled with LysoTracker® Red DND-99 (red); (c) Merged image of a and b: ×40 (scale bar: 30 μm)

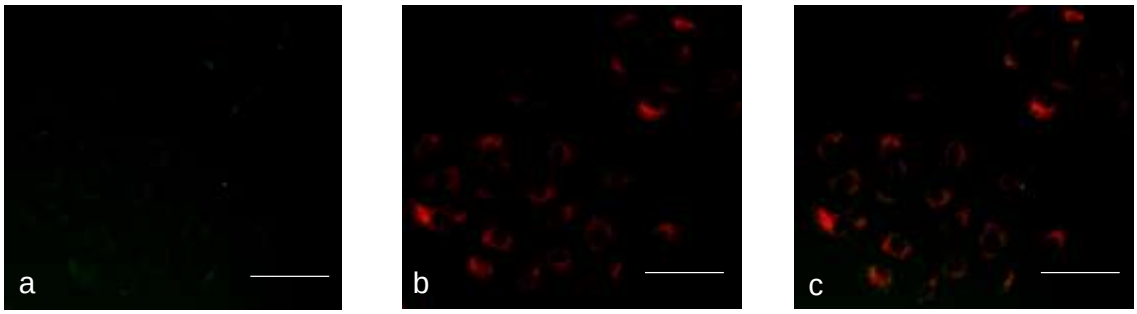

Figure 4.22. Fluorescence microscopic images of A549 cells after 1 hour incubation with (a) Oregon green labeled with PEG 20K (green), (b) colabelled LysoTracker® Red DND-99 (red); (c) Merged image of a and b: ×40 (scale bar: 30 μm)

CHAPTER 5

CONCLUSION

To the best of the author's knowledge, there has been no reports in literature on the comparison of the physicochemical characteristics and *in vitro* cell interactions of linear and comb-type PEGs. Therefore, the first specific objective of this study was to investigate the morphology and hydrodynamic size of comb-type and linear PEGs of equivalent molecular weights. The second specific objective was to provide a preliminary work on *in vitro* cytotoxicity, cell uptake, cell cycle and intracellular distribution profiles of comb-type and linear PEGs.

In this context, linear PEGs having two different molecular weights (M_n=10 000 g/mol and 20 000 g/mol (PEG 10K and PEG 20K)) were purchased from a manufacturer. These molecular weights were selected as they are in the range of molecular weights that are used commonly in PEGylation applications. The comb-type PEGs, p(PEG-A), with two different molecular weights (M_n= 10 700 g/mol and M_n= 20 200 g/mol p(PEG-A) 10K and p(PEG-A) 20K) were synthesized by a controlled polymerization technique, RAFT polymerization, according to a method reported in previous publications. Polymers were characterized by using Nuclear Magnetic Resonance (NMR), Gel Permeation Chromatography (GPC), Dynamic Light Scattering (DLS) and Atomic Force Microscopy (AFM) methods. A combination of the results obtained from NMR spectroscopy and GPC measurements showed clearly the successful synthesis of the controlled molecular weight and narrow polydisperse comb-type PEGs. DLS was used to measure the hydrodynamic diameter (D_h) of polymers in 5 different media: phosphate buffer saline (PBS) at pH 7.4, PBS containing 10% fetal bovine serum (FBS), cell culture medium RPMI-1640, and RPMI-1640 containing 10% FBS. Compared to linear PEG, the comb-type polymers had a smaller D_h in water and PBS. All polymers tested in aqueous solutions had a D_h value less than 7.8 nm. The D_h values of all polymers showed a significant increase in cell culture media, RPMI 1640 and RPMI 1640 containing 10% FBS, indicating the existence of interactions between medium components and polymers possibly through hydrogen bonding. While p(PEG-A) 10K in RPMI 1640 had the smallest size of 44.4 nm, p(PEG-A) 20K in the same

medium had the largest size of 58 nm. The linear PEGs in RPMI 1640 had D_h values between 54.5 nm and 55.9 nm. Similar D_h values were obtained for polymers in RPMI 1640 containing 10% FBS. The morphology of both PEG 10K and p(PEG-A) 10K was investigated by AFM. The AFM image of PEG 10K displayed the formation of linear structures whereas supramolecular spherical structures were observed clearly with p(PEG-A) 10K, indicating significant differences between interchain interactions of linear and comb-type PEGs.

The interactions of comb-type and linear poly(ethylene glycol) with equivalent molecular weights with *in vitro* cultured cells were investigated using A549 human lung adenocarcinoma epithelial cells as a model cancer cell line, as lung cancer is one of the most common cancers worlwide and the uptake of linear PEG by A549 cells has been shown in literature to be inefficient.

The cytotoxic effect of polymers on the viability of A549 cells was investigated 3-(4,5-dimethylthiazol-2-yl)-2,5-diphenyl tetrazolium bromide (MTT) Cell Viability assay. Comb-type PEGs were statistically more cytotoxic than linear PEGs after 24 hours treatment. Nevertheless, the minimum cell viability observed after 24 with the comb-type polymers at the highest concentration tested (200 μM) was above 59%. The cell viability after treatment with p(PEG-A) (10K and 20K) for 72 hours increased when compared with the cell viability after 24 hours, and reached the similar values with those of linear PEGs. This was attributed to the the growth of cells in 72 hours minimizing the cytotoxic effects of polymers.

The uptake of comb-type and linear PEGs by A549 cells was investigated as a function of incubation time (1-6 hours), incubation temperature (37 and 4 ºC) and polymer concentration (12.5 – 50 μM). Overall the cell uptake results showed that all polymers are taken up efficiently by A549 cells at 37 ºC in 1 hour, however when compared to other polymers, p(PEG-A) 10K is taken up at significantly higher amounts by the cells at 37 ºC. The cell uptake of polymers at 37 °C increased with increasing polymer concentrations in the studied range. When compared to 37 °C, the cell uptake of all polymers significantly decreased at 4 °C. This indicated that the main cell entry mechanism of the polymers is via an energy-dependent mechanism such as phagocytosis, pinocytosis and endocytosis. The intracellular distribution of polymers by A549 cells was visualized by a fluorescence microscope. Both type of polymers were found in the cytoplasm and lysosomes of the cells. None of the polymers entered the nucleus of cells. The microscopy data support the results observed by flow cytometry.

Furthermore the effect of polymers on the cell cycle was investigated by flow cytometry for 24 and 72 hour. Both polymers p(PEG-A) 10K and 20K , and PEG 10K and 20K did not affect at all the cell cycle phases under the conditions tested compared to control experiments.

Overall the study presented in this thesis provided for the first time a preliminary comparative investigation on the physicochemical properties of linear and comb-type PEGs and their interactions with an *in vitro* cultured cancer cell line.

Future investigations on the topic may include the following suggestions:

1. The morphology of the cells can be investigated by AFM under liquid, which will show the hydrodynamic conformation or organization of the polymers. This would make the AFM data be more comparable with DLS data although liquid AFM still requires a substrate surface.

2. The cytotoxicity, cell uptake, cell cycle and intracellular distribution experiments can be done using various healthy cells and other cancer cells to derive general conclusions.

3. The cytotoxicity, cell uptake and cell cycle experiments can be performed at significantly higher concentrations of polymers to determine the critical concentrations of polymers causing significant effects on cells.

REFERENCES

Asayama, S., M. Nogawa, Y. Takei, T. Akaike, and A. Maruyama. 1998. "Synthesis of novel polyampholyte comb-type copolymers consisting of a poly (L-lysine) backbone and hyaluronic acid side chains for a DNA carrier." *Bioconjugate chemistry* no. 9 (4):476-481.

Bailon, P., A. Palleroni, C.A. Schaffer, C.L. Spence, W.J. Fung, J.E. Porter, G.K. Ehrlich, W. Pan, Z.X. Xu, and M.W. Modi. 2001. "Rational design of a potent, long-lasting form of interferon: a 40 kDa branched polyethylene glycol-conjugated interferon α-2a for the treatment of hepatitis C." *Bioconjugate chemistry* no. 12 (2):195-202.

Bendele, A., J. Seely, C. Richey, G. Sennello, and G. Shopp. 1998. "Short communication: renal tubular vacuolation in animals treated with polyethylene-glycol-conjugated proteins." *Toxicological sciences* no. 42 (2):152-157.

Berg, K., M.B. Hansen, and S.E. Nielsen. 2009. "A new sensitive bioassay for precise quantification of interferon activity as measured via the mitochondrial dehydrogenase function in cells (MTT-method)." *Apmis* no. 98 (1-6):156-162.

Bhawe, K.M., R.A. Blake, D.O. Clary, and P.M. Flanagan. 2004. "An automated image capture and quantitation approach to identify proteins affecting tumor cell proliferation." *Journal of biomolecular screening* no. 9 (3):216-222.

Bihari, P., M. Vippola, S. Schultes, M. Praetner, A.G. Khandoga, C.A. Reichel, C. Coester, T. Tuomi, M. Rehberg, and F. Krombach. 2008. "Optimized dispersion of nanoparticles for biological in vitro and in vivo studies." *Particle and Fibre Toxicology* no. 5 (1):14.

Bouladjine, A., A. Al-Kattan, P. Dufour, and C. Drouet. 2009. "New advances in nanocrystalline apatite colloids intended for cellular drug delivery." *Langmuir* no. 25 (20):12256-12265.

Boyer, C., V. Bulmus, and T.P. Davis. 2009. "Efficient usage of thiocarbonates for both the production and the biofunctionalization of polymers." *Macromolecular Rapid Communications* no. 30 (7):493-497.

Boyer, C., J. Liu, V. Bulmus, and T.P. Davis. 2009. "RAFT polymer end-group modification and chain coupling/conjugation via disulfide bonds." *Australian Journal of Chemistry* no. 62 (8):830-847.

Bures, P., Y. Huang, E. Oral, and N.A. Peppas. 2001. "Surface modifications and molecular imprinting of polymers in medical and pharmaceutical applications." *Journal of Controlled Release* no. 72 (1):25-33.

Caliceti, P., O. Schiavon, and F.M. Veronese. 1999. "Biopharmaceutical properties of uricase conjugated to neutral and amphiphilic polymers." *Bioconjugate chemistry* no. 10 (4):638-646.

Caliceti, P., and F.M. Veronese. 2003. "Pharmacokinetic and biodistribution properties of poly (ethylene glycol)–protein conjugates." *Advanced drug delivery reviews* no. 55 (10):1261-1277.

Chang, C.W., E. Bays, L. Tao, S.N.S. Alconcel, and H.D. Maynard. 2009. "Differences in cytotoxicity of poly (PEGA) s synthesized by reversible addition–fragmentation chain transfer polymerization." *Chemical Communications* (24):3580-3582.

De, P., M. Li, S.R. Gondi, and B.S. Sumerlin. 2008. "Temperature-Regulated Activity of Responsive Polymer− Protein Conjugates Prepared by Grafting-from via RAFT Polymerization." *Journal of the American Chemical Society* no. 130 (34):11288-11289.

Eto, Y., J.Q. Gao, F. Sekiguchi, S. Kurachi, K. Katayama, M. Maeda, K. Kawasaki, H. Mizuguchi, T. Hayakawa, and Y. Tsutsumi. 2005. "PEGylated adenovirus vectors containing RGD peptides on the tip of PEG show high transduction efficiency and antibody evasion ability." *The journal of gene medicine* no. 7 (5):604-612.

Gao, W., W. Liu, T. Christensen, M.R. Zalutsky, and A. Chilkoti. 2010. "In situ growth of a PEG-like polymer from the C terminus of an intein fusion protein improves pharmacokinetics and tumor accumulation." *Proceedings of the National Academy of Sciences* no. 107 (38):16432-16437.

Gao, W., W. Liu, J.A. Mackay, M.R. Zalutsky, E.J. Toone, and A. Chilkoti. 2009. "In situ growth of a stoichiometric PEG-like conjugate at a protein's N-terminus with significantly improved pharmacokinetics." *Proceedings of the National Academy of Sciences* no. 106 (36):15231-15236.

Gilbert, C.W., and M. Park-Cho. 2000. Interferon polymer conjugates. Google Patents.

Grace, M., S. Youngster, G. Gitlin, W. Sydor, L. Xie, L. Westreich, S. Jacobs, D. Brassard, J. Bausch, and R. Bordens. 2001. "Structural and biologic characterization of pegylated recombinant IFN-α 2b." *Journal of interferon & cytokine research* no. 21 (12):1103-1115.

Graham, M.L. 2003. "Pegaspargase: a review of clinical studies." *Advanced drug delivery reviews* no. 55 (10):1293-1302.

Gunasekaran, K., T.H. Nguyen, H.D. Maynard, T.P. Davis, and V. Bulmus. 2011. "Conjugation of siRNA with Comb-Type PEG Enhances Serum Stability and Gene Silencing Efficiency." *Macromolecular Rapid Communications* no. 32 (8):654-659.

Harris, J.M., N.E. Martin, and M. Modi. 2001. "Pegylation: a novel process for modifying pharmacokinetics." *Clinical pharmacokinetics* no. 40 (7):539-551.

Heredia, K.L., T.H. Nguyen, C.W. Chang, V. Bulmus, T.P. Davis, and H.D. Maynard. 2008. "Reversible siRNA–polymer conjugates by RAFT polymerization." *Chemical Communications* (28):3245-3247.

Hermanson, G.T. 1996. *Bioconjugate techniques*: Academic press.

Jevševar, S., M. Kunstelj, and V.G. Porekar. 2010. "PEGylation of therapeutic proteins." *Biotechnology journal* no. 5 (1):113-128.

Kim, S.H., J.H. Jeong, S.H. Lee, S.W. Kim, and T.G. Park. 2006. "PEG conjugated VEGF siRNA for anti-angiogenic gene therapy." *Journal of Controlled Release* no. 116 (2):123-129.

Kompella, U.B., and V.H.L. Lee. 2001. "Delivery systems for penetration enhancement of peptide and protein drugs: design considerations." *Advanced drug delivery reviews* no. 46 (1):211-245.

Kunath, K., T. Merdan, O. Hegener, H. Häberlein, and T. Kissel. 2003. "Integrin targeting using RGD-PEI conjugates for in vitro gene transfer." *The journal of gene medicine* no. 5 (7):588-599.

Levy, Y., M.S. Hershfield, C. Fernandez-Mejia, S.H. Polmar, D. Scudiery, M. Berger, and R.U. Sorensen. 1988. "Adenosine deaminase deficiency with late onset of recurrent infections: response to treatment with polyethylene glycol-modified adenosine deaminase." *The Journal of pediatrics* no. 113 (2):312-317.

Li, M., P. De, S.R. Gondi, and B.S. Sumerlin. 2008. "End group transformations of RAFT-generated polymers with bismaleimides: Functional telechelics and modular block copolymers." *Journal of Polymer Science Part A: Polymer Chemistry* no. 46 (15):5093-5100.

Linegar, K.L., A.E. Adeniran, A.F. Kostko, and M.A. Anisimov. 2010. "Hydrodynamic radius of polyethylene glycol in solution obtained by dynamic light scattering." *Colloid journal* no. 72 (2):279-281.

Lowe, A.B., C.E. Hoyle, and C.N. Bowman. 2010. "Thiol-yne click chemistry: A powerful and versatile methodology for materials synthesis." *Journal of Materials Chemistry* no. 20 (23):4745-4750.

Lowe, A.B., and C.L. McCormick. 2007. "Reversible addition–fragmentation chain transfer (RAFT) radical polymerization and the synthesis of water-soluble (co) polymers under homogeneous conditions in organic and aqueous media." *Progress in Polymer Science* no. 32 (3):283-351.

Magnusson, J.P., S. Bersani, S. Salmaso, C. Alexander, and P. Caliceti. 2010. "In Situ Growth of Side-Chain PEG Polymers from Functionalized Human Growth Hormone · A New Technique for Preparation of Enhanced Protein− Polymer Conjugates." *Bioconjugate chemistry* no. 21 (4):671-678.

Marsh, M., and HT McMahon. 1999. "The structural era of endocytosis." *Science* no. 285 (5425):215-220.

Masters, J. 2000. "Animal cell culture."

Matsushima, A., Y. Kodera, M. Hiroto, H. Nishimura, and Y. Inada. 2001. "Polyethylene Glycol-Modified Enzymes in Hydrophobic Media." *METHODS IN BIOTECHNOLOGY* no. 15:49-64.

Moad, G., E. Rizzardo, and S.H. Thang. 2005. "Living radical polymerization by the RAFT process." *Australian Journal of Chemistry* no. 58 (6):379-410.

Moad, G., E. Rizzardo, and S.H. Thang. 2009. "Living Radical polymerization by the RAFT process–a second update." *Australian Journal of Chemistry* no. 62 (11):1402-1472.

Ng, E.W.M., D.T. Shima, P. Calias, E.T. Cunningham, D.R. Guyer, and A.P. Adamis. 2006. "Pegaptanib, a targeted anti-VEGF aptamer for ocular vascular disease." *Nature Reviews Drug Discovery* no. 5 (2):123-132.

Pacetti, S., and W.E. Roorda. 2010. ZWITERIONIC TERPOLYMERS, METHOD OF MAKING AND USE ON MEDICAL DEVICES. Google Patents.

Pissuwan, D., C. Boyer, K. Gunasekaran, T.P. Davis, and V. Bulmus. 2010. "In vitro cytotoxicity of RAFT polymers." *Biomacromolecules* no. 11 (2):412-420.

Roberts, MJ, MD Bentley, and JM Harris. 2012. "Chemistry for peptide and protein PEGylation." *Advanced drug delivery reviews*.

Rogošić, M., H.J. Mencer, and Z. Gomzi. 1996. "Polydispersity index and molecular weight distributions of polymers." *European polymer journal* no. 32 (11):1337-1344.

Ryan, S.M., J.M. Frías, X. Wang, C.T. Sayers, D.M. Haddleton, and D.J. Brayden. 2011. "PK/PD modelling of comb-shaped PEGylated salmon calcitonin conjugates of differing molecular weights." *Journal of Controlled Release* no. 149 (2):126-132.

Ryan, S.M., G. Mantovani, X. Wang, D.M. Haddleton, and D.J. Brayden. 2008. "Advances in PEGylation of important biotech molecules: delivery aspects."

Ryan, S.M., X. Wang, G. Mantovani, C.T. Sayers, D.M. Haddleton, and D.J. Brayden. 2009. "Conjugation of salmon calcitonin to a combed-shaped end functionalized poly (poly (ethylene glycol) methyl ether methacrylate) yields a bioactive stable conjugate." *Journal of Controlled Release* no. 135 (1):51-59.

Sayers, C.T., G. Mantovani, S.M. Ryan, R.K. Randev, O. Keiper, O.I. Leszczyszyn, C. Blindauer, D.J. Brayden, and D.M. Haddleton. 2009. "Site-specific N-terminus conjugation of poly (mPEG1100) methacrylates to salmon calcitonin: synthesis and preliminary biological evaluation." *Soft Matter* no. 5 (16):3038-3046.

Schiebener, P., J. Straub, J.M.H.L. Sengers, and JS Gallagher. 1990. *Refractive index of water and steam as function of wavelength, temperature and density*: American Chemical Society.

Silverstein, S.C., R.M. Steinman, and Z.A. Cohn. 1977. "Endocytosis." *Annual review of biochemistry* no. 46 (1):669-722.

Srividhya, M., S. Preethi, A. Gnanamani, and BSR Reddy. 2006. "Sustained release of protein from poly (ethylene glycol) incorporated amphiphilic comb like polymers." *International journal of pharmaceutics* no. 326 (1):119-127.

Thomas, D.B., A.J. Convertine, R.D. Hester, A.B. Lowe, and C.L. McCormick. 2004. "Hydrolytic susceptibility of dithioester chain transfer agents and implications in aqueous RAFT polymerizations." *Macromolecules* no. 37 (5):1735-1741.

Torchilin, V.P., V.G. Omelyanenko, M.I. Papisov, A.A. Bogdanov, V.S. Trubetskoy, J.N. Herron, and C.A. Gentry. 1994. "Poly (ethylene glycol) on the liposome surface: on the mechanism of polymer-coated liposome longevity." *Biochimica et Biophysica Acta (BBA)-Biomembranes* no. 1195 (1):11-20.

Trainer, P.J., W.M. Drake, L. Katznelson, P.U. Freda, V. Herman-Bonert, AJ Van Der Lely, E.V. Dimaraki, P.M. Stewart, K.E. Friend, and M.L. Vance. 2000. "Treatment of acromegaly with the growth hormone–receptor antagonist pegvisomant." *New England Journal of Medicine* no. 342 (16):1171-1177.

Vermeulen, K., D.R. Van Bockstaele, and Z.N. Berneman. 2003. "The cell cycle: a review of regulation, deregulation and therapeutic targets in cancer." *Cell proliferation* no. 36 (3):131-149.

Veronese, F.M. 2001. "Peptide and protein PEGylation: a review of problems and solutions." *Biomaterials* no. 22 (5):405-417.

Veronese, F.M., and G. Pasut. 2005. "PEGylation, successful approach to drug delivery." *Drug discovery today* no. 10 (21):1451-1458.

Whittaker, M.R., Y.K. Goh, H. Gemici, T.M. Legge, S. Perrier, and M.J. Monteiro. 2006. "Synthesis of monocyclic and linear polystyrene using the reversible coupling/cleavage of thiol/disulfide groups." *Macromolecules* no. 39 (26):9028-9034.

Wiogo, H.T.R., M. Lim, V. Bulmus, and R. Amal. 2011. Effects of surface functional groups on the aggregation stability of magnetite nanoparticles in biological media containing serum. Paper read at Nanotechnology (IEEE-NANO), 2011 11th IEEE Conference on.

Yamaoka, T., Y. Tabata, and Y. Ikada. 1994. "Distribution and tissue uptake of poly (ethylene glycol) with different molecular weights after intravenous administration to mice." *Journal of pharmaceutical sciences* no. 83 (4):601-606.

YAMAOKA, T., Y. TABATA, and Y. IKADA. 1995. "Comparison of Body Distribution of Poly (vinyl alcohol) with Other Water-soluble Polymers after Intravenous Administration." *Journal of pharmacy and pharmacology* no. 47 (6):479-486.

Yılmazel Çakmak, Özgür. 2011. *DNA Fragmantasyonu, Hücre Döngüsünün Analizi ve Apoptatik Hücre Analizi (Annexin V) Hücre ölümü araştırma teknikleri Teorik kursu, kitap bölümü* Vol. 978-975-411-349-6

Yunus, W., and A.A. Rahman. 1988. "Refractive index of solutions at high concentrations." *Applied optics* no. 27 (16):3341-3343.

Zalipsky, S. 1995. "Functionalized poly (ethylene glycols) for preparation of biologically relevant conjugates." *Bioconjugate chemistry* no. 6 (2):150-165.

Zalipsky, S., and J. Milton Harris. 1997. Introduction to chemistry and biological applications of poly (ethylene glycol).

APPENDIX A

CHARACTERIZATION

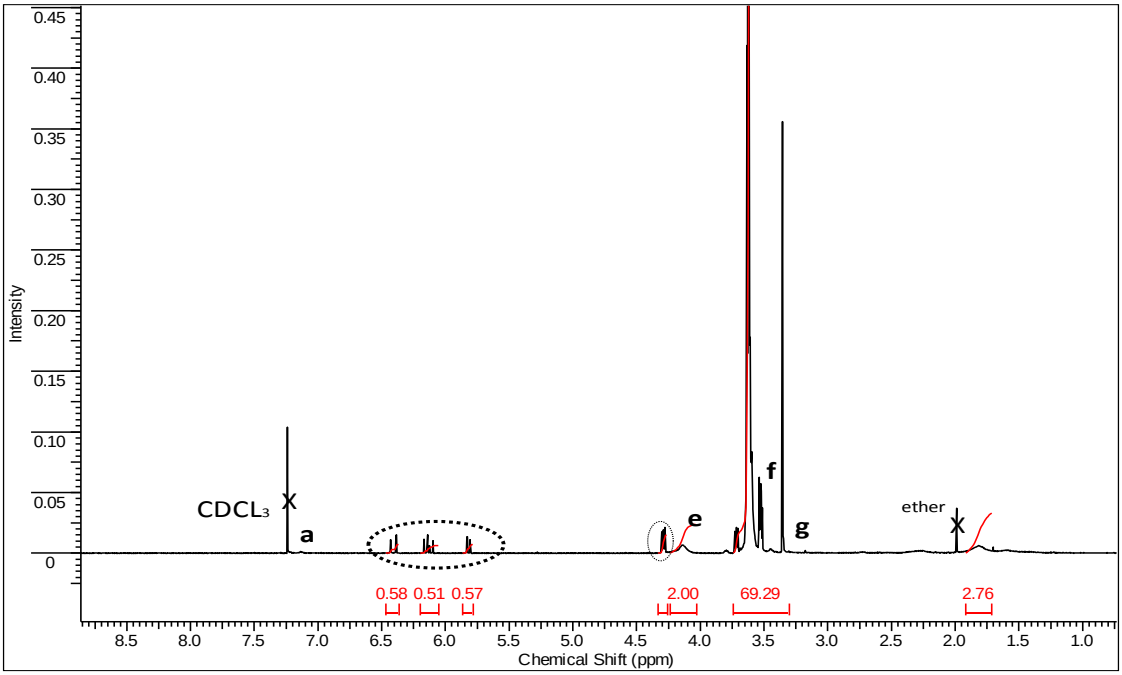

Figure A.1. ^{1}H-NMR spectrum of non-purified p(PEG-A) 10 K Conversion determined by ^{1}H-NMR spectrum of non-purified PEG-A that synthesized by RAFT polymerization at 65 °C, at a [BSPA]0/[PEG-A]0/[AIBN]0 = 1/30/0.2

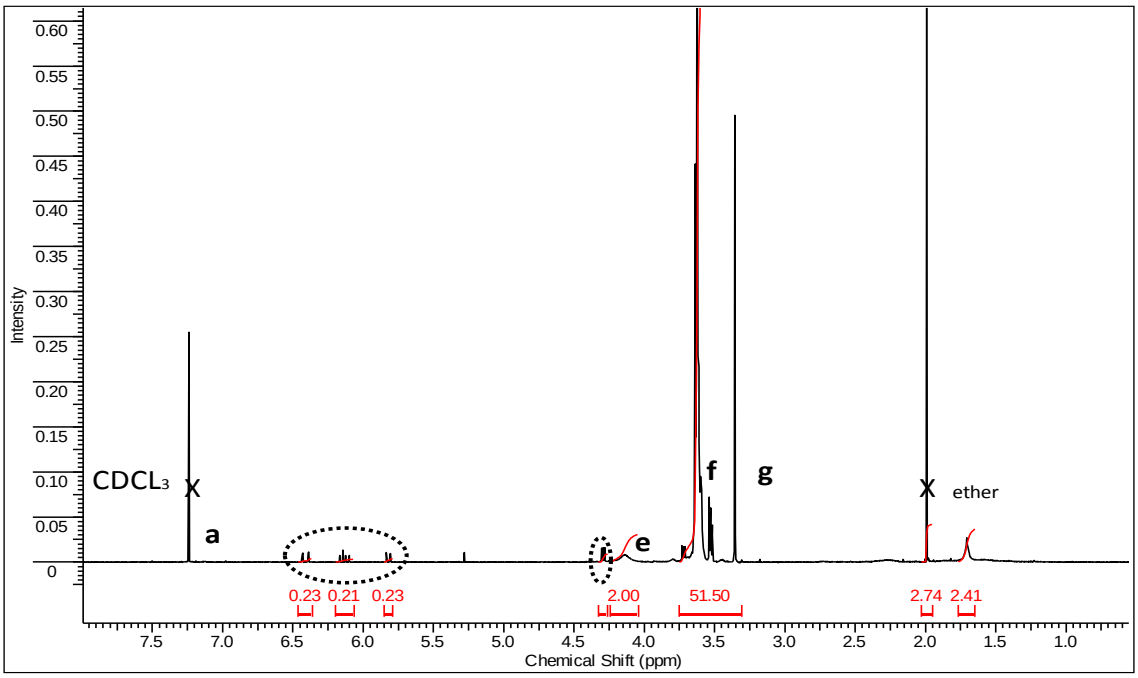

Figure A.2. ^{1}H-NMR spectrum of non-purified p(PEG-A) 20K. Conversion determined by ^{1}H-NMR spectrum of non-purified PEG-A that synthesized by RAFT polymerization at 65 °C, at a $[BSPA]_0/[PEG\text{-}A]_0/[AIBN]_0$ = 1/60/0.2

$$\text{Yield (mol \%)} = ((I_e - I_{e'})/(I_e + I_{e'})) \times 100 \text{ mol \%} \quad \text{(A.1)}$$

In this equation; Ie refers to integration values of reacted PEG-A and Ie' refers to un-reacted PEG-A.

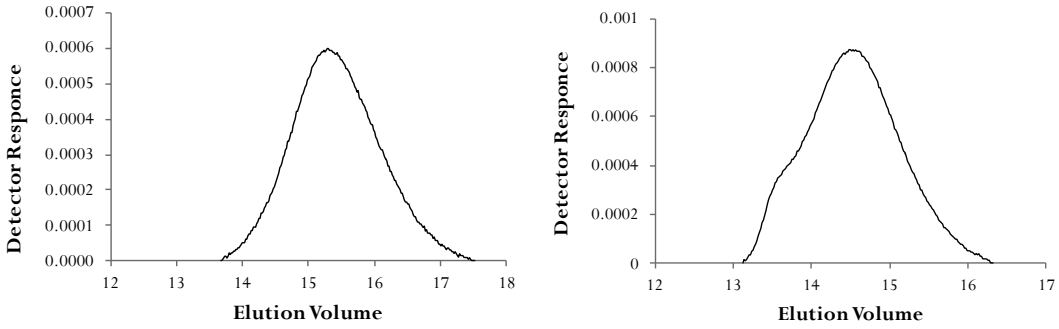

Figure A.3. GPC chromotograms of p(PEG-A) (10 and 20K) synthesized via RAFT polymerization. (a) elugram of p(PEG-A) (Mn = 10 700 g/mol, PDI =1.21) b) elugram of p(PEG-A) (Mn = 20 200 g/mol PDI = 1.26)

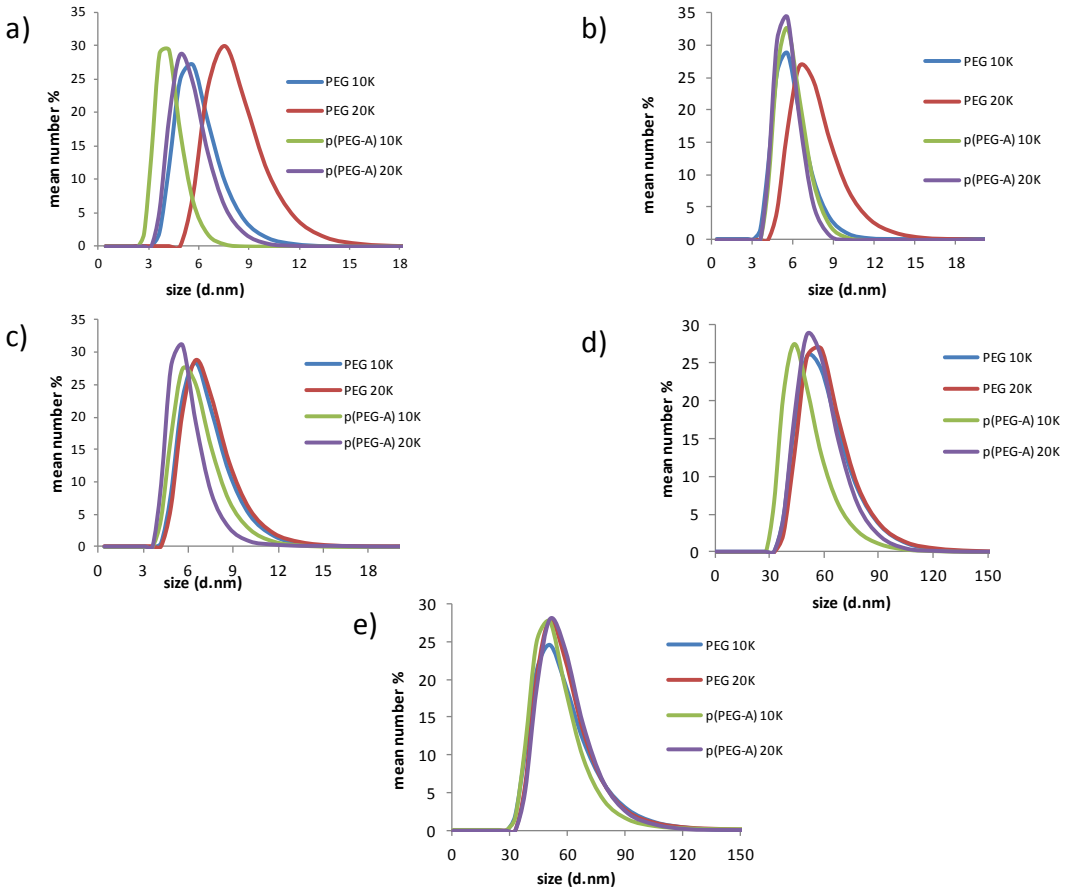

Figure A.4. Hydrodynamic diameter (D_h) of polymers obtained by DLS (measurement range 0.3nm – 10.0 microns). The D_h of linear PEGs (PEG 10K and 20K) and comb-type PEGs (p(PEG-A) 10K and p(PEG-A) 20K) in (a) water (b) PBS (c) PBS containing 10% FBS (d) RPMI 1640(e) RPMI 1640 containing 10% FBS

APPENDIX B

ETHYLENE GLYCOL ENDED-POLYMERS

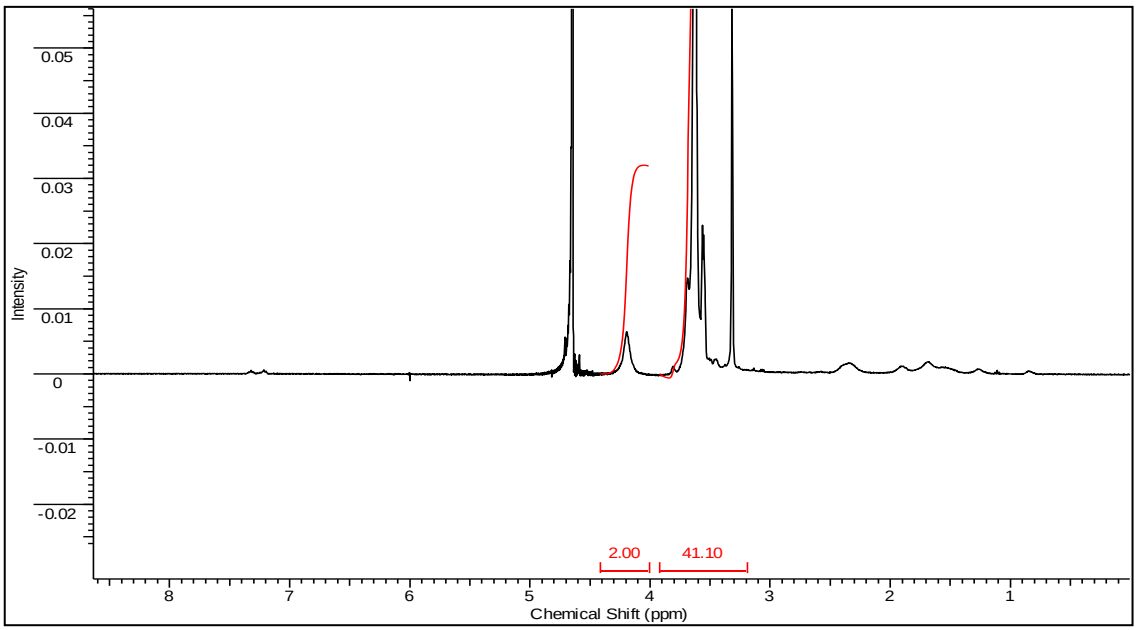

Figure B.1. ^{1}H-NMR spectrum of p(PEG-A) 10K after binding of PEG-A and purification by dialysis.

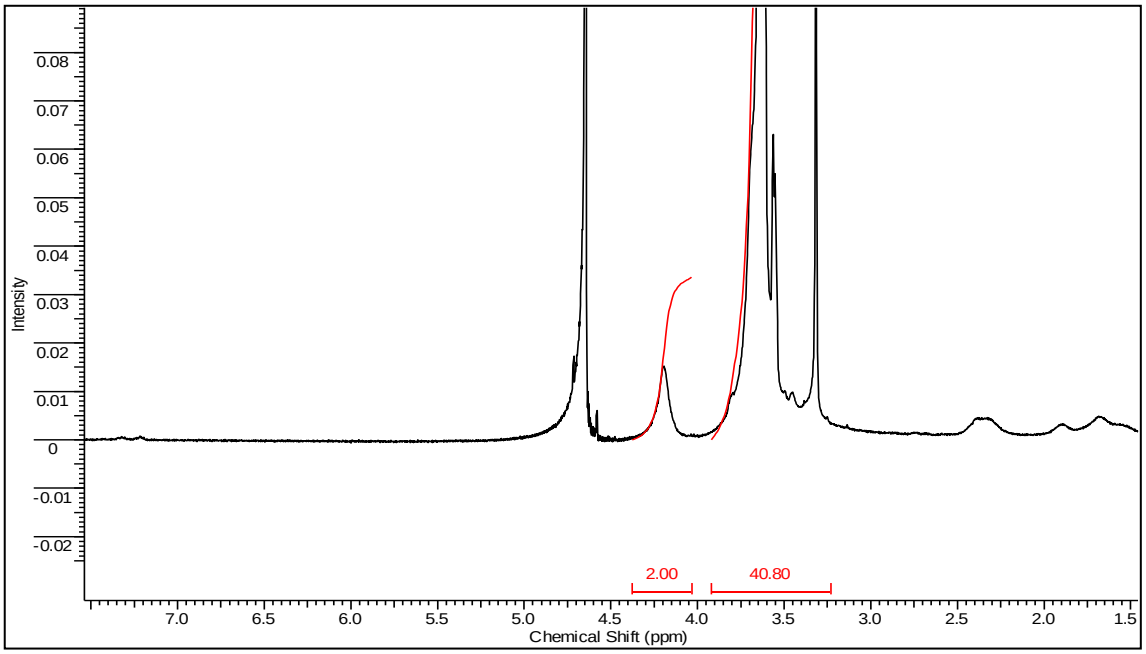

Figure B.2. ^{1}H-NMR spectrum of p(PEG-A) 20K after binding of PEG-A and purification by dialysis

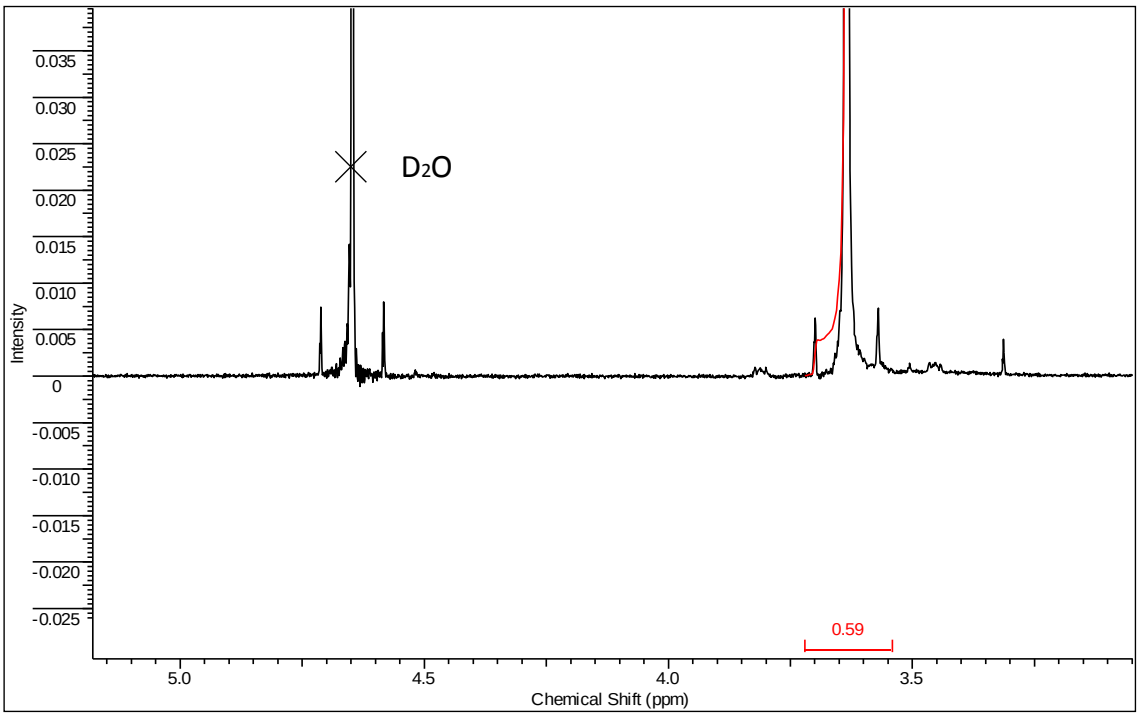

Figure B.3. [1]H-NMR spectrum of PEG 10K after binding of PEG-A and purification by dialysis.

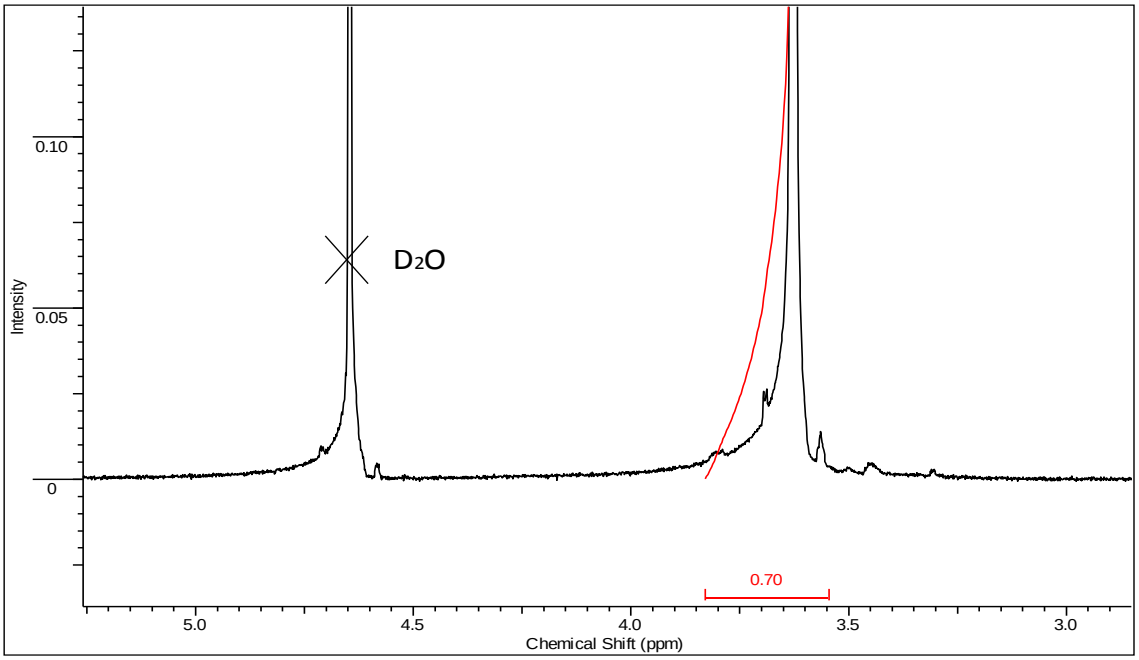

Figure B.4. [1]H-NMR spectrum of p(PEG-A) 20K after binding of PEG-A and purification by dialysis.

APPENDIX C

CELL UPTAKE OF LINEAR PEG (10K AND 20K) AND COMB-TYPE PEG p(PEG-A) (10K AND 20K)

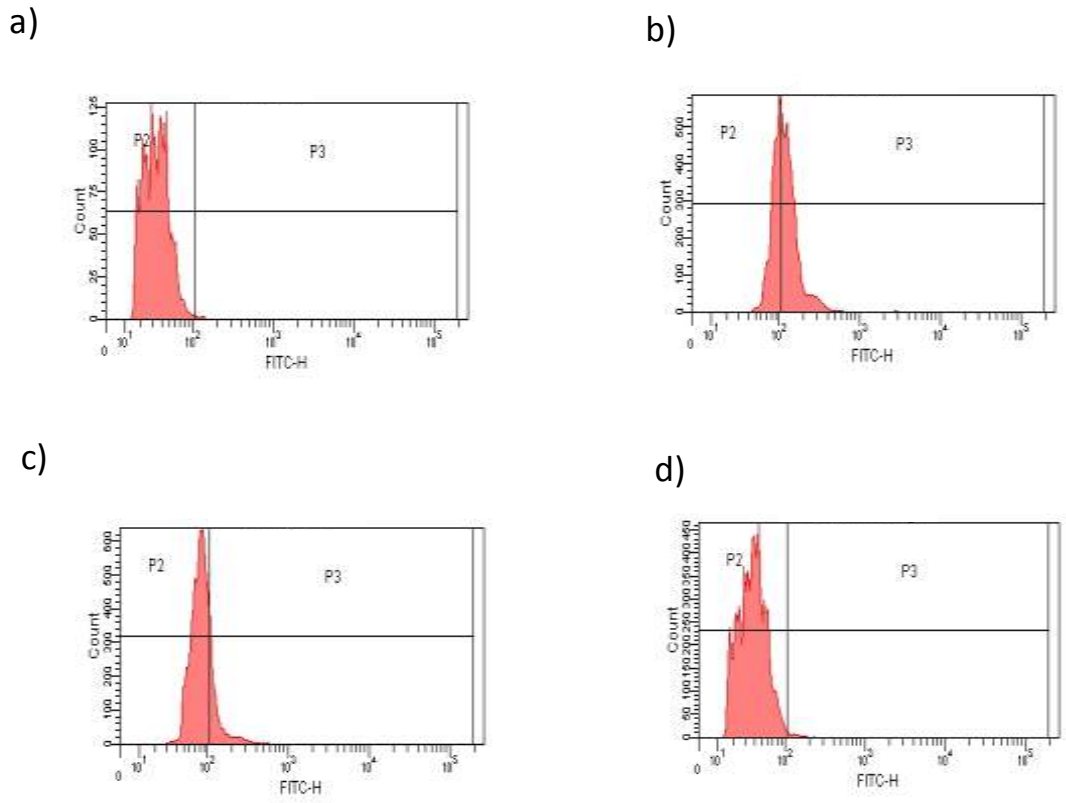

Figure C.1. Uptake of polymers (12,5 µM) by A549 cells in 1 hour at 37 ˚C a) Control b) Linear PEG 10K c) Comb-type PEG, p(PEG-A) 10K d) no labelled linear PEG 10K

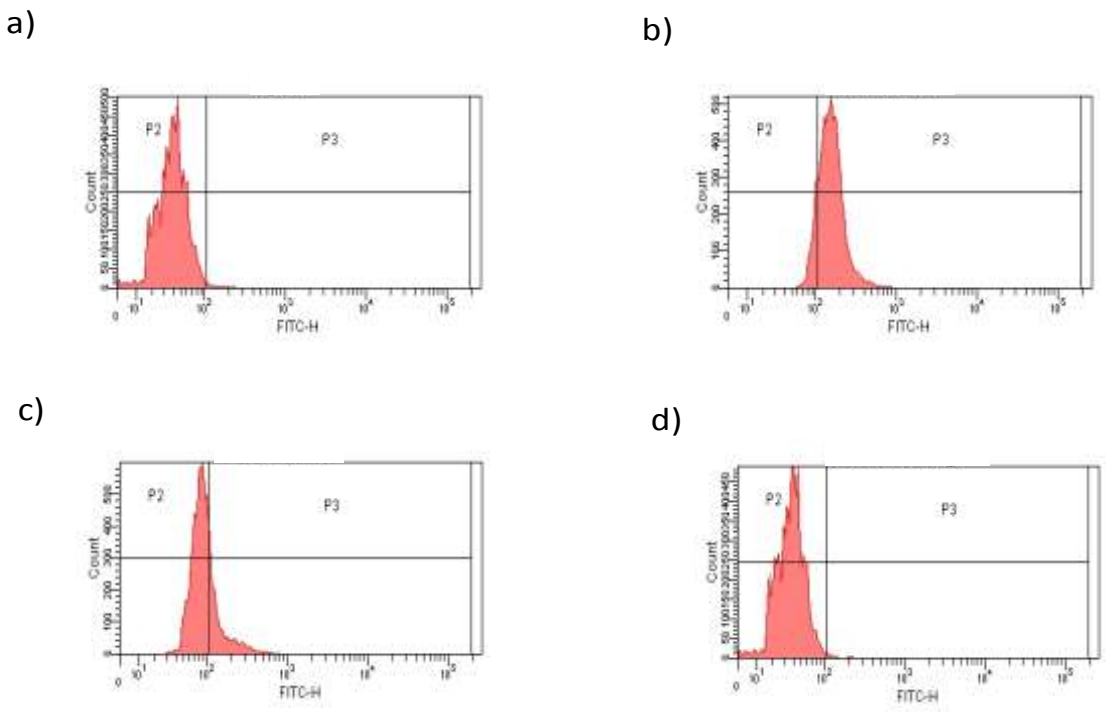

Figure C.2. Uptake of polymers (12,5 μM) by A549 cells in 3 hour at 37 ˚C a) Control b) Linear PEG 10K c) Comb-type PEG, p(PEG-A) 10K d) no labelled linear PEG 10K

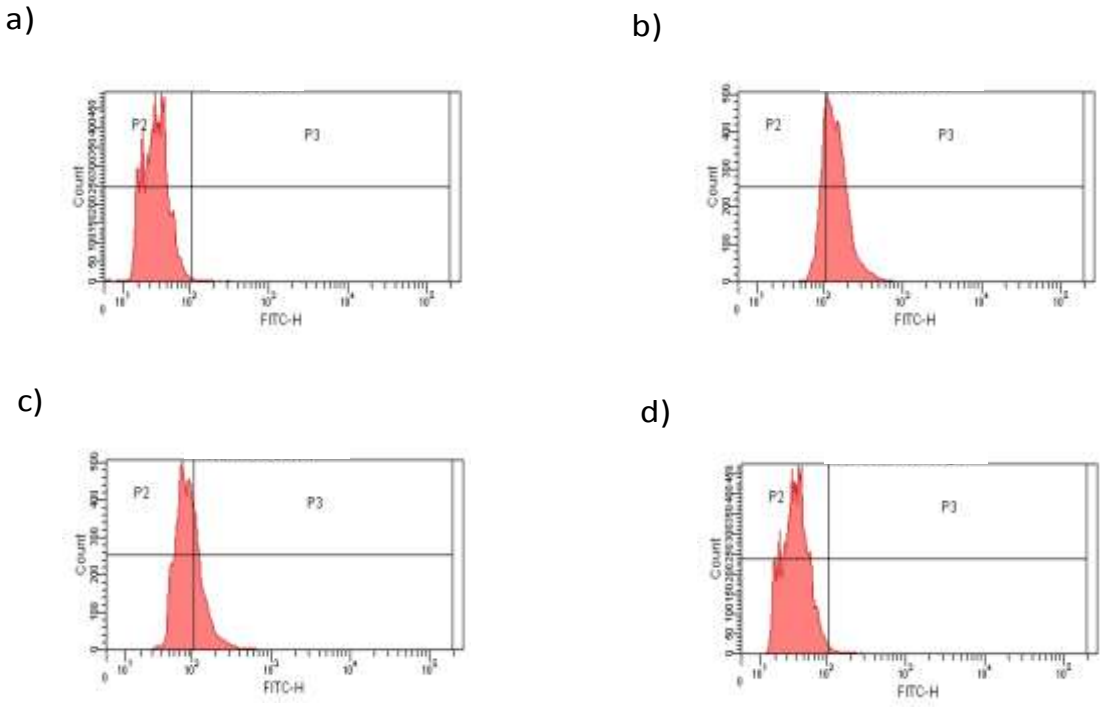

Figure C.3. Uptake of polymers (12,5 μM) by A549 cells in 6 hour at 37 ˚C a) Control b) Linear PEG 10K c) Comb-type PEG, p(PEG-A) 10K d) no labelled linear PEG 10K

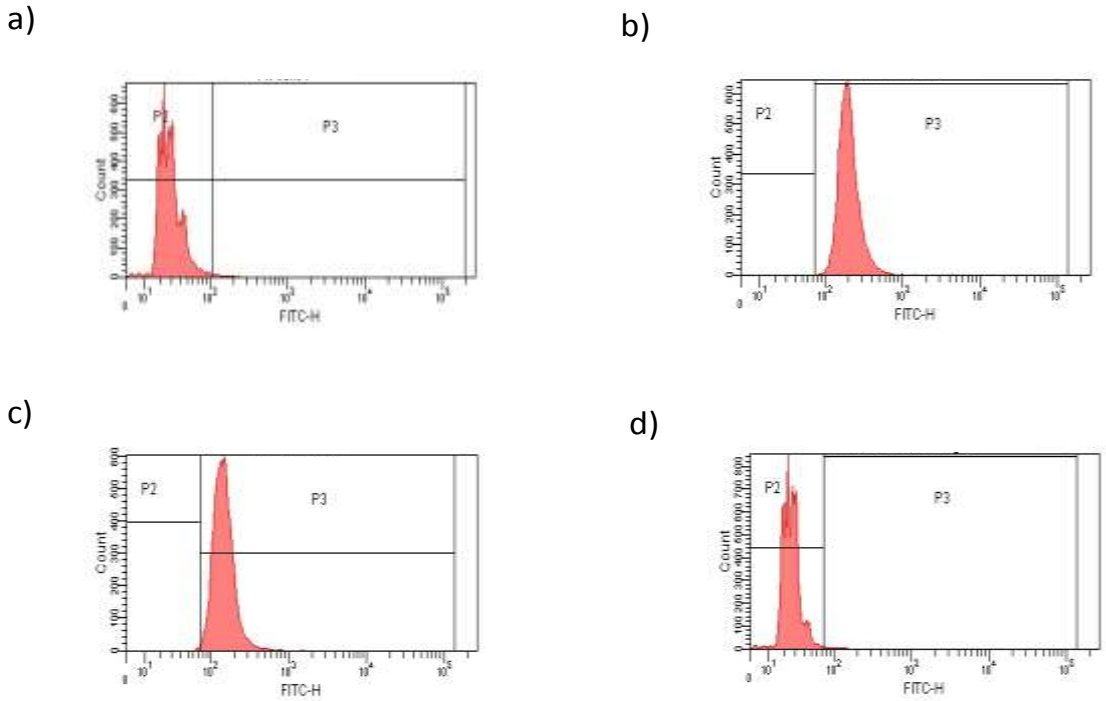

Figure C.4. Uptake of polymers (12,5 μM) by A549 cells in 1 hour at 37 ˚C a) Control b) Linear PEG 20K c) Comb-type PEG, p(PEG-A) 20K d) no labelled linear PEG 20K

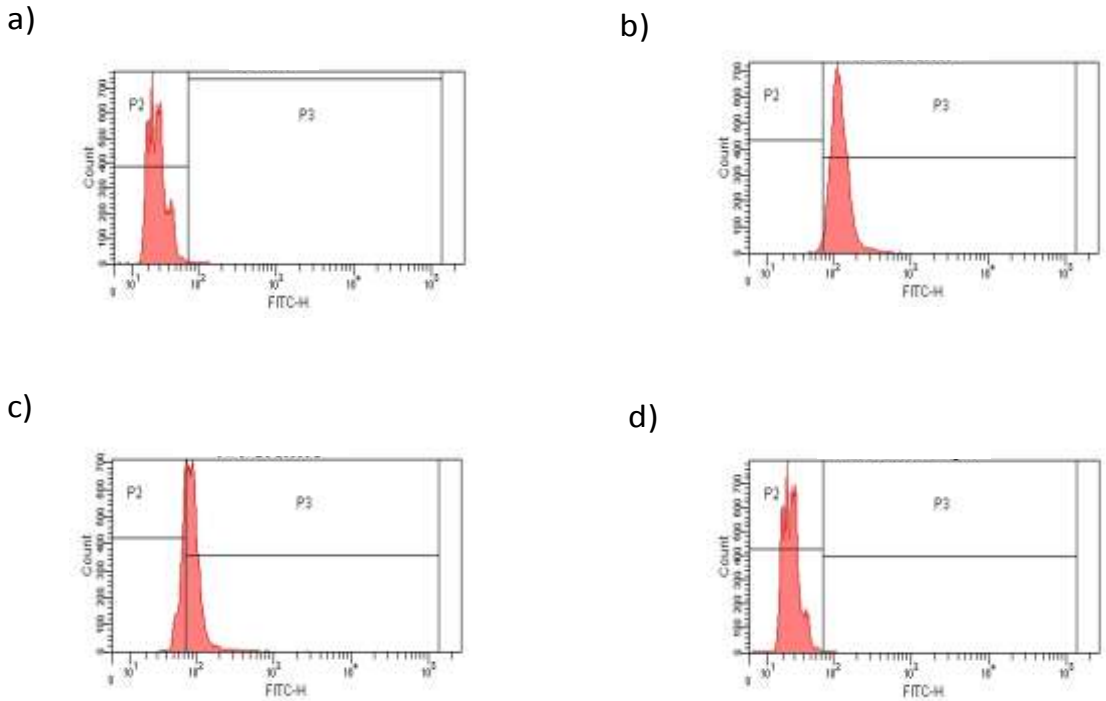

Figure C.5. Uptake of polymers (12,5 μM) by A549 cells in 3 hour at 37 ˚C a) Control b) Linear PEG 20K c) Comb-type PEG, p(PEG-A) 20K d) no labelled linear PEG 20K

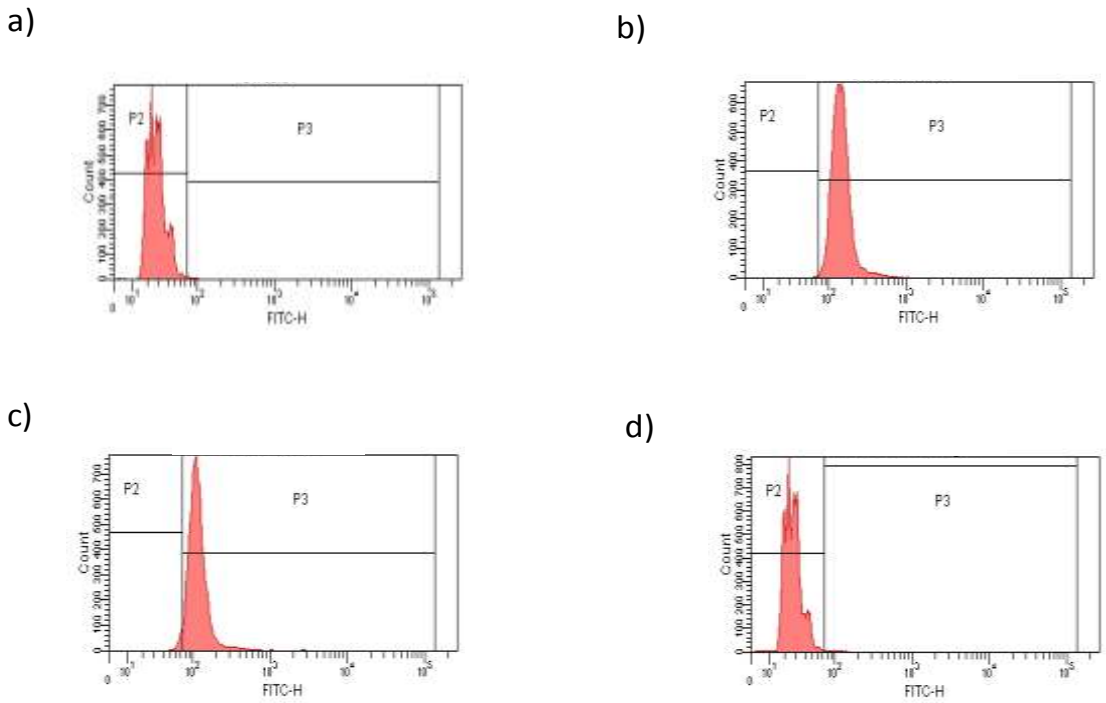

Figure C.6. Uptake of polymers (12,5 μM) by A549 cells in 6 hour at 37 ˚C a) Control b) Linear PEG 20K c) Comb-type PEG, p(PEG-A) 20K d) no labelled linear PEG 20K

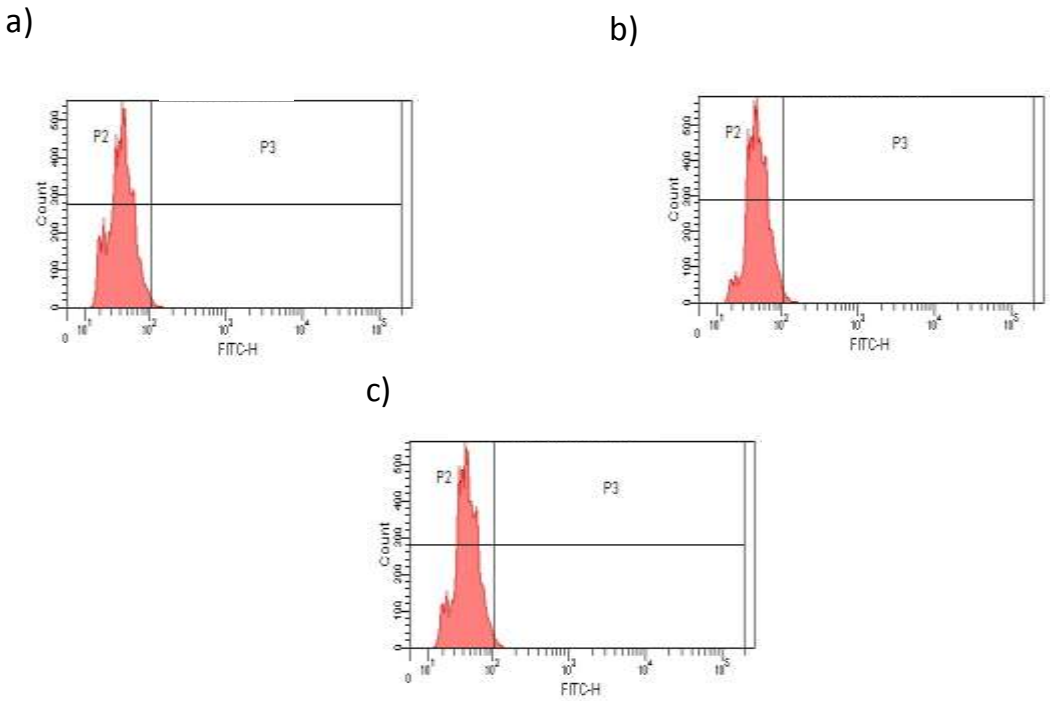

Figure C.7. Uptake of polymers (12,5 μM) by A549 cells in 1 hour at 4˚C a) Control b) Linear PEG 10K c) Comb-type PEG, p(PEG-A) 10K

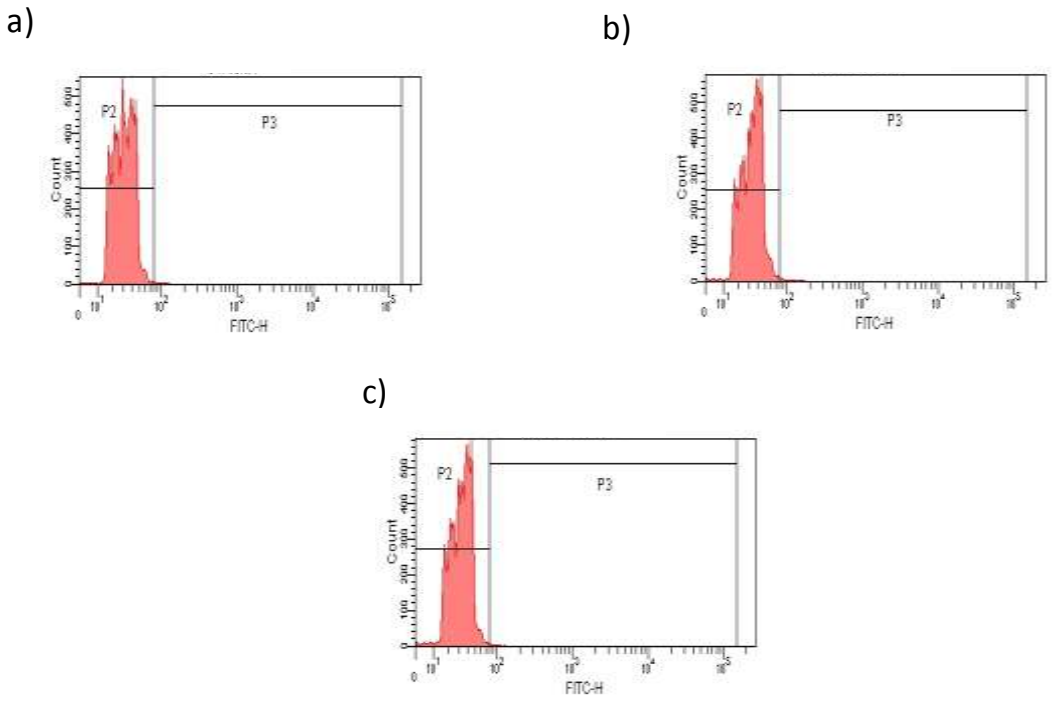

Figure C.8. Uptake of polymers (12,5 μM) by A549 cells in 3 hour at 4 ˚C a) Control b) Linear PEG 10K c) Comb-type PEG, p(PEG-A) 10K

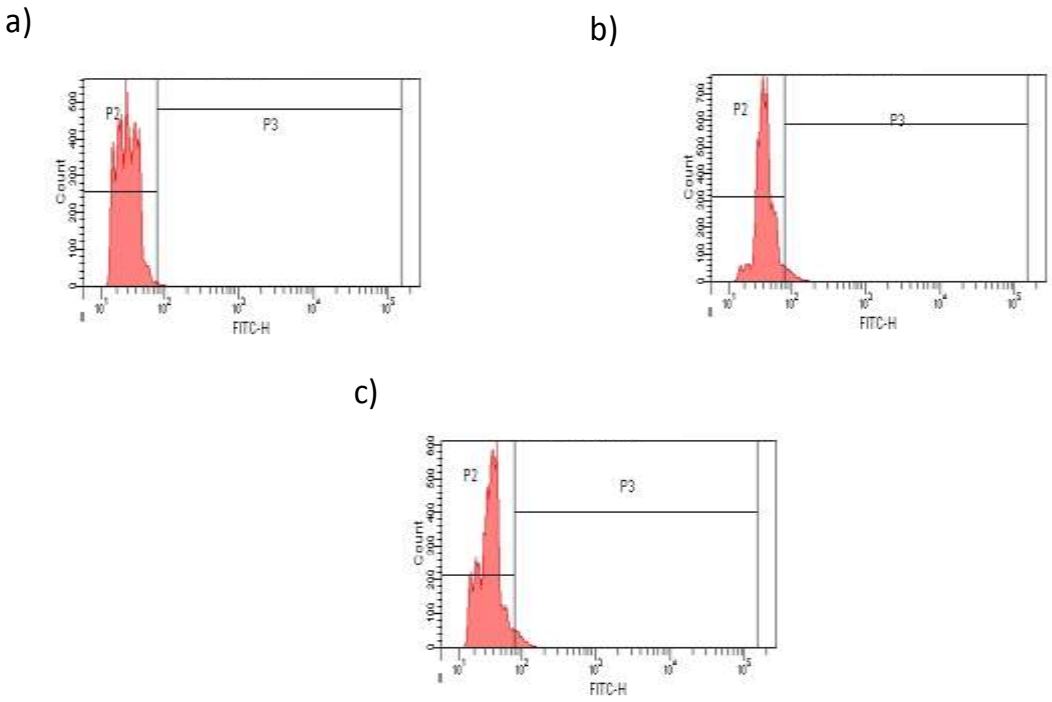

Figure C.9. Uptake of polymers (12,5 μM) by A549 cells in 6 hour at 4 ˚C a) Control b) Linear PEG 10K c) Comb-type PEG, p(PEG-A) 10K

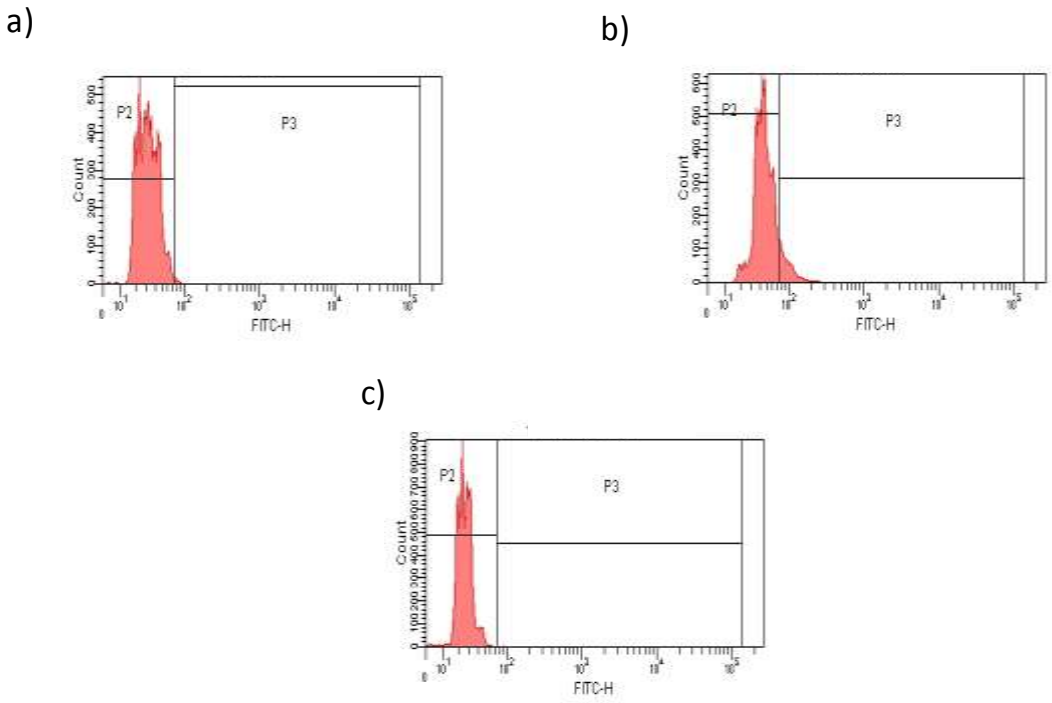

Figure C.10. Uptake of polymers (12,5 μM) by A549 cells in 1 hour at 4 ˚C a) Control b) Linear PEG 20K c) Comb-type PEG, p(PEG-A) 20K

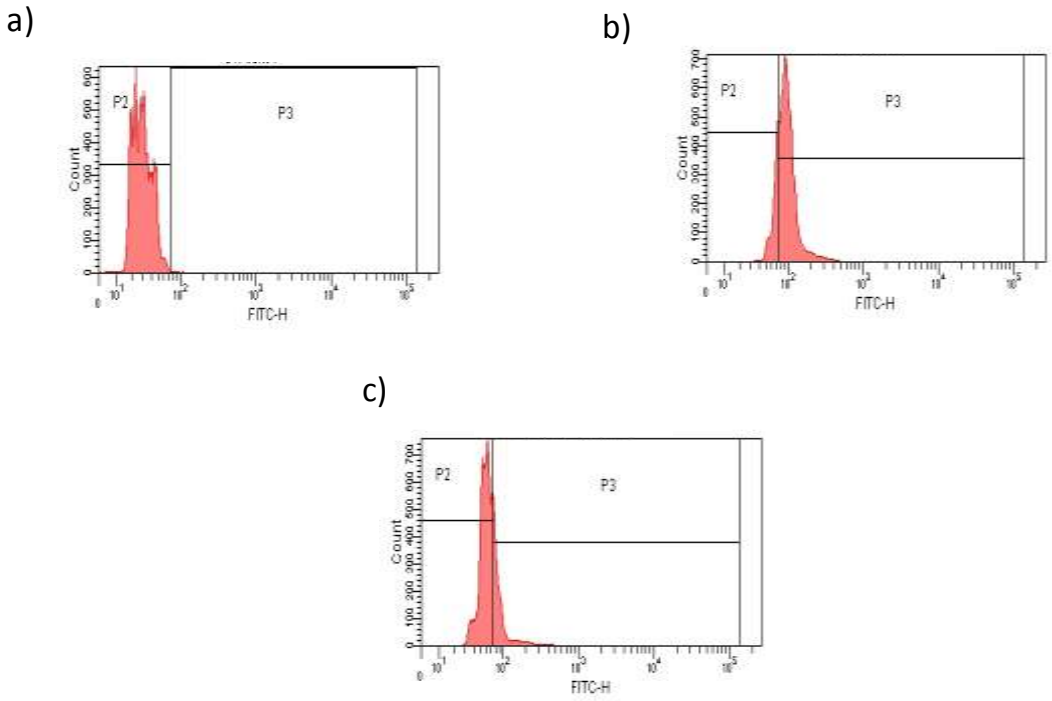

Figure C.11. Uptake of polymers (12,5 μM) by A549 cells in 3 hour at 4 ˚C a) Control b) Linear PEG 20K c) Comb-type PEG, p(PEG-A) 20K

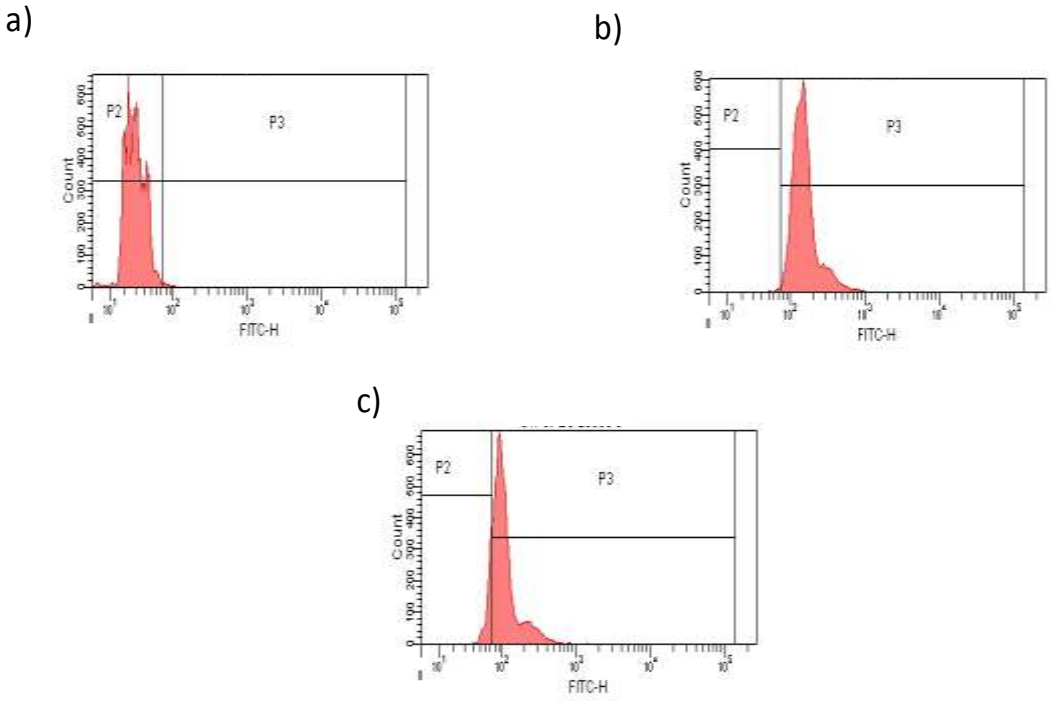

Figure C.12. Uptake of polymers (12,5 μM) by A549 cells in 6 hour at 4 ˚C a) Control b) Linear PEG 20K c) Comb-type PEG, p(PEG-A) 20K

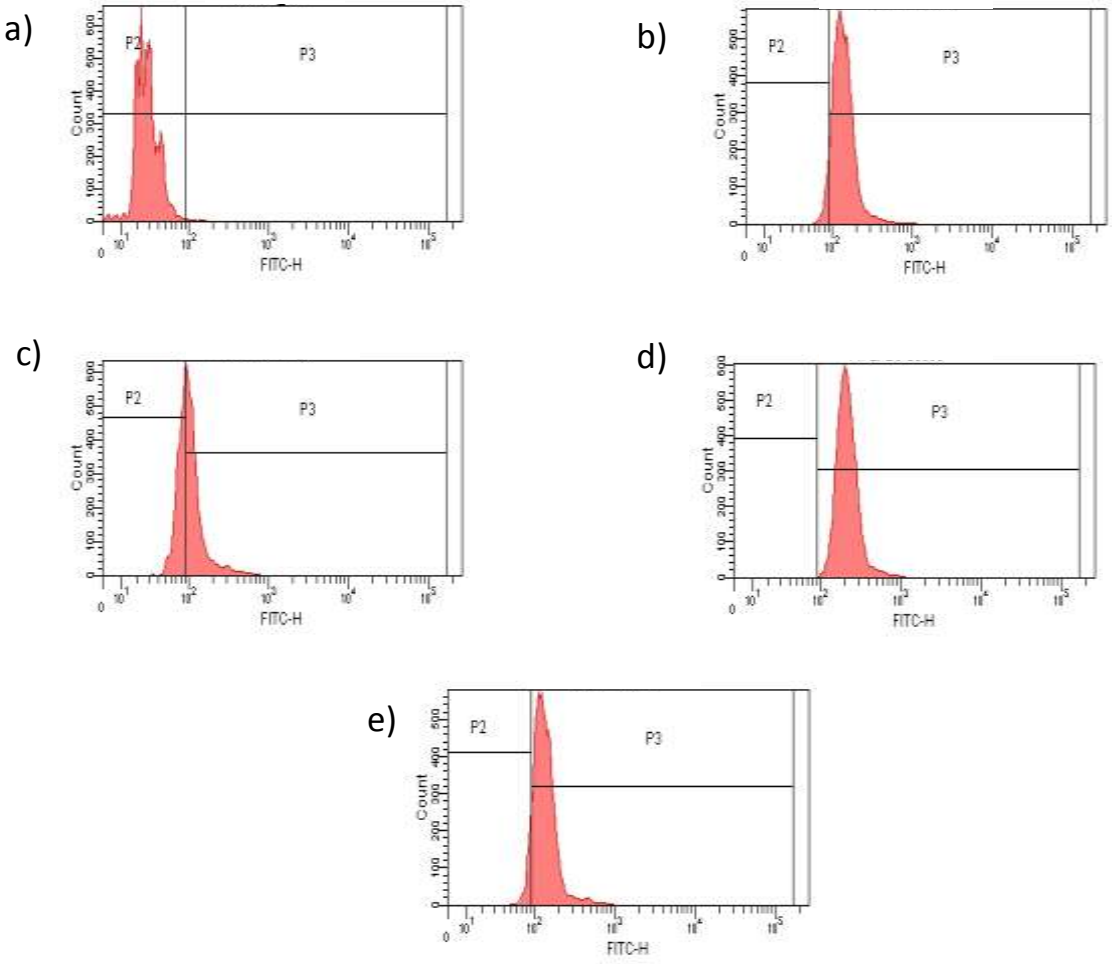

Figure C.13. Uptake of polymers (25 μM) by A549 cells in 1 hour at 37 ˚C a) Control b) Linear PEG 10K c) Comb-type PEG, p(PEG-A) 10K d) Linear PEG 20K, e) Comb-type PEG, p(PEG-A) 20K

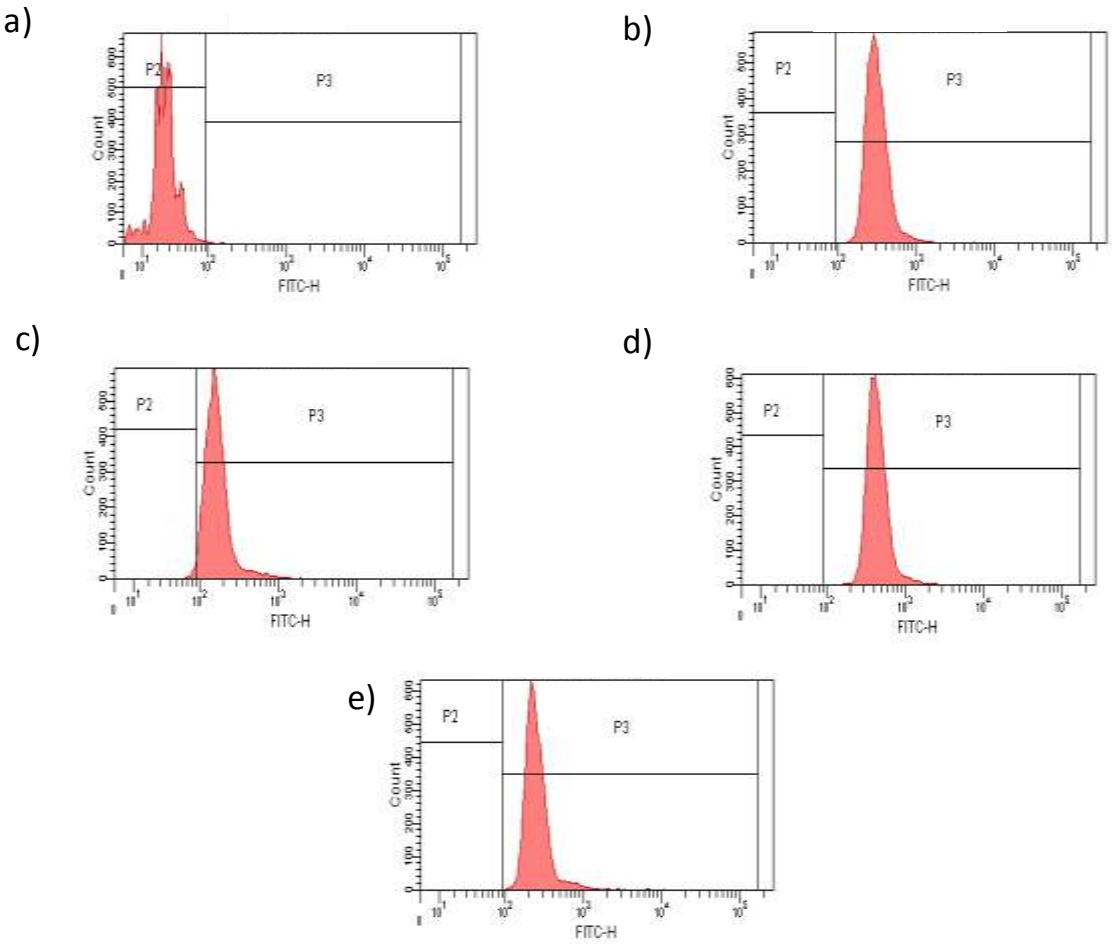

Figure C.14. Uptake of polymers (50 μM) by A549 cells in 1 hour at 37 ˚C a) Control b) Linear PEG 10K c) Comb-type PEG, p(PEG-A) 10K d) Linear PEG 20K, e) Comb-type PEG, p(PEG-A) 20K

APPENDIX D

FACS ANALYSIS OF CELL CYCLE

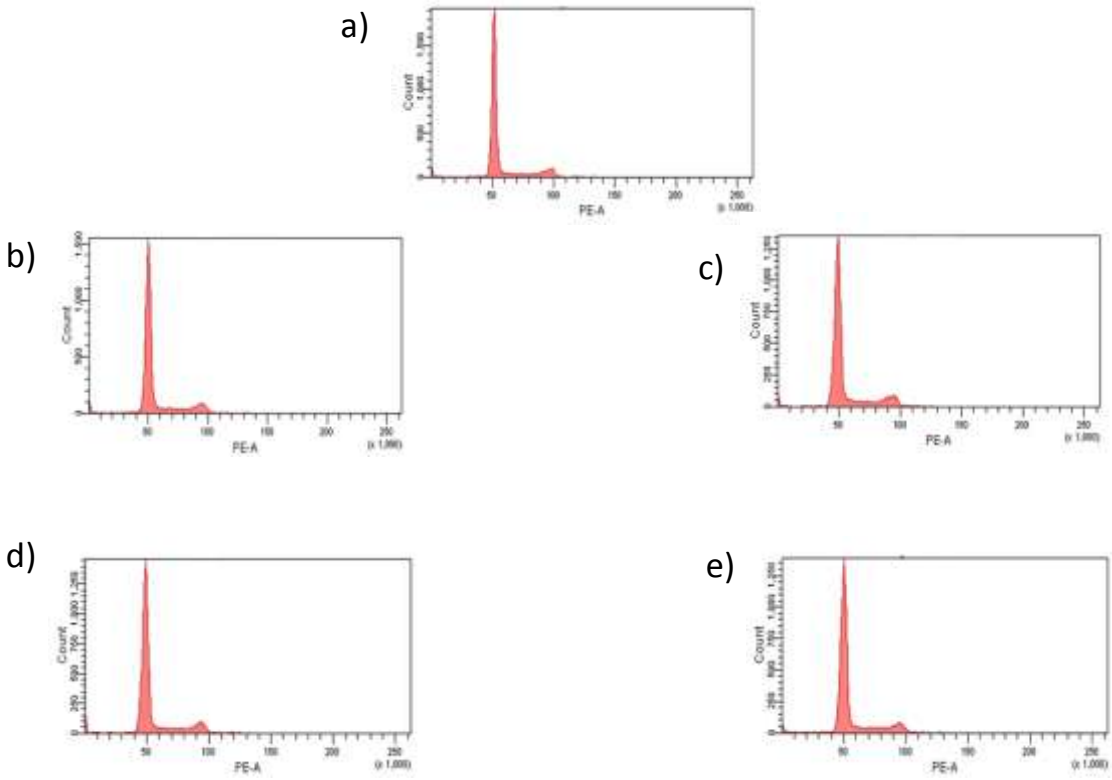

Figure D.1. FACS analysis of cell cycle induced by polymers for 24 hour. a) Control experiment b) PEG 10K, c) PEG 20K, d) p(PEG-A) 10K, e) p(PEG-A) 20K

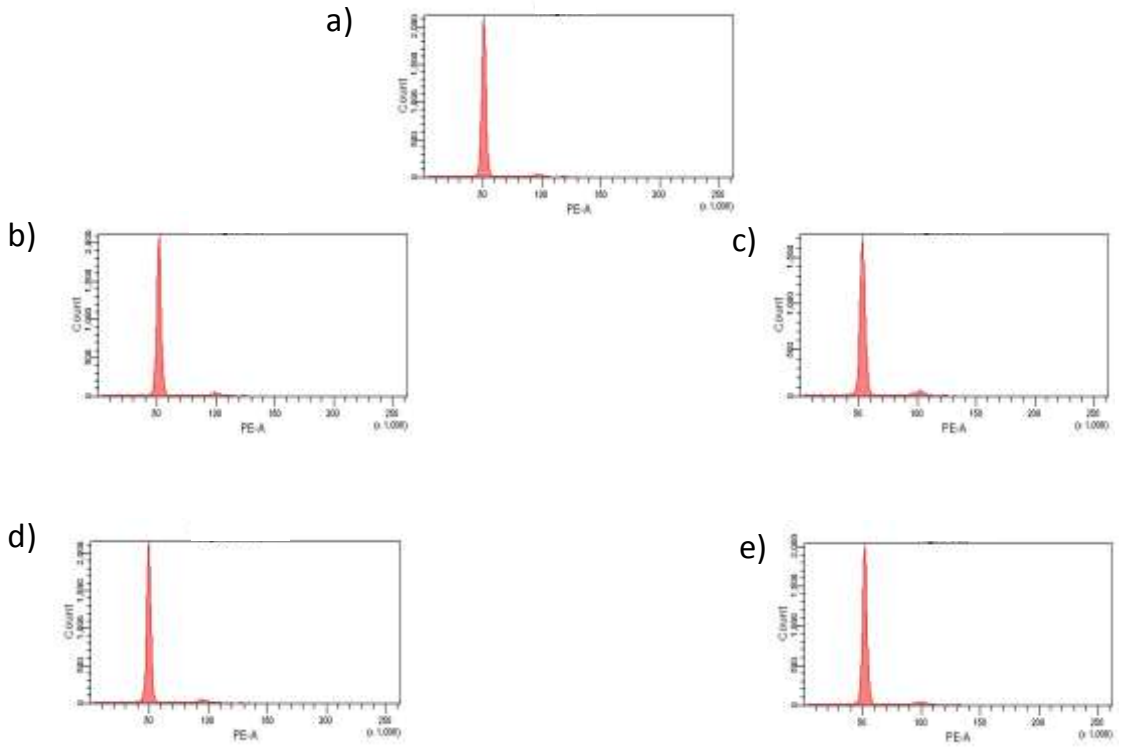

Figure D.2. FACS analysis of cell cycle induced by polymers for 72 hour. a) Control experiment b) PEG 10K, c) PEG 20K, d) p(PEG-A) 10K, e) p(PEG-A) 20K

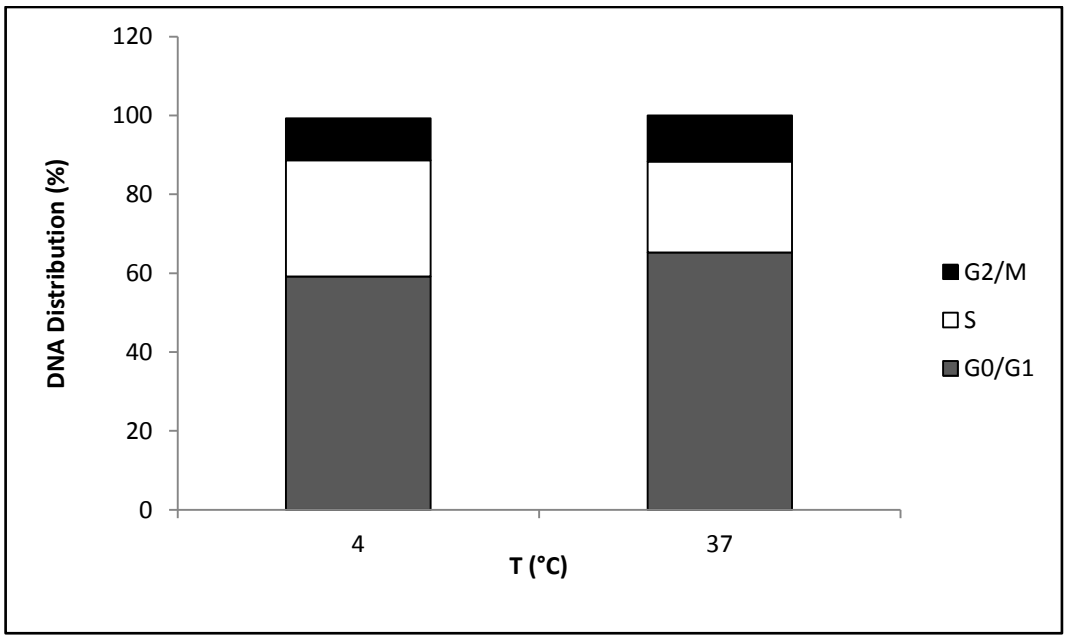

Figure D.3. DNA distribution of A549 cells after 24 hour treatment at 4 and 37 °C Experiments were performed in triplicate.